POLITECNICO DI TORINO

SCUOLA DI DOTTORATO
Dottorato di Ricerca in Scienza e Tecnologia dei Materiali – XXVII ciclo

Tesi di Dottorato

Development of a Novel Electrically Conductive Flame Retardant Bio-based Thermoplastic Polyurethane

A dissertation submitted in partial
fulfillment of the requirements for the degree of
Doctor of Philosophy in Materials Science and Technology

Relatori

Prof. Giulio Malucelli

Dr. Andrea Castrovinci

Candidato

Rosane Moura Dos Santos

2015

This thesis is approved by the following Thesis Examining Committee:

Prof. Alberto Fina (Chairman)

Prof. Giovanni B. Appetecchi

Prof. Davide Beneventi

Prof. Giulio Malucelli (Principal Advisor)

Prof. Andrea Castrovinci (Co-advisor)

To my mother Maria Rosa and my husband Diego, whose love, support, and example have helped me find my dreams and for never letting me give up.

Abstract

The central topic of this thesis was the design and development of a bi-functional thermoplastic polyurethane (TPU) composite, which is halogen-free bio-based flame retardant (UL94-V0) with an electrical resistivity ≤ 1000 Ω.cm and a filler load that does not exceed 25 wt.%.

In order to reach this goal, the experimental activities were divided into the following tasks: (a) materials pre-selection, (b) design of experiment (DOE), (c) materials compounding, (d) specimens preparation (injection moulding), and (e) materials characterization (electrical resistivity tests, flammability tests, and microstructure analysis).

In other words, the main tasks were identifying the ingredients (in a first stage) and defining the optimal proportions of additives (in a second stage) capable of simultaneously conferring to the polymer of interest the most desirable values of flame retardancy (as high as possible) and electrical resistivity (as low as possible); followed by the material preparation (third stage) and the material characterization (forth stage).

The materials (flame retardants and electrically conductive additives) used in the development of this novel formulation were pre-selected mainly based on bibliographical studies.

Then, the experimental activities and the analysis of the test results allowed to identify positive and negative effects among the components of the formulation such as synergistic effects among flame retardants on the improvement of the fire resistant performance.

The obtained final formulation accomplished the desired target values of flame retardancy (V0 compliant) and electrical resistivity (≤1000 Ω.cm). It was compared to commercial products from the companies RTP, BASF and LUBRIZOL, which are used in the same field of application. The material developed during this work showed a lower electrical resistivity than these commercially available products while being bio-based and V0 (UL-94 test) at the same time.

In addition, an innovative online acquisition apparatus for monitoring the surface growth of flame retardant protective layers was designed and developed during this thesis, which provided a deep insight of the dynamic behaviour of a phosphorous-based flame retarded material. The measurement of the surface protective layer growth rate provided a better understanding of the behaviour of the flame retardant systems, correlating the speed of the chemical reaction with the performances of the material.

Riassunto

Il tema centrale di questa tesi è stata la progettazione e lo sviluppo di un compound a base poliuretano termoplastico (da fonti rinnovabili) bi-funzionale. Il materiale risulta ritardato alla fiamma (UL94 V0) con una resistività elettrica ≤ 1000 Ω.cm. Queste caratteristiche sono state raggiunte senza l'uso di ritardanti alla fiamma a base alogeni e con una carica complessiva che non supera 25% in peso.

Le attività possono essere raggruppate come segue:

- preselezione dei materiali
- progettazione dell'attività sperimentale (DOE)
- compounding di materiali
- preparazione dei provini (stampaggio ad iniezione)
- caratterizzazione dei materiali (test di resistività elettrica, prove di infiammabilità ed analisi microstrutturale)

I compiti principali erano identificare gli ingredienti (in una prima fase) e definire le proporzioni ottimali di additivi (in una seconda fase) in grado di conferire contemporaneamente al polimero di interesse valori più desiderabili di resistenza alla fiamma (il più alto possibile) e resistività elettrica (il più basso possibile); seguita dalla preparazione del materiale (terza fase) e la caratterizzazione dello stesso (quarta fase).

Le cariche utilizzate nello sviluppo di questa nuova formulazione sono state pre-selezionate principalmente sulla base di studi bibliografici. Successivamente, le attività sperimentali e l'analisi dei risultati delle prove hanno permesso di individuare gli effetti positivi e negativi tra i componenti delle varie formulazioni, come per esempio gli effetti sinergici tra ritardanti di fiamma.

La formulazione finale ottenuta ha raggiunto i target desiderati di ritardo alla fiamma (UL94-V0) e resistività elettrica (≤1000 Ω.cm). La stessa è stata confrontata con prodotti commerciali delle aziende RTP, BASF e Lubrizol, che vengono utilizzati nello stesso campo di applicazione. Il materiale sviluppato durante questo lavoro ha mostrato una resistività elettrica inferiore ai prodotti commerciali disponibili essendo a base biodegradabile e V0 (UL-94 test) allo stesso tempo.

Inoltre, è stato progettato e sviluppato durante questa tesi un nuovo sistema di acquisizione visiva on-line in grado di monitorare la superficie di un campione di materiale polimerico sottoposto alla fiamma. Il sistema filtra la luce emessa dall'innesco e permette di studiare l'evoluzione della superficie del campione anche in caso di fiamme e fumo persistenti. L'uso di questo set-up ha permesso di valutare la lo sviluppo degli strati protettivi generati dai ritardanti alla fiamma a base fosforo. La misurazione del tasso di crescita dello strato protettivo superficiale ha migliorato la comprensione del comportamento dei sistemi ritardanti di fiamma, correlando la velocità della reazione chimica con le prestazioni del materiale.

Resumo

O tema central desta tese foi o planejamento e desenvolvimento de um compósito bifuncional a base de poliuretano termoplástico (42% de origem vegetal), retardador de chamas (UL94-V0) livre de halogenados, com uma resistividade elétrica ≤ 1,000 Ω.cm e uma carga de compositos que não excede 25 wt.%.

Para alcançar este objetivo, as atividades experimentais foram divididas nas seguintes tarefas: (a) pré-seleção de materiais, (b) planejamento experimental (DOE), (c) preparação dos materiais (extrusão), (d) preparação das amostras (moldagem por injeção), e (e) caracterização dos materiais (testes de resistividade elétrica, testes de inflamabilidade, e análise da microestrutura).

Em outras palavras, as principais tarefas foram identificar os ingredientes (numa primeira fase), definir as proporções ótimas de aditivos (numa segunda fase) capaz de conferir, simultaneamente, ao polímero de interesse os mais desejáveis valores de retardância à chamas (o mais alto possível) e resistividade elétrica (o mais baixo possível); seguido da preparação (terceira fase) e da caracterização (quarta fase) dos materiais.

Os aditivos (materiais retardadores de chama e condutores electricamente) utilizados no desenvolvimento desta nova formulação foram pré-selecionados principalmente com base em estudos bibliográficos.

Em seguida, as atividades experimentais e a análise dos resultados dos testes permitiram identificar efeitos positivos e negativos entre os componentes da formulação, tais como efeitos sinérgicos entre os retardadores de chama na melhoria da resistência a chama.

O material obtido alcançou os valores-alvo desejados de retardância à chama (Ul94-V0) e resistividade elétrica (≤1000 Ω.cm). Ele foi comparado com produtos comerciais das empresas RTP, BASF e Lubrizol, que são utilizados no mesmo campo de aplicação. O mesmo revelou uma resistividade elétrica inferior a estes produtos comercialmente disponíveis sendo, ao mesmo tempo, de base biodegradável e UL-94-V0.

Além disso, um aparelho inovador de aquisição on-line para monitorar o crescimento da superfície das camadas protetoras contendo retardadores de chama foi projetado e desenvolvido durante esta tese, o que proporcionou uma visão profunda do comportamento dinâmico de um material contendo retardadores de chama à base de fósforo. A medição da taxa de crescimento da camada protectora de superfície forneceu uma melhor compreensão do comportamento dos sistemas de retardadores de chama, correlacionando a velocidade de reação química com os desempenhos do material no teste UL94.

Contents

1 Introduction

1.1 Scope of the thesis

This PhD thesis is focused on the development of a bi-functional TPU composite, which is halogen-free UL94-V0 bio-based with electrical resistivity ≤ 1000 Ω.cm and the filler load does not exceed 25 wt.%. To achieve these features, bio-based TPUs have to be modified with a certain number of additives like flame retardants (phosphorous and mineral based) and potential synergists, micro and nanofillers (e.g. electrically conductive fillers). The work will exploit fundamental know-how, focusing on its potential applications.

1.2 Objectives

This work has established a set of *Scientific and Technological Objectives*.

Scientific Objectives:

The main scientific objective of the present work aims to set some correlations among the raw materials characteristics and concentrations, the nano-microstructure, and the processing with the new materials properties/performances. Therefore, the following studies are necessary:

(i) *Identification of synergistic effects.* The relative percentage of selected fillers is driven by the interaction among them. Synergisms would allow minimizing the overall amount of additives and fillers, as well as maximizing their effect on the material properties. A clear identification of the interaction between the additives is therefore required.

(ii) *Correlation between materials micro-nanostructure and performances.* The definition of a map of the correlations between the intrinsic characteristics of the composites (e.g. microstructure, composition, additive nature, etc.) with the performances (i.e. flammability, electrical conductivity, mechanical properties) is needed.

(iii) *Correlation between materials processing and their performances*. The identification of the processing parameters that bring benefits, in terms of

nano/micro structure and final properties of the materials, deserves investigation.

(iv) *Additional tests.* UL94 pass/fail test does not provide qualitative and quantitative data capable to support the development of new formulations. Therefore, an innovative image processing system is used to monitor the first step of material combustion, i.e. the ignition and growth of the protective layer, delivering results far beyond the limit of the human operator.

Technological Objectives:

The main technological objectives of this work can be summarized as follows: (a) to obtain a bio-based TPU-ester/ether compound that, being simultaneously halogen-free fire-safe and electrically conductive, overcomes the currently used soft PVC products in the target application fields, (b) to identify the best preparation processing conditions; and (c) to define an effective formulation. These technological objectives are further detailed as follows:

(i) *Halogen-free, fire-safe, electrically conductive bio-based TPU composites with suitable mechanical properties.* Production of polymeric materials in compliance with the project stated objectives, i.e. the design of a new UL94 V0 electrically conductive (resistivity $\leq$ 1000Ω/cm) halogen-free TPU ether/ester compound.

(ii) *Optimization of blending process parameters*. Dispersion of nano and microfillers and other additives is a fundamental step to achieve the targeted material performances. The know-how in terms of process parameters is therefore a fundamental technological objective of this work, being a competitive advantage with respect of the competitors.

(iii) *Definition of the effective formulation domain.* This work explores a relatively large formulation domain, intended to find: (a) the total proportion of additives to be used in the mixture; (b) the number and identity of additives; (c) the proportion of each additive in the mixture. The design of experiment (DOE) approach was used to define the effective formulation

domain potentially suitable to (a) tune the formulation on the basis of specific (already existing) needs, and (b) explore new formulations suitable for other markets.

2 Background

2.1 Flammability of polymeric materials

Polymers can be classified depending on their structures, physical properties, technological uses, etc. They can be natural or synthetic, processed in different ways into different shapes. They are light in weight and show low thermal and electrical conductivity, good toughness and chemical resistance; last but not least, their cost is relatively low.[1]

There are a few reasons that make the market of synthetic polymer-based materials (plastics) continuously growing. One refers to the emergence of new applications for plastics. In addition, polymeric materials are replacing other materials, e.g. metals, in some applications such as transports (e.g. automotive, aircraft, public transports, etc.), buildings (e.g. thermal insulation), furniture (e.g. upholstery, etc.), and electronic devices (e.g. cables, external case for computers and notebook, etc.). [2, 3]

Although synthetic polymer materials are rapidly replacing more traditional materials, their easy burning behavior under certain conditions represent a weak point as compared, for instance, to metals. Therefore, the fraction of the fire load in homes, commercial environments, and transports has also growth. [3-5]

Being carbon-based polymeric materials, polymers easily burn producing gases and smoke when subjected to a flame, and degrade at high temperatures into volatile and gaseous combustion products. [3-5]

Most polymers are inherently flammable, although at different levels. Flammability refers to the propensity of a substance to ignite easily and burn rapidly with a flame, and it is one indicator of fire hazard. [6] The damages caused by fire are staggering: as an example, 12 people die and 120 people are severely injured every day in Europe. In addition, the global economic impact of the deaths and injuries caused by fire is estimated to be around 1% of GDP in the developed world. As an example, the total cost of fires in England and Wales was estimated at approximately £7.03bn in 2004.

The most important sources of fires are electrical faults and electrical apparatuses, which caused 10% of all the recorded fire incidents. After the introduction of the 1988 UK legislation, requiring domestic furniture to be fire resistant, the numbers of saved lives and fire injuries has improved considerably and it is estimated to have resulted in at least 50% savings in injuries and domestic fire deaths in 2002. [7]

To avoid potential fire hazard and risks, it is important to understand how synthetic polymers burn and how to make these materials less flammable. Therefore, the combustion of synthetic polymer materials will be explained in the next section.

2.2 Combustion process of polymers

Combustion of synthetic polymer materials is characterized by a complex coupling between condensed and gas phase phenomena. Furthermore, the phenomena in each phase consist of a complex coupling of chemical reactions with heat and mass transfer processes.[5] Figure 1 shows a scheme of the polymers combustion cycle.

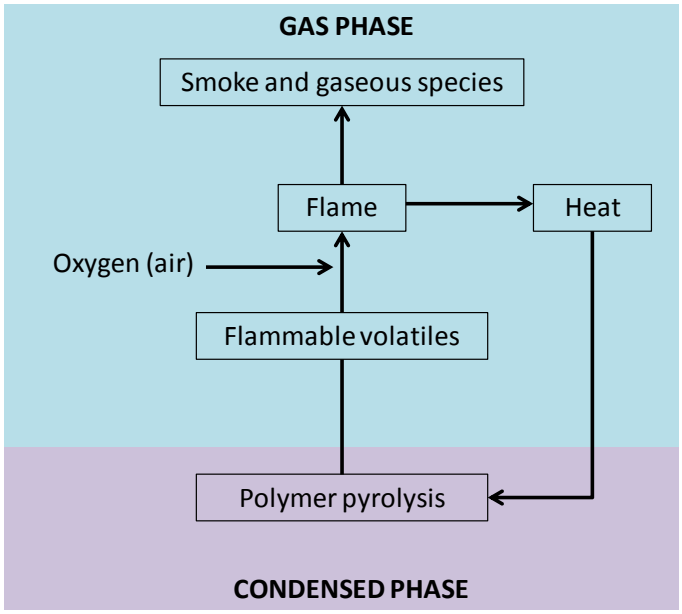

Figure 1 Combustion of polymeric materials

The burning process of polymeric materials can be divided into subsequent stages [3,8-12]:

- *Heating.* Thermal energy is supplied by radiation, convection or conduction by an external source to the polymer, which increases its temperature. The rate of temperature rise depends on the heat flux, temperature difference, specific heat and thermal conductivity.
- *Degradation and decomposition.* At a certain temperature, thermal decomposition takes place. The degrading polymer releases combustible volatiles. Polymer degradation depends on the mechanism of decomposition of macromolecules, which in turn is strictly related to their chemical structure. The presence of additives, i.e. flame retardants, can modify the degradation mechanism, decreasing, for example, the production of volatiles.

- *Ignition.* Combustible volatiles mix with atmospheric oxygen and ignite. Ignition is affected by temperature, concentration of volatiles and depends on the possible presence of an ignition source (a flame or a spark, etc.).
- *Combustion*. The fraction of the heat generated by the flame is partially dispersed (that is, re-radiation from the surface to the surrounding ambient occurs), thus increasing both the material and volatiles temperature. If enough heat is released, the surrounding material is heated up to ignition and a self-sustaining combustion takes place.
- *Propagation*. The flame propagates through the material, which decomposes to volatiles and, depending on the chemical nature of the polymer, to an inert carbonaceous char.

Physical and chemical processes take place in each of three separate phases: *gas*, *mesophase* (that is, the interface between the gas and condensed phase during burning), and *condensed* (liquid/solid) phases [3,13], as shown in Figure 2.

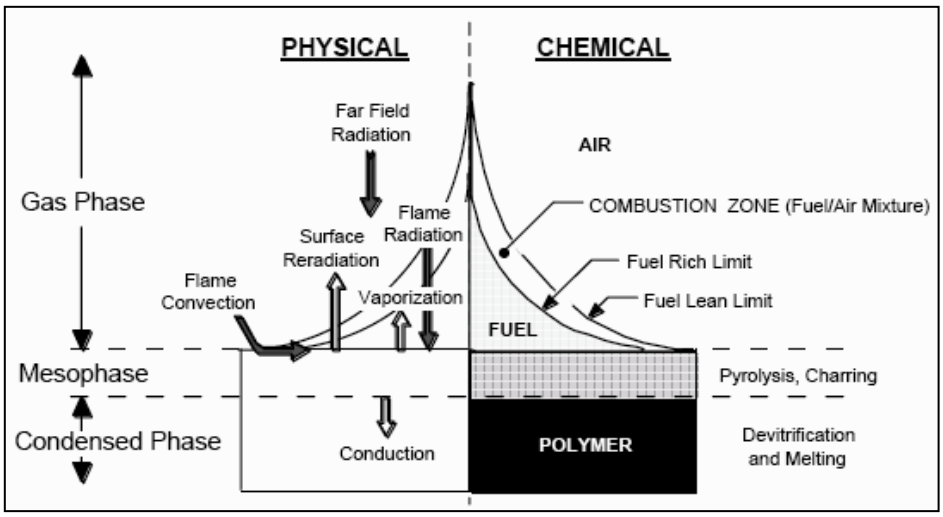

Figure 2 Physical and chemical processes in the flaming combustion of polymers [10]

Figure 2 shows an schematic diagram of a horizontal polymer slab that is burning with a diffusion flame. The physical processes, shown on the left-hand side of Figure 2, include: (a) energy transport by radiation and convection between the gas phase (flame) and the mesophase and (b) energy loss from mesophase by mass transfer (vaporization and pyrolysis gases) and conduction into the solid. The chemical processes, shown on the right-hand side of Figure 2, include: (a) the thermal degradation of the polymer in a thin surface layer (the mesophase), as a consequence of the physical processes involving energy transport, (b) the mixing of the volatile

pyrolysis products with air by diffusion, and (c) the combustion of the fuel-air mixture in a combustion zone that produces radiant energy over a spectrum of wavelengths including the visible spectrum. The combustion zone is bounded by a fuel-rich region on the inside and a fuel-lean region on the outside.

The consequences of polymers combustion in terms of fire hazard and risks can be described for representing a model scenario. To this purpose, the fire development in an enclosure (for example, a room, a train compartment, etc.) is described in terms of the temperature development in the compartment, as reported in Figure 3 [3,9,11].

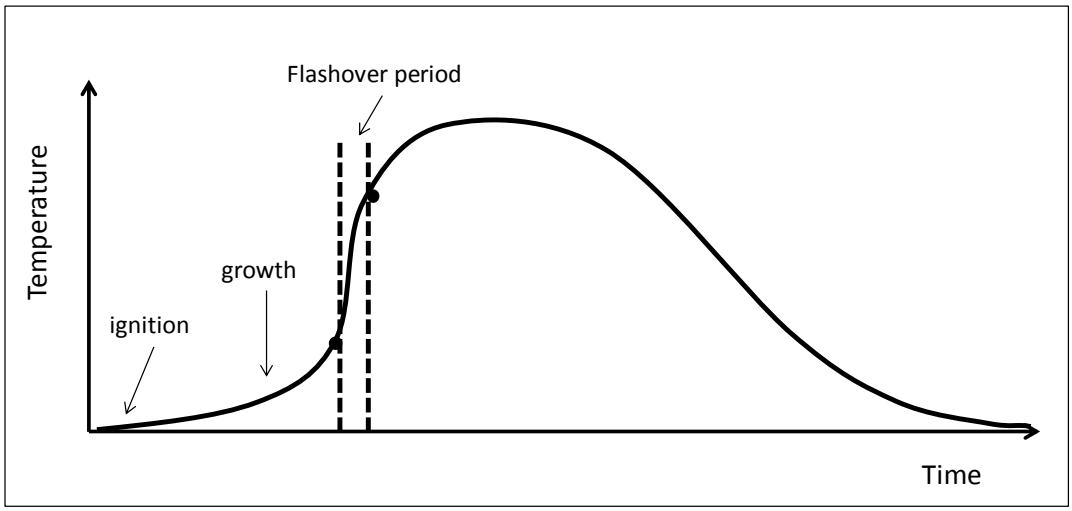

Figure 3 Enclosure fire development in terms of gas temperatures

Different steps can be identified [3]:

- *Ignition.* Ignition can be considered as a process that produces an exothermic reaction characterized by an increase in temperature greatly above the ambient. The accompanying combustion process can be either flaming combustion or smouldering combustion.
- *Growth.* Following ignition, the fire may grow at a slow or a fast rate, depending on the type of combustion, the type of fuel, the interaction with the surroundings, and the access to oxygen. The fire can be described in terms of the rate of energy released and the production of combustion gases. A smouldering fire can produce hazardous amounts of toxic gases, while the energy release rate may be relatively low. The growth period of such a fire may be very long, and it may die out before subsequent stages are reached. The growth stage can also occur very rapidly, especially with flaming combustion, according to which the fuel is flammable enough to allow rapid flame spread over its surface, where heat flux from the

first burning fuel package is sufficient to ignite adjacent fuel packages, and where sufficient oxygen and fuel are available for rapid fire growth. Fires with sufficient oxygen available for combustion are classified as fuel-controlled.

- *Flashover*. Flashover is the transition from the growth period to the fully developed stage in fire development. In fire safety engineering, the word is used as the demarcation point between two stages of a compartment fire, i.e., pre-flashover and post-flashover. Flashover is not a precise term: indeed, several variations in its definition can be found in the literature. The given criteria usually demands that the temperature in the compartment has reached 500–600°C, or that the radiation to the floor of the compartment is 15 to 20 kW/m^2.
- *Fully developed fire.* At this stage the energy released in the enclosure is at its greatest and is very often limited by the availability of oxygen. This is called ventilation-controlled burning (as opposed to fuel-controlled burning), since the oxygen needed for the combustion is assumed to enter through the openings. In ventilation-controlled fires, unburned gases can collect at the ceiling level, and as these gases leave through the openings, they burn, causing flames to stick out through the openings. The average gas temperature in the enclosure during this stage is often very high, within 700 and 1200°C.
- *Decay.* As the fuel becomes consumed, the energy release rate diminishes and thus the average gas temperature in the compartment declines. The fire may go from ventilation-controlled to fuel-controlled in this period.

The reduction of fire hazard and risks related to plastics burning represents a goal continuously pursued by industries, governments (e.g. by evolving regulations) and scientists from several disciplines (material and chemical experts, physics, fire safety engineers, etc.). Fire hazard and risks related to the use of combustible plastic are due to a combination of factors including flammability of the polymeric material related to material properties and characteristics (i.e. intrinsic factors such as thermal stability, heat capacity, etc), as well as to the fire scenario (i.e. extrinsic factors such as the shape of burning objects, orientation, ventilation conditions, etc.).

The combination of intrinsic and extrinsic factors determines the fire characteristics for a specific scenario: amount of heat released on burning, rate of heat release, flame spread, smoke obscuration and evolved volatiles toxicity.

2.3 Flame retardancy of polymeric materials

There are general mechanisms of action applicable to various classes of flame retardants. Usually, two kinds of flame retardants can be identified: gas-phase-active and condensed-phase-active. Gas-phase-active flame retardants provide their main activity by scavenging free radicals responsible for the branching of radical chain reactions in the flame, as shown in Figure 4 [3]. This is the chemical mechanism of action in the gas phase.

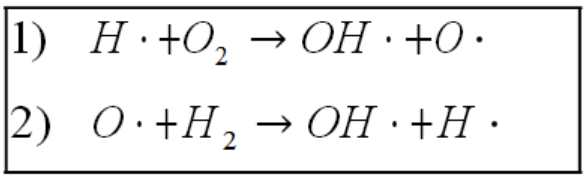

Figure 4 Branching chain reactions in the flame

Some other flame retardants generate large amounts of non-combustible gases, which dilute flammable gases, sometimes dissociate endothermically and decrease the temperature by absorbing heat. This slows down the combustion and eventually may result in flame extinguishment. This is the physical mechanism of action in the gas phase.

Condensed-phase mechanisms of action are more numerous than the gas-phase ones. Charring is the most common condensed- phase mode of action. Charring could be promoted either by chemical interaction of the flame retardant and the polymer or by physical retention of the polymer in the condensed-phase. Intumescent flame retardant, upon heating, build up a multicellular carbonaceous structure that acts as a barrier to heat and mass transfer between the surface of the polymer and the flame [3,15].

Charring can be also promoted by catalysis of oxidative dehydrogenation. [3,16-19]

Some flame retardants show almost exclusively a physical mode of action. Examples are aluminium hydroxide and magnesium hydroxide. On the other hand, there is no single flame retardant that will operate exclusively through a chemical mode of action. Chemical mechanisms are always accompanied by one or several physical mechanisms, most commonly endothermic dissociation or dilution of fuel. Combinations of several mechanisms can often be synergistic.

2.4 Halogen-free flame retardants

Flame retardants are used to retard or to stop the process of polymer combustion [20-27]. Flame retardant systems are intended to inhibit or to stop the polymer combustion process described in the previous paragraphs. According to their nature, flame retardant systems can either act physically (by cooling, formation of a protective layer or fuel dilution) or chemically (reaction in the condensed or gas phase) [20].

- *Physical action*. The endothermic decomposition of some flame retardant additives induces a temperature decrease by heat consumption. This involves some cooling of the reaction medium down below the polymer combustion temperature. In this category, hydrated tri-alumina or magnesium hydroxide, which start liberating water vapour at approximately 200 and 300 °C, respectively, can be mentioned. Such a marked endothermic reaction is known to act as a ‘‘heat sink’’. When the flame retardants decompose with the formation of inert gases (H_2O, CO_2, NH_3, etc.), the combustible gas mixture is diluted, hence limiting the concentration of reagents and the possibility of ignition. In addition, some flame retardant additives lead to the formation of a protective solid or gaseous layer between the gaseous phase where combustion occurs and the solid phase where thermal degradation takes place. Such a protective layer limits the transfer of matter like combustible volatile gases and oxygen. As a result, the amount of decomposition gases produced is significantly decreased. Furthermore, the fuel gases can be physically separated from the oxygen, which prevents the combustion process being sustained [20].
- *Chemical action.* Flame retardancy through chemical modification of the fire process can occur in either gaseous or condensed phase. The free-radical mechanism of the combustion process can be stopped by the incorporation of flame retardant additives that preferentially release specific radicals (e.g. Cl· and Br·) in the gas phase. These radicals can react with highly reactive species (such as H· and OH·) to form less reactive or even inert molecules. This modification of the combustion reaction pathway leads to an important decrease in the exothermicity of the reaction, and consequently to a decrease in temperature and to a reduction in the fuel produced. In the condensed phase, two types of chemical reactions triggered by flame retardants are possible: first, the flame retardants can accelerate the rupture of the polymer chains. In this case, the

polymer drips and thus moves away from the flame action zone. Alternatively, the flame retardant can cause the formation of a carbonized (perhaps also expanded) or vitreous layer at the surface of the polymer by chemical transformation of the degrading polymer chains. This char or vitrified layer acts as a physical insulating layer between the gas phase and the condensed phase.

Flame retardants can be classified into two main categories [3]:

- *Additive flame retardants*: these are generally incorporated during the transformation process and do not react at this stage with the polymer but only at higher temperature, at the start of a fire; they are usually mineral fillers, hybrids or organic compounds, which can include macromolecules.
- *Reactive flame retardants*: unlike additive flame retardants, these are usually added to the polymer during its synthesis (as monomers or precursor polymers) or in a post-reaction process (e.g. via chemical grafting). These flame retardants are integrated in the polymer chains.

Traditionally, halogen-containing compounds have been highly used due to their effectiveness in reducing the heat release rate of commodities. However, the halogenated flame retardants have been the focus of public scrutiny since they are usually toxic or carcinogenic. The environmental impact of the processing and combustion of certain halogenated flame retardants, which are persistent and easily bio-accumulative, has also become an issue in Europe. Therefore, the market is orienting itself to a progressive phase-out of halogen containing polymers, pushing the industrial sector to develop highly effective halogen-free flame retardants capable to replace halogen flame retardants as well as halogen containing polymer (i.e. Polyvinylchloride – PVC) in a number of applications.

There are several possible alternatives to halogenated flame retardant, like the use of aluminum hydroxide or magnesium hydroxide. They are relatively cheap, easy to obtain, in addition are non toxic and environmentally friendly. However, high loadings are necessary in order to obtain flame retardancy: this gives a negative effect on the mechanical properties of the filled material. [28]

Flame retardants based on chemicals containing phosphorus and nitrogen have also been developed and proved their environmental benefits [9, 12,13,29]. One example is the melamine polyphosphate, which is usually used in combination with other flame

retardants, such as metal phosphinates, metal hydroxides and phosphates. Melamine polyphosphate presents good thermal stability and a small impact on the glass transition temperature. It acts decomposing endothermically and giving rise to the formation of inert nitrogen gases that dilute oxygen and the flammable gases in the flame. In addition, phosphoric acid is commonly formed as a decomposition product and promotes the formation of insulating char on the surface of the polymer.[28]

Phosphorus flame retardants are considered environmentally friendly, and during the past few years red phosphorus, and organic phosphinic acid salts have grown on the flame retardant market. They have become established flame retardants for polyamides, thermoplastic polyethers and polyesthers, certain thermosets, and some additional niche applications. Red phosphorus, for instance, is considered nontoxic, non-spontaneously flammable, and its thermal stability can reach 450 °C. Some of the drawbacks of red phosphorus include its reaction with moisture to form toxic phosphine gases; furthermore, and red phosphorus-containing products are limited to be brown and red due to its inherent colour.[28]

In general, organic and inorganic Phosphorus flame retardants (FRs) are not detrimental and do not contribute to the formation of toxic gases. These findings can be justified as these flame retardants, during a thermal stress, act in the gas phase forming a considerable amount of phosphorus containing radicals and gases that oxidise to P_2O_5 and then to polyphosphoric acid. This latter acts as a carbonaceous char former. [28]

The phosphinate-based FRs are mainly used to achieve a V-0 classification according to the UL 94 test. The required loading depends on several parameters, such as the type of polymer or blend, thickness of material, glass-fiber content, and flame retardant grade used. In contrast to other halogen-free FRs, such as melamine cyanurate or red phosphorus, the phosphinate-based systems can be used at nearly all glass levels and with non-reinforced polymers as well [29].

2.5 Electrical conductivity of polymers: properties, performance and applications

Nowadays, the European demand of polymers is growing in terms of both volume and performance. In particular, the market segment of electrical and electronics represents 6% on the overall plastic industry in Europe [30], as shown in Figure 5:

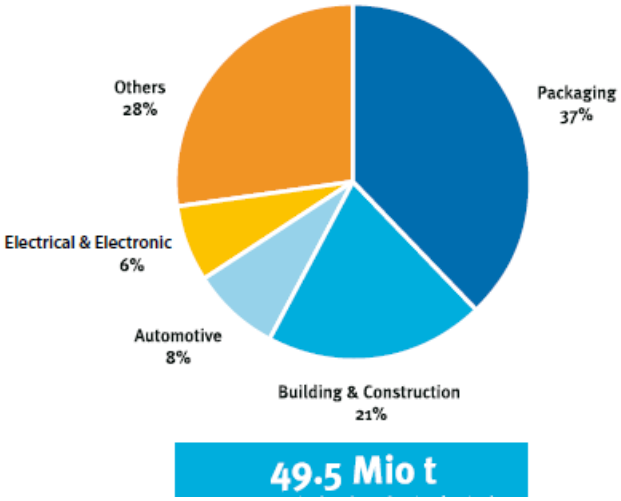

Figure 5: Demand by End Use Segment (Source : Association of Plastics Manufactures Europe)

The effects of electromagnetic interference are becoming more and more pronounced, caused by the demand for high-speed electronic devices operating at higher frequencies, the more intensive use of electronics in e.g. computers, communication equipment and cars, and the miniaturisation of these electronics. As an example, mobile phones and smartphones are typically operating at 800-1900 MHz, and around 2 GHz for data transmission through Universal Mobile Telecommunications Systems (UMTS). Compact, densely packed electronic components produce more electronic noise. The market of electrically conductive polymer composites is growing: in particular, the global demand for EMI/RFI shielding options is expected to increase to $5.2 billion by 2016, a projected compound annual growth rate of 2.8%.[31]

Electrically conductive polymeric composites are intrinsically nonconductive polymers loaded with conductive fillers like carbon black, carbon nanotubes, graphite fibers, metal particles, or metal oxide particles [20,32-47]. Polymers containing electrically conductive fillers show interesting electrical properties like semiconductors and metals without losing the processability of polymers. Filled polymers have the longest history and broadest application in electronic devices. Typical applications are as antistatic (electrostatic dissipation) materials, electromagnetic interference shielding materials, heaters and sensors. The extensive use of these materials lies in their ease of processing, wide range of electrical properties, and relatively low cost [20].

Electrically conductive polymer composites of our interest can be roughly divided into two categories according to their conductivity and application [41,42]:

- *Low conductivity region*, electrical resistivity 10^6-10^{11} Ω.cm, mainly for

antistatic properties for preventing dust attraction on TV-cabinets, etc.

- *Semiconducting/conducting region*, electrical resistivity 10^2-10^4 Ω.cm, for electromagnetic interference (EMI) shielding of electronic devices and prevention of static electricity hazards in the handling of electronic chips and explosives (electrostatic discharge, ESD), or for semiconducting layers to maintain the surface of high voltage cable insulation at a uniform potential (otherwise ionization occurs resulting in breakdown of the insulating polymer).

When a sufficient amount of filler is loaded, a ‘‘percolation’’ path of connected fillers forms and allows charge transport through the sample. At this critical concentration, called the percolation threshold, the conductivity suddenly and rapidly increases. [48] It is worthy to note that for predicting the electronic properties of nanocomposites, tunnelling effect has to be taken into consideration. This phenomenon shows that for electrical conduction between particles no direct contact is needed since statistical electrons jump of facing surfaces may occur. [49]

The conductivities and percolation thresholds of conducting polymeric composites strongly depend on the morphology and the compatibility between the insulating polymer matrix and the conductive filler. [50] The intrinsic properties of the filler and polymer matrix, including particle shape, orientation, aspect ratio, distribution and dispersion in the polymer matrix, have also turned out to contribute to the electrical conductivity of the resulting polymer composite. [51,52] At a low filler concentration, the fillers are present as small clusters or individual elements. When the average distance between the filler elements exceeds their size, the conductivity of the nanocomposite is very close to that of the pure insulating matrix. [48]

Carbon Nanotubes (CNTs) are an attractive filler used in polymer matrices for improving their electrical conductivity. CNTs belong to the fullerene family, and they are cylinders formed by concentrically rolled grapheme layers. The type of CNT depends on the number of concentric cylinders sheets. They can be classified as single-walled carbon nanotubes (SWCNTs), double-walled carbon nanotubes (DWCNTs) or multi-walled carbon nanotubes (MWCNTs) [53,54] as shown in Figure 6.

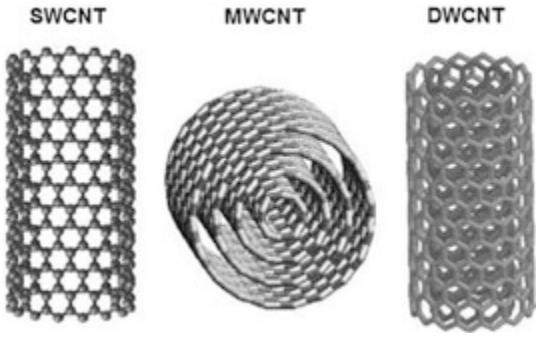

Figure 6: Different types of CNTs—based on the number of tube walls. Reprinted from [53], Copyright (2003)

CNTs are typically of a few nanometers in diameter and microns in length. CNTs possess an excellent electrical conductivity (10^5–10^8 S/m), combined with a high aspect ratio (reaching 100–1000 for μm-long single-wall and multi-wall CNTs) [48].

The intrinsic properties of the CNTs depend on the way their graphene sheets are rolled, the type of CNT and their individual geometric dimensions. The rolling up of the graphene sheets and hence the atomic structure of the CNTs is well defined by tube chirality. The chirality, which gives the electronic conduction of the CNTs, is given by the chiral vector and gives rise to three possible orientation forms for the carbon atoms of the CNTs: armchair, zigzag, and chiral structures. In the case of MWCNTs, the chirality is very complex since each of the concentric nanotubes walls can show different chiralities. [48,53]

SWCNTs have higher electrical conductivity than MWCNTs, with an order of 10^4 to 10^8 S/m and 10^5 to 10^7 S/m, respectively. However, purified SWCNTs are significantly more expensive than MWCNTs due to the high cost needed to purify SWCNTs.[53]

Electrically conductive composites can be obtained starting at 2wt% addition of CNTs, which have an excellent dispersability leading to a quite homogeneous dispersion.[55] Conductive polymer composites with a fixed CNTs content can display very different conductivity values depending on different processing conditions. For instance, higher conductivity and lower percolation thresholds are found for low viscosity rather than simple melt compounding of thermoplastics, and for processes involving high temperatures and long times (e.g. compression molding).[56]

2.6 Multifunctional materials: a brief introduction

Materials with multifunctional properties can be designed in order to guarantee the

integration of different properties (electrical, magnetic, optical features). The integration of more than one function impacts their structural performance by reducing size, weight, cost, power consumption, and complexity, while improving efficiency, safety, and versatility. The synergism between the various elements contributes to these functionalities and may be achieved while keeping the structural integrity of the overall material. [53,57]

In this work, a new class of bi-functional polymeric composites, which is capable of satisfying the requirements of fire safety polymers, bio-based polymers and EMS shielding, thus delivering high added value materials to meet demanding applications and providing easy to process multifunctional class of products, is thoroughly developed. The bi-functionality derives from the combination of thermal and electrical properties. Therefore, the introduction of electrical conductive fillers and flame retardants additives into the same polymeric material is implemented in this work to achieve the requirements mentioned above.

2.7 Synergistic effect of electrically conductive fillers and flame retardants

When developing or optimizing new formulations through the combination of additives, it is important to take into consideration the concepts of addition, synergism, and antagonism. The *additive effect* is considered as the sum of the effects of the individual actions. The *synergistic effect* can be achieved when the performance of the additive mixtures is greater than that predicted from the linear combination of the single effects of each additive. On the other hand, when the performance of the additives mixtures is lower, it is defined as an *antagonistic effect*. [20,58-60]

Flame retardants synergistic systems are important because they are less expensive with respect to the use of individual flame retardants.[59] In addition, when applied to polymers, they can reduce the loss on other properties, such as the mechanical features [20,58-61]. Therefore, it is better to use synergistic agents (or additives) in the system in order to reduce the amount of flame retardant as much as possible.[58,61]

The synergism of flame retardants systems can be achieved in two ways: (i) by combining the flame retardancy mechanisms (e.g. char formation by a Phosphorated flame retardant combined with a gas phase action by a halogenated flame retardant); or (ii) by combining flame retardant agents reinforcing the same mechanism (e.g., using Nanoclays and Phosphorated flame retardant agents, which both act in the condensed

phase).[20]

Apart from the synergism between flame retardants, the synergism between flame retardants and nanofillers may be interesting to this work, as less amount of fillers and additives could be used to reach the desired performance, while preserving the composite mechanical properties. An example already reported in the literature is the synergistic effect between carbon nanotubes and phosphorous compounds, which showed a considerable effect on reduction of heat release rate and on delaying the time to ignition.[62]

2.8 References

[1] S.V. Kailas. Material Science. Chapter 11. "Applications and Processing of Polymers". Dept. of Mechanical Engineering, Indian Institute of Science, Bangalore, India.

[2] G.L. Nelson in "Fire retardancy of polymeric materials", eds. A.F. Grant, C.A. Wilkie, Marcel Dekker, New York: 2000, 1-26.

[3] A. Castrovinci (2007). "Intrinsic properties and Combustion Behaviour of Polymeric Materials". Ph.D. Thesis. Politecnico di Torino: Italy.

[4] J.H. Troitzsch in "Plastics Flammability Handbook", eds. J. Troitzsch, Hanser Publishers, Munich: 2004.

[5] Twenty-Fifth Symposium (International) on Combustion- The Combustion Institute, 1994/pp,1423-1437. Invited Topical Review Polymer Combustion And Flammability-Role of The Condensed Phase. Takashi Kashiwagi, Building and Fire Research Laboratory, National Institute of Standards and Technology. Gaithersburg, MD 20899, USA]

[6] DOT/FAA/AR-05/14 Office of Aviation Research. Washington, D.C. 20591. Polymer Flammability . May 2005. Final Report . This document is available to the U.S. public through the National Technical Information Service (NTIS), Springfield, Virginia 22161. U.S. Department of Transportation Federal Aviation Administration.

[7] T.R. Hull, R.J. Law, Ake Bergman. "Polymer Green Flame Retardants. Constantine" D. Papaspyrides, Pantelis Kiliaris, editors. Chapter 4: Environmental Drives for replacement of halogenated Flame retardants. Elsevier: 2014.

[8] D. Drysdale in "An Introduction to Fire Dynamics", Wiley and Sons, New York: 2002.

[9] G. Pál, H. Macskásy in “Plastics, their behaviour in fires”, Elsevier, Amserdam: 1991.

[10] M.A. Hirschler in “Fire retardancy of polymeric materials”, eds. A.F. Grant, C.A. Wilkie, Marcel Dekker, New York: 2000, 27-79.

[11] B. Karlsson, G. Quintiere in “Enclosure fire dynamics”, CRC Press LLC, US, 2000.

[12] D. Price, G. Anthony, P. Carty in “Fire Retardant materials”, eds. A. R. Horrocks, D. Price, Woodhead Publishing Limited, Cambridge: 2000, 1-30.

[13] R.E. Lyon and M. Janssens, “Polymer flammability”, U.S. Government Final Report number DOT/FAA/AR-05/14, 2005.

[14] D. Drysdale in “Fire Retardant materials”, eds. A. R. Horrocks, D. Price, Woodhead Publishing Limited, Cambridge: 2000, 378-397.

[15] M. Lewin in “Fire Retardancy of polymers: the use of intumescence”, eds. M. Le Bras, G. Camino, S. Bourbigot, R. Delobel, The Royal Society of Chemistry, Cambridge, 1998, 3-32.

[16] S. Cheng, “From layer compounds to catalytic materials”. Catalysis Today 49 (1999), 303-312.

[17] A. Marcilla, A. Gómez, S. Menargues, R. Ruiz, “Pyrolysis of polymers in the presence of a commercial clay”. Polymer Degradation and Stability 88 (2005), 456-460.

[18] K. Gobin, G. Manos, “Polymer degradation to fuels over microporous catalysts as a novel tertiary plastic recycling method”. Polym. Deg. Stab. 83 (2004), 267-279.

[19] K. Gobin, G. Manos. Polymer Degradation and Stability 86 (2004), 225-231.

[20] F. Laoutid, L. Bonnaud, M. Alexandre, J.-M. Lopez-Cuesta, Ph. Dubois, “New prospects in flame retardant polymer materials: From fundamentals to nanocomposites”, Materials Science & Engineering: R 63 (2009), 100-125.

[21] US 2009/0048377 A1 – Flame Retardant Resin Processed Article.

[22] US 4877823 – Fireproofed Thermoplastic Molding Materials Containing Red Phosphorus and Based on Polyesters or Polyamides.

[23] WO 2003/066723 A2 – Flame Retardant Thermoplastic Polyurethane Containing Melamine Cyanurate.

[24] EP 1640411 B1 – Reactive Flame Retardants And Flame-Retarded Resin Products.

[25] US 2006/01679148 A1 – Flame Retardant Thermoplastic Article.

[26] US 7608651 B2– Flame Retardant Thermoplastic Article.

[27] US 4500748 – Flame Retardant Electrical Cable

[28] M. Rakotomalala, S. Wagner and M. Döring. “Review: Recent developments in Halogen free flame retardants for epoxy resins for electrical and electronic applications”. Materials 3 (2010), 4300-4327.

[29] T. Kuang-Chung, D. Drysdale, “Using cone calorimeter data for the prediction of fire hazard”. Fire Safety Journal 37 (2002), 697–706

[30] Polymer innovation program- Dutch Polymer Institute.

[31] EMI/RFI: Materials and technologies, BCC Research April 1, 2011.

[32] S. Hamdani, C. Longuet, D. Perrin, “Flame retardancy of silicone-based materials”. Polymer Degradation and Stability 94 (2009), 465-495.

[33] W.C. Zhang, X.M. Li, X.Y. Guo, “Mechanical and thermal properties and flame retardancy of phosphorus containing polyhedral oligomeric silsesquioxane (DOPO-POSS)/polycarbonate composites”. Polymer Degradation and Stability 95 (2010), 2541-2546.

[34] A. Beard and T. Marzi, “New phosphorus based flame retardants for E&E applications: A case study on their environmental profile in view of European legislation on chemicals and end-of-life (REACH, WEEE, RoHS)”, Addcon 2005.

[35] E.K. Sichel, “Carbon black-polymer composites”. Marcel Dekker, New York: 1982.

[36] J.M. Margolis, “Conductive polymers and plastics”. Chapman and Hall, New York: 1989.

[37] R.H. Norman, “Conductive rubbers and plastics”. Elsevier, Amsterdam: 1970.

[38] S.K. Bhattacharya, “Metal-filled polymers: Properties and applications”. Marcel Dekker, Inc., New York: 1986.

[39] W.M. Wright and G.W. Woodham, ”Conductive polymers and plastics” in J.M. Margolis, ed. Chapman and Hall, New York: 1989.

[40] K.M. Jager, D.H. McQueen, I.A. Tchmutin, N.G. Ryvkina, M. Kluppel, “Electron transport and ac electrical properties of carbon black polymer composites”. Journal of Physics D: Applied Physics 34 (2001), 2699.

[41] C. Klason, D.H. McQueen, J. Kubat, Macromol. Symp. 108 (1996) 247-260

[42] X.S. Yi, G. Wu and Y. Pan, “Properties and applications of filled conductive polymer composites”. Polymer International 44 (1997), 117–124.

[43] A. Rybak, G. Boiteux, F. Melis, “Conductive polymer composites based on

metallic nanofiller as smart materials for current limiting devices". Composites Science and Technology 70 (2010), 410-416.

[44] B.H. Cipriano, A.K. Kota, A.L. Gershon, "Conductivity enhancement of carbon nanotube and nanofiber-based polymer nanocomposites by melt annealing". Polymer 49 (2008), 4846-4851.

[45] D. Kumar and R.C. Sharma, "Advances in conductive polymers". European Polymer Journal 34 (1998), 1053-1060.

[46] M. Kohan, S. Mestemacher, R.U. Pagilagan, "Polyamides". Ullmann's Encyclopedia of Industrial Chemistry, 2003.

[47] R. Sengupta, M. Bhattacharya, S. Bandyopadhyay, A.K. Bhowmicka, "A review on the mechanical and electrical properties of graphite and modified graphite reinforced polymer composites". Progress in Polymer Science 36 (2011), n.5, 638-670.

[48] N. Grossiord, J. Loos, L. van Laake, M. Maugey, C. Zakri, C.E. Koning, and J. Hart, "High-conductivity polymer nanocomposites obtained by tailoring the characteristics of carbon nanotube fillers". Advanced Functional Materials 18 (2008), 3226–3234.

[49] N. Hu1, Z. Masuda and H. Fukunaga, "electrical properties of a carbon nanotube/polymer nanocomposite and its application as highly sensitive strain sensors". Department of Aerospace Engineering, Tohoku University, Japan.

[50] R. Zhang (2009), "Conductive TPU/CNT composites for strain sensing". PhD thesis. Queen Mary, University of London, United Kingdom.

[51] H.S. Gokturk, T.J. Fiske, D.M. Kalyon, "Effects of particle shape and size distribution on the electrical and magnetic properties of nickel/polyethylene composites". Journal of Applied Polymer Science. 50 (1993), 1891-1901.

[52] K. Kalaitzidou , H. Fukushima and L.T. Drzal, "A route for polymer nanocomposites with engineered electrical conductivity and percolation threshold". Materials 3 (2010), 1089-1103.

[53] S. Sathyanarayana and C. Hübner, "Thermoplastic nanocomposites with carbon nanotubes". J. Njuguna (ed.), Structural Nanocomposites, Engineering Materials, Springer-Verlag Berlin Heidelberg: 2013.

[54] X. Marino, "Funcional Fillers for Plastics". Chapter 10: Carbon nanotubes/nanofibers and carbon fibers. Ed Wiley. Second Edition: 2010.

[55] A.M.F. Lima, V.G. de Castro, R.S. Borges, G.G. Silva, "Electrical conductivity and thermal properties of functionalized carbon nanotubes/polyurethane composites".

Polímeros 22 (2012), n. 2, 117-124.

[56] E. Bilotti, R. Zhang, H. Deng, M. Baxendale and T. Peijs, “Fabrication and property prediction of conductive and strain sensing TPU/CNT nanocomposite fibres”. Journal of Materials Chemistry, 2010.

[57] S. Nemat-Nasser, S. Nemat-Nasser, T. Plaisted, A. Starr, and A. Vakil Amirkhizi. Chapter 12: Multifunctional materials. Biomimetics: Biologically inspired technologies. Edited by Yoseph Bar-Cohen. CRC Press (2005).

[58] D.M. Marquis, E.G. and C. Chivas-Joly. “Properties of nanofillers in polymer”. In: Nanocomposites and polymers with analytical methods. Edited by Dr. John Cuppoletti (2011), 261-284. Laboratoire national de métrologie et d’essais (LNE) France.

[59] N.H. Huang, Z.J. Chen, C.H. Yi, J.Q. Wang, “Synergistic flame retardant effects between sepiolite and magnesium hydroxide in ethylene-vinyl acetate (EVA) matrix”. eXPRESS Polymer Letters 4 (2010), n. 4, 227–233.

[60] J. H. Troitzsch, “Overview of flame retardants. Fore and fire safety, markets and application, mode of action and main families, role in fire gases and residues”. Chimica Oggi/ Chemistry Today 16 (1998).

[61] E. Kandare, G. Chigwada, D. Wang, Charles A. Wilkie, J. M. Hossenlopp, “Probing synergism, antagonism, and additive effects in poly(vinyl ester) (PVE) composites with fire retardants”. Polymer Degradation and Stability 91 (2006), n. 6, 1209-1218.

[62] D. Wesolek and W. Gieparda, “Single- and multiwalled carbon nanotubes with phosphorus based flame retardants for textiles”. Journal of Nanomaterials 2014 (2014), Article ID 727494, 6 pages.

3 Experimental

3.1 Introduction

The experimental activities are divided into the following tasks: (a) materials pre-selection, (b) design of experiment (DOE), (c) materials compounding, (d) specimens preparation (injection moulding), (e) materials characterisation (electrical resistivity tests, flammability tests, and microstructure analysis).

Each task will be described in detail in the following sections.

3.2 Materials pre-selection

In the first step, the materials (flame retardants and electrically conductive additives) to be used for developing this novel formulation, were pre-selected based mainly on bibliographical studies. The creation of a database was essential to identify important commercial available additives to be used in the final formulation, like, for instance, (i) high efficient organic and inorganic phosphinates for improving the flame retardant properties; and (ii) conductive fillers to improve the electrical conductivity properties.

The database consisted of 37 materials organised by material manufacturer, product name, aggregation state, chemical structure, and a brief description of the material features as shown in Annex 1.

This database was constructed with the following materials selection criteria:

(a) guarantee the best processability of the polymeric-based matrices,

(b) address synergistic combinations of different flame retardants, promoting chemical interactions among the chemical systems on heating before ignition, particularly promoting both condensed phase actions, such as the rapid formation of a protective shield on the surface of the polymeric material (e.g. glass forming/ceramic forming chemical systems) and gas-phase actions (release of radical quenchers such as P×, PO×, etc.),

(c) combine conductive nano- and micro- fillers addressing the percolation thresholds,

(d) explore the potential synergisms between conductive nano- and micro- fillers with flame retardants, to maximise their effectiveness

(e) address the preservation/enhancement of the mechanical properties.

Then, economic aspects and fundamental know-how of these materials were considered, thus reducing the number of material candidates from 37 to 16. The remaining 16 material candidates and their contributions in the formulation are described in Section 3.2.1.

After evaluating the economic aspects and previous fundamental know-how, preliminary compounding tests were carried out with the remaining 16 material candidates in order to assess their processability. Based on the results of these preliminary compounding tests and the partner company (SIPsa) practical decisions, the number of material candidates was reduced even more from 16 to 13. The preliminary compounding tests are described in Section 3.2.2.

3.2.1 Materials description and contribution in the formulation

3.2.1.1 Bio-based TPU

TPU is a synthetic polymer with exceptional properties. It is an elastomeric linear segmented block copolymer having a hard and a soft segment. The soft segment consists of long flexible polyether or polyester chains (long chain diols- polyols), which interconnect two hard segments (short chain diols). [1,2] The hard segments behave as multifunctional tie points acting both as physical crosslinks and reinforcing fillers. The soft segments give the TPU elastic properties and offer new possibilities on tuning the polymeric matrix properties, but they give to the TPU some inconveniencies such as weak mechanical and gas barrier properties. These drawbacks (especially for the TPU with low hard segment content) can be overcome with the addition of nanofillers allowing its use in several applications like injection moulded products, coatings, adhesives, fire-retardants, packaging materials, etc. [1,2]

Bio-based polymers are renewable materials, which offer potential possibilities for chemical recycling [3]. They have already found extensive use in the packaging sector and new applications are increasingly emerging in other engineering fields in an effort to move away from petrochemical raw materials. Therefore, a positive trend related to the bio-based polymers can be observed. As a consequence, compounders have interest in developing novel products based on a bio-based polymeric matrix.

This is the case of the ELYSA project, which supports this work and shares some scientific and technical objectives, like, in particular, the development of a new electrically-conductive flame-retarded material using a bio-based TPU polymeric matrix, due to the progressive introduction of bio-based TPU polymers targeting high

performance applications.

The selected commercial bio-based TPUs was Pearlthane®Eco D12T80 from Merquinsa (now Lubrizol), which is a TPU based on renewable sources with ca. 42% renewable content according to ASTM D6866. According to the supplier of Pearlthane® Eco, the polyols segments derive from vegetable oils and fatty acids (Figure 7).

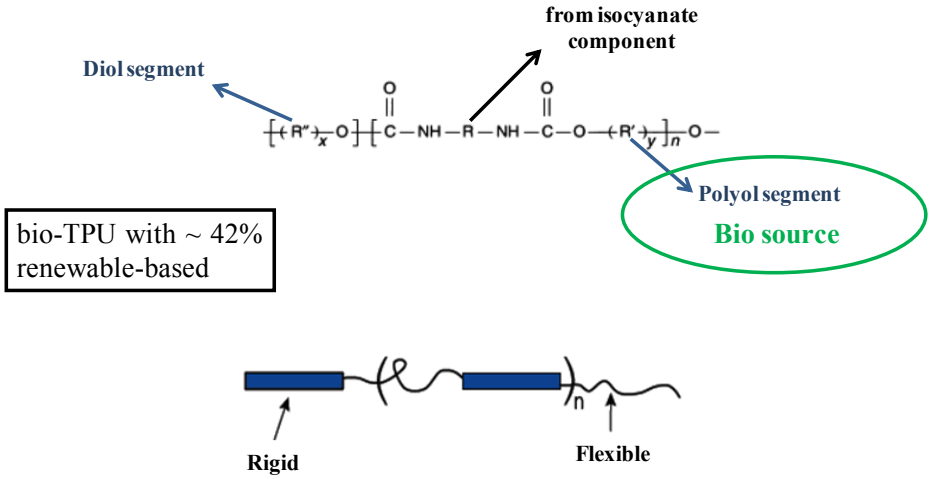

Fig 7. Short-chain diols and long chain diols (polyols) of a TPUs

The selection of Pearlthane®Eco was supported by its hardness, elongation at break and abrasion loss values (Table 1), which could give excellent mechanical properties to the final formulation. In addition, this TPU is a suitable material for extrusion and injection moulding applications.

Property	Value
Density at 20ºC (g/cm^3)	1.10
Shore Hardness (ShA)	82
Tensile Strength (MPa)	33
Abrasion Loss (mm^3)	20
Elongation at Break (%)	604
Melting Temperature Range (°C)	167-177

Table 1: Feature properties of Pearlthane® Eco (42% renewable-soft segment)

3.2.1.2 Flame retardants and synergists

3.2.1.2.1 Pre-selected Halogen-Free Flame retardant

According to the background information described in Chapter 2, phosphorous-based components were selected as the main flame retardant family to be used in the

development of this novel electrically-conductive flame retardant TPU composite.

Phosphorus-based flame retardants are significantly more effective in oxygen- or nitrogen-containing polymers. It is thus important to have oxygen or nitrogen atoms in the polymer chain: hence, polyurethanes can contribute as charring agents in intumescent flame retardant systems. [4]

The number of commercial organic phosphorus derivatives is limited by the processing temperature and the nature of the polymer to be modified. The organic phosphorus derivatives can act as additives or as reactive (co)monomers/oligomers. The main groups of organophosphorus compounds are phosphinates, phosphate esters, and phosphonates.[4]

The use of organic phosphinates in TPU has been already reported in the literature, showing that the addition of aluminium phosphinate successfully reduced the melt-dripping and enhanced flame retardancy of TPU matrix.[5] Therefore, the selection of a commercially available aluminium phosphinates, was considered in this work. In addition, an inorganic phosphinate salt was also chosen for comparing the efficiency of organic and inorganic phosphinates in the formulation.

For plastics engineering, oligomeric phosphates like resorcinol bis(diphenyl phosphate) (RDP) and bisphenol A bis(diphenyl phosphate) (BDP), with lower volatility and higher thermal stability than triaryl phosphates, can be incorporated in some polymers to provide also UL 94 V0 rate [4]. Therefore, they were considered as potential flame retardant candidate for the development of this work.

The use of polyphosphonate homopolymers or copolymers in flame retardant TPUs compositions to achieve UL94 V0 ratings, was also mentioned in a patent [6]. This information suggested to consider the use of polyphosphonate homopolymers for the development of the novel formulation.

Ammonium polyphosphate (APP), an inorganic salt of polyphosphoric acid and ammonia, is known to be an additive which can induce the formation of intumescent char in oxygen- and/or nitrogen-containing polymers thermoplastic materials [4,7]. The effectiveness of APP depends also on the level of incorporation: indeed, it is more efficient at high concentration, e.g. >10wt%. The literature mentions that TPUs containing ammonium polyphosphate could be a more effective flame retardant in the presence of a synergistic co-additive [7]. Therefore, it was thought that ammonium polyphosphate could be used in combination with other flame retardants to get synergistic interactions leading to better performance than it would have been achieved

with any individual flame retardant additive.

In addition, based on the fact that phosphoric acids can act as a char forming agent, thus physically limiting oxygen access and fuel volatilization was also pre-selected as flame retardant additive.

3.2.1.2.2 Pre-selected synergists additives

The addition of a relatively low amount of silicon-based compounds (silicones, silicas, organosilanes, silsesquioxanes and silicates) to polymers has been reported to substantially improve their flame retardancy.[4] Depending on the polymer, silicon-based additives used in combination with phosphorous based additives can generate a synergistic effect in the flame retardancy system.[8] Organic silicon-based flame retardants have the possibility to attach to specific groups, such as phosphorous and nitrogen based, thus improving the flame retardancy. Studies have shown that silicon-based compounds as flame retardants contribute mainly in the formation of a protective layer in the condensed phase. [8] Another relevant characteristic of this additive is that, during fire, it does not release toxic gases. In addition, it can preserve the mechanical properties of the polymer. [8] The commercially available silicon-based systems are limited and mainly in the form of silica and organically-modified montmorillonite. Silicone gum was selected to be combined with others halogen-free flame retardant fillers to improve burning characteristics of the TPU.

Carbon source polymers, such as aromatic polymers, are usually used as flame retardants for underneath polymers, mainly acting in the char formation.[9] The main composition of a char is carbon and hydrogen, therefore less quantity of carbon and hydrogen are released from char-forming materials to the gas phase as combustible gaseous products during the pyrolysis of aromatic polymers. In addition, this carbonaceous protective layer acts as a thermal barrier to the transfer of combustible gases to the gas phase. Furthermore, because the char has a lower thermal conductivity than the polymer, it acts as thermal insulation layer to protect the underneath polymer.[9] Carbon source polymer was also used during the development of this work.

The development of a glassy/ceramic surface layer on polymers represents an important way to produce some efficient flame retarded polymers. [10] Metal borates and particularly zinc borates have frequently been used as synergistic agents in some thermoplastics due to their direct physical flame retardant action. As the temperature

rises, these fillers absorb energy and decompose between 290 and 450 °C liberating water, boric acid and boron oxide (B_2O_3).[4,11] The B_2O_3 formed softens at 350°C and flows above 500°C leading to the formation of a protective vitreous layer. In the case of polymers containing oxygen atoms, the presence of boric acid causes dehydration, leading to the formation of a carbonized layer. This layer protects the polymer from heat and oxygen. The release of combustible gases is thus reduced.[4] Based on this information, zinc borates was selected to be used as ceramic precursor.

It is known that nanofillers added to a polymeric matrix can improve specific features of a polymeric material without sacrificing the melt rheological properties [12,13]: (i) mechanical properties; (ii) thermal stability; (iii) flame retardancy and reduced smoke emissions; (iv) electrical conductivity; etc.

Indeed, effective flame retardancy can be obtained by combining the nanoparticles with conventional flame-retardants like metal hydroxides or phosphorous.[14,15] For instance, nanoclay have been added to flame retardants in a polymeric matrix, significantly contributing to the material flame retardancy and gas barrier properties [16]. The incorporation of a relatively low quantity of (organomodified) nanoclay in the polymer matrix creates a protective layer during combustion.[4] The nanoclay has been used as flame retardant to improve the burning behaviour of TPUs. [17] However, it is worthy to note that the fire behaviour of the polymer depends on the dispersion of nanocomposite fillers in a matrix, therefore fillers should be well dispersed in order to confer flame-retardant properties.[14] Nanofillers were used to improve the flame retardancy of the polymer.

3.2.1.3 Electrically-conductive fillers pre-selection

Three types of electrically conductive fillers were evaluated in this work: *CNTs*, *Carbon black* and *Graphite*.

CNTs are commonly used in many polymeric matrices to improve the electrical conductivity, as mention in Chapter 2. Low amounts of CNTs (e.g. 2wt%) added to polymeric matrix can be enough to exploit the advantage of the CNT properties. The pre-selection of MWCNTs was based mainly on their availability in bulk and their costs. Furthermore, MWCNTs can be used for high volume industrial applications, and at the same time can be well dispersed into thermoplastic polyurethanes. MWCNTs was pre-selected to reach the desired electrical conductivity in the polymeric material.

Carbon black is an amorphous form of carbon with a structure similar to disordered

graphite.[19] It is made up of hollow spheres of partially graphitized carbon, and has a bulk resistivity of about 10^{-3} Ω.cm at room temperature. [20] Carbon black is of special interest because it is characterized by high surface area and high degrees of porosity, which are critical characteristics that impart electrical conductivity at lower loadings in polymer composites. [19-21] Highly conducting carbon black powder was also pre-selected as conductive filler.

Graphite is frequently used as electrical conductive filler for manufacturing high-performance antistatic, thermal and electrical conductivity of plastics articles.[22] In addition, graphite is cheaper as compared to other materials with similar performance, like carbon nanotubes [23,24]. Synthetic graphite was also considered as pre-electrical conductive filler.

As described above, 16 materials were identified as potential pre-selected candidates to be used in the development of the novel electrically conductive flame retarded polymer formulation. Table 2 summarizes these pre-selected materials.

Material Type	Description
Bio-based polymer	Thermoplastic polyurethanes (TPU) (injection moulding and extrusion grades)
Flame Retardants	Organic and inorganic phosphorous systems
	Silicon-based systems
	Carbon sources polymers (e.g. aromatic polymers)
	Ceramic and low melting glass precursors
	Nanofillers (e.g. montmorillonites, POSS, sepiolites, bentonites, etc.)
Electrically Conductive Fillers	Carbon nanotubes (multiwall), carbon fibres

Table 2. Pre-selected materials to be used in development of the electrically conductive halogen-free UL94-V0 bio-based TPUs composite.

3.2.2 Preliminary compounding tests

The pre-selection of the 16 materials, based on the fundamental know-how, was an important step to narrow down the huge list of possible material candidates.

In addition, preliminary compounding tests were also carried out in order to assess the processability of the polymer and additives, before bringing them to next

experimental stage.

Different formulations were compounded using a twin screw extruder type ZSE 18 HP – 40 D from Leistritz, which is described in detail in Section 3.4. The addition of the liquid flame retardants was done using a liquid gravimetric pumper from Brabender Technologie.

The fraction of each component in the formulations was defined on the basis of (i) the information found in the material datasheet; or (ii) previous studies in the literature, which reported the load of the components in TPUs or in thermoplastics in general.

In the first set of preliminary experiments (Preliminary tests 1), the fraction of CNTs (0.03) was kept constant together with TPU (0.85). These components sum a total of 0.88, and five flame retardants count a total fraction of 0.12. The mixed systems with all the formulations are shown in Table 3 and the extrusion parameters used for these laboratory preliminary tests are presented in Table 4.

	A	B	C	D	E	Polymer + 3wt% CNTs
Run 1	0.03	0.03	0.03	0	0.03	0.88
Run 2	0.03	0.03	0	0.03	0.03	0.88
Run 3	0.12	0	0	0	0	0.88
Run 4	0	0	0	0	0.12	0.88
Run 5	0	0.12	0	0	0	0.88
Run 6	0	0	0	0.12	0	0.88
Run 7	0	0	0.12	0	0	0.88

Table 3. Formulations used in the preliminary tests 1

Extrusion Parameters	**Values**
Temperature [°C]- Zone 1	150
Temperature [°C]- Zone 2	210
Temperature [°C]- Zone 3	210
Temperature [°C]- Zone 4	200
Temperature [°C]- Zone 5	200
Temperature [°C]- Zone 6	200
Temperature [°C]- Zone 7	190
Temperature [°C]- Zone 8	180
Screw speed [rpm]	600
Lateral screw speed [rpm]	200

Table 4. Extrusion process parameters used for the preliminary tests 1

In the second set of preliminary experiments (Preliminary tests 2), the fraction of CNTs (0.03) and TPU (0.77) were kept constant summing a total of 0.80. A synergistic additive was included in the formulations together with five flame retardants counting a total fraction of 0.20. The mixed systems with all formulations are shown in Table 5. The extrusion parameters were the same used in the previous tests.

	A	B	C	D	E	F	Polymer + 3% CNTs
Run 1	0	0.1	0	0	0.05	0.05	0.80
Run 2	0.1	0	0.05	0	0	0.05	0.80
Run 3	0.1	0	0	0	0.05	0.05	0.80
Run 4	0	0.1	0.05	0	0	0.05	0.80
Run 5	0.1	0	0	0.05	0	0.05	0.80
Run 6	0	0.1	0	0.05	0	0.05	0.80

Table 5. Formulations used in the preliminary tests 2

In the third set of preliminary experiments (Preliminary tests 3), the amount of flame retardant varied from 0.20 to 0.25, consequently the amount of CNTs/TPU decreased from 0.80 to 0.75. In this test, a viscous liquid flame retardant was also considered. The tested formulations (Table 6) were compounded at the same conditions of preliminary test 1, with the exception of the screw speed, which was decreased to 400 rpm.

	A	B	G	Polymer + 3wt% CNTs
Run 1	0	0.25	0	0.75
Run 2	0	0.20	0	0.80
Run 3	0.25	0	0	0.75
Run 4	0.20	0	0	0.80
Run 5	0	0	0.20	0.80

Table 6. Formulations used in the preliminary tests 3

The fourth set of preliminary experiments (Preliminary tests 4), consisted of one test (Table 7) with a new viscous liquid flame retardant. The conditions in which this formulation was compounded are shown in Table 8.

	H	Polymer + 3wt% CNTs
Run 1	0.25	0.75

Table 7. Formulations used in the preliminary tests 4

Extrusion Parameters	Values
Temperature [°C]- Zone 1	150
Temperature [°C]- Zone 2	210
Temperature [°C]- Zone 3	210
Temperature [°C]- Zone 4	200
Temperature [°C]- Zone 5	190
Temperature [°C]- Zone 6	180
Temperature [°C]- Zone 7	170
Temperature [°C]- Zone 8	160
Screw speed [rpm]	600
Lateral screw speed [rpm]	30

Table 8. Extrusion process parameters used for the preliminary tests 4

The fifth set of preliminary experiments (Preliminary tests 5), Flame retardant E was compounded together with CNTs/TPU (0.75) in conditions similar to preliminary test 1, but the screw speed was increased to 800 rpm (Table 9).

	E	Polymer + 3wt% CNTs
Run 1	0.25	0.75

Table 9. Formulations used in the preliminary tests 5

In order to observe the processability of the pre-selected polymeric matrix and additives, 20 formulations were submitted to compounding. The polymeric matrix and additives did not present any compounding problem during the experiments. In addition, this compounding feasibility test helped to identify the best processability conditions for the tested materials.

3.2.3 Conclusions

In principle, to develop the novel formulation, the materials (the polymer and the additives) must be defined; however, narrowing down the huge list of possible candidates to a manageable number proved to be a very hard task. At the end, 16 materials were identified as potential pre-selected materials to be used in the development of the novel electrically conductive flame retarded polymer formulation.

However, according to the partner company of this project (SIPsa), the use of liquid additives at industrial scale would not be practical or feasible. Therefore, the two liquid flame retardants tested were excluded from the pre-selected materials.

In addition, although the two polyphosphonate homopolymer flame retardant used did not show any processability problem, it was decided to keep only one.

In summary, the number of material candidates to be used for the next experimental step was reduced to 13.

3.3 Design of Experiment (DOE)

The Design of Experiments (DOE) technique allows the designers to determine, at the same time, both (i) the individual and (ii) the interactive effects of many factors that could influence the yield results in any design. This tool contributes to the understanding of the interactions among the design elements helping to point out the sensitive parts and areas in the designs that could cause problems in the output. Therefore, it is possible to fix these problems and produce robust and higher yield designs before going into production.

The application of the DOE to the study and optimization of flame retardants is not new, as DOE is universally considered to be the best experimental strategy in many fields of science and technology [25-28].

The complexity of our system is due to the remarkable high number of additives, which requires the application of a structured experimental strategy. Furthermore, the present work is characterized by multiple responses to be simultaneously optimized, therefore, the desirability function methodology was applied.

Based on the above premises, the scientific and technological objectives of this work were pursued mainly by means of the DOE methodology applied to mixtures under the general guidance of the Subject-Matter Expert Knowledge (SMEK), meant to effectively explore a relatively wide formulation domain, to test remarkably high number of additives (some of which were novel for this application) spanning a large loading interval.

In addition, DOE was adopted in order to: (i) enhance the rate between the number of experiments and the relative information output, and (ii) scout the nonlinear blending effects among the mixture components, leading to synergistic or antagonistic behaviours.

The details of the DOE applied to mixtures are explained in Annex 2. [29]

The DOE briefly comprised the following sequential stages of experiments consisting of 4 phases, where, initially, 10 out of the 13 pre-selected materials (as known as *components*) were used:

- **Screening - Phase (I):** it was used to identify which components turn out to have a desirable effect in determining the responses of interest and therefore should be retained in the next stage of experimentation. Linear mixture models were adopted to reach this objective. In this phase, the percentage proportions of polymer and CNTs were kept at constant levels; therefore, the system had 8 variable components out of 10 components.

The system required 20-run experiments. This phase was carried out experimentally at a laboratory scale and data analysis was also carried out after the experiments.

- **Rational reduction of the mixture complexity- Phase (II):** it was used to investigate whether any of the mixtures components identified in Phase (I) could be reduced to simplify the mixture. This could happen if, for example, two components turn out to exhibit similar effects on the responses, which may not be unlikely because some of the synergistic agents are just varieties of the same chemical class of materials.

At this phase, the number of components identified in Phase (I), which had to undergo the following optimization phase, was reduced from 10 to 6.

- **Optimization and verification- Phase (III):** it was used to define the optimal formulation of the mixture based on the components defined in Phase (II), i.e., the proportion of components capable of delivering the most desirable combination of the values taken on by the responses of interest. This predicted global optimum was verified carrying out some experimental trials at the identified mixture composition.

The composition of the mixture system in this phase consisted of 6 components, that required about 10-run experiments (plus 2-runs replication) and another 4 runs for the model verification (16 runs in total).

- **Process strengthening and verification- Phase (IV):** it was used to carry out a critical study of the final statistical models generated in Phase (III) in order to verify whether the emerged global optimum is robust enough towards the variation

transmitted by the variance in the composition set-up and the natural variation in the responses due to the "common causes" of variation (in the Sheward's sense of Statistical Process Control).

This phase was carried out experimentally both at a laboratory scale and industrial scale, with an estimated number of 10 runs.

It should be noted that some additional experiments were carried out in this work, like the preliminary compounding tests described in Section 3.2.2, which were made in order to assess the processability of the polymer and additives. Therefore, in total, around 100 experiments were carried out, and around 1000 kg of material were used for preparing all the formulations.

3.4 Materials compounding

A high volume manufacturing process in which plastic material is melted and moves towards a screw mechanism is called *extrusion process*. In this process, the screw rotates thus forcing the plastic material to advance through the extruder cavity and pushing it through the die. After exiting the die, it is cooled, solidified and cut into pellets. [30]

In most applications, solid polymer pellets are fed to the extruder, which gives three different zones: (i) solid transport zone, which is filled with polymer pellets from the hopper; (ii) melt zone, where the polymer melts; and (iii) pump zone, which is completely filled with material and pressure is built up to overcome the die resistance.

There are some important process parameters to be considered for the extrusion process: melting temperature of plastic, speed of the screw, extrusion pressure required, etc.[30]

A schematic showing a general description of the component parts of an extruder is presented in Figure 8.

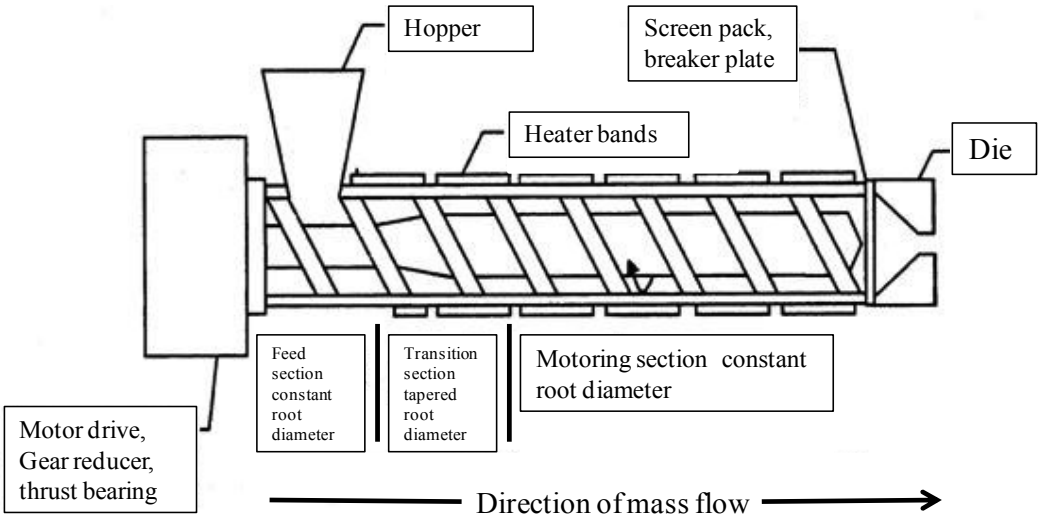

Fig 8. Component parts of an extruder

Screw extruders are divided into single screw and multi screw extruders.[30] In particular, the twin screw extruder is a kind of multi screw extruder, which is used in polymer industry and has become increasingly important in the extrusion industry. It is a continuous processing operation, in which a material is extruded by means of the action of two screws.

In this work, composites of different formulations, at laboratory scale, were blended in a co-rotating twin-screw extruder type ZSE 18 HP – 40 D from Leistritz (Figure 9), and cut into pellets. The screw geometry and some other extruder data are shown in Figure 10.

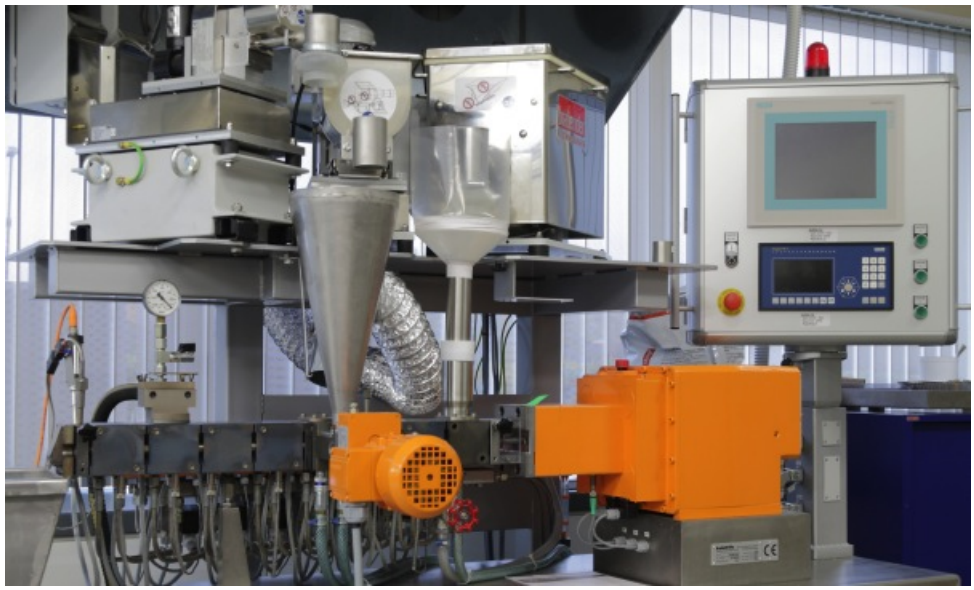

Fig 9. Twin-screw extruder ZSE 18 HP – 40 D from Leistritz

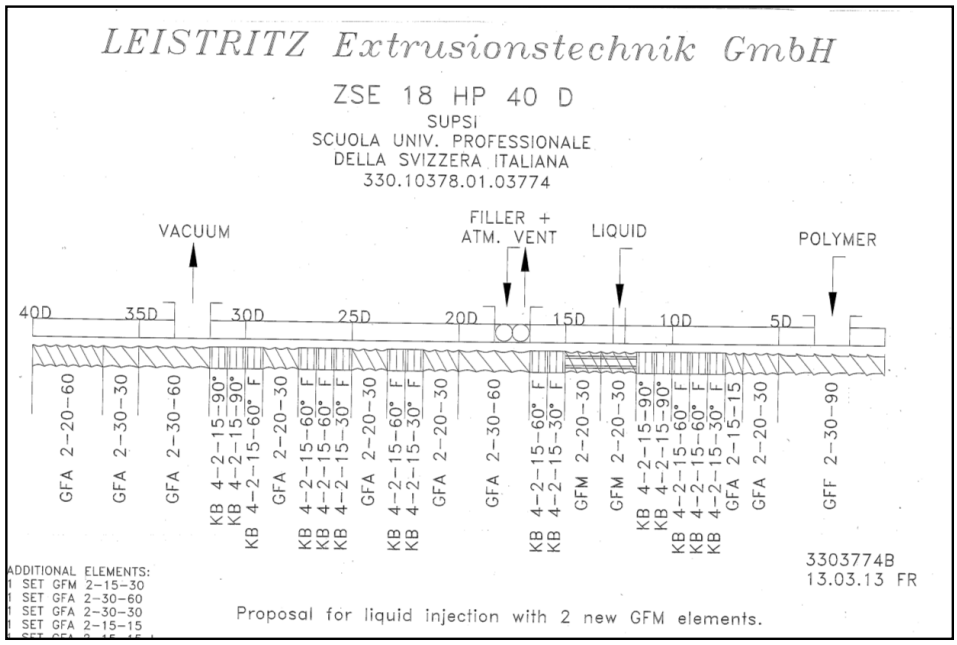

Fig 10. Co-rotating twin-screw extruder ZSE 18 HP – 40 D from Leistritz

The extrusion parameters used in the preliminary tests were variable and they are mentioned in Section 3.2.2. After the preliminary tests, however, the extrusion parameters used for the laboratory scale tests were kept the same for all the experiments: they are presented in Table 10.

Extrusion Parameters	Values
Temperature [°C]- Zone 1	150
Temperature [°C]- Zone 2	210
Temperature [°C]- Zone 3	210
Temperature [°C]- Zone 4	200
Temperature [°C]- Zone 5	200
Temperature [°C]- Zone 6	200
Temperature [°C]- Zone 7	190
Temperature [°C]- Zone 8	180
Screw speed [rpm]	900
Lateral screw speed [rpm]	200
Output [kg/hour]	7

Table 10. Extrusion process parameters used for the laboratory test scale

At industrial scale, composites were blended in a co-rotating twin-screw extruder type EBC 30HT– 29D from COMAC. The screws had three lobes and a speed value of

600 rpm. Further details about the extruder, the screw geometry and the process parameters used to compound the formulations at industrial scale are treated as confidential.

3.5 Specimens preparation

The formulations were subjected to injection-moulding in order to produce moulded standard test samples. Figure 11 shows an schematic overview of the injection moulding process.

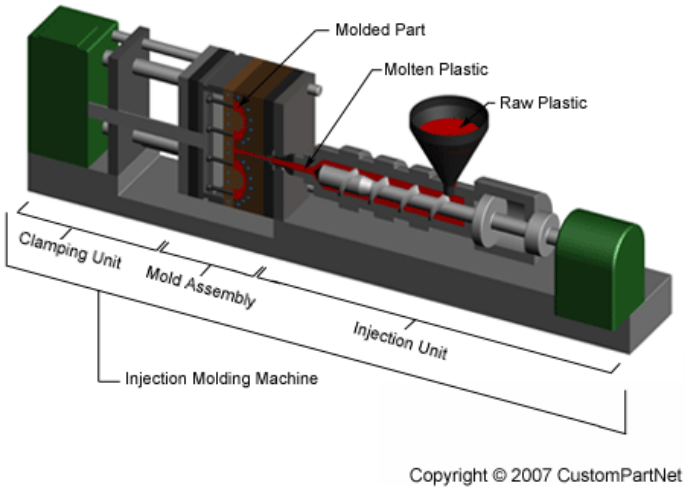

Fig 11. Overview of the injection moulding process

In the first step of the preparation, each material formulation was dried at the TPU recommended temperature of 90-110°C [17] for a period of approximately 2 hours using a vacuum oven. Moisture levels were kept below 0.2% to avoid a reduction in the quality of the finished part (specimens). After that, the material was cooled down to room temperature and then transferred to the feeder of the injection moulding machine model Allrounder 320C 600-225 from Arburg. The testing specimens were moulded with sample dimensions of 125mm x 13mm x 3.2 mm according to the UL-94 standard.

The state-of-the-art literature indicates a very strong influence of the mass temperature and the injection speed on the orientation of the nanotubes and on the resistivity by some orders of magnitude. This may lead to the conclusion that injection moulding conditions have to be adapted in these nanocomposites [31]. Therefore, the process parameters were modified depending on the formulation in order to achieve the best quality of the specimen.

The injection moulding parameters used to mould the samples are listed in Table 11.

Injection Moulding Parameters	Values
Temperature [°C]- Zone 1	170 (170 - 200)
Temperature [°C]- Zone 2	180 (180 - 210)
Temperature [°C]- Zone 3	185 (185 - 215)
Temperature [°C]- Zone 4	190 (190 - 220)
Temperature [°C]- Zone 5	190 (190 - 220)
Mould Temperature [°C]	40
Injection Speed [ccm/s]	20 (5-60)
Injection Pressure [bar]	550 (300-1000)
Screw Speed [rpm]	20
Back Pressure [bar]	50

Table 11. Injection moulding parameters used to mould the samples

After moulding, some samples were thermally treated (annealing) in order to evaluate the optimal functional properties in a shorter period. In general, the annealing is recommended for a period of 20 hours at a temperature of 100°C [32]. If the moulded parts are not annealed, they would require several weeks of storage at room temperature to attain full mechanical properties. In addition, the samples were thermally treated also to evaluate the influence of annealing on the electrical resistivity measurements. [33,34]

3.6 Materials characterisation

3.6.1 Electrical resistivity tests of conductive plastics

This part of work is focused on the electrical properties of TPUs. Therefore, after the moulding of the material samples, it was necessary to study their electrical behaviour. For this purpose, the two probe method was used to evaluate the electrical resistivity of the materials developed in this work.

Electrical conductivity is defined as the ability of a substance to conduct electrical current. The SI unit for the electrical conductivity is the Siemens per meter ($S \cdot m^{-1}$). Electrical conductivity is the reciprocal of the electrical resistivity, the unit of which is

Ohm meter or Ω.m.[35]

As known from the Ohm's law, if physical conditions remains unchanged, the potential difference (V) across two ends of a conductor is proportional to the current (I) flowing through a conductor:

$$V = I \cdot R$$

The constant of proportionality R is named resistance of the conductor.

At a constant temperature, the resistance (R) of a conductor is proportional to its length (l) and inversely proportional to its area of cross section (A) as presented in the equations below:

$$R = \rho \cdot l/A,$$

where ρ is a constant of proportionality called resistivity of material. The resistivity of a material is equal to the resistance offered by a wire of this material of unit length and unit cross-sectional area. [35]

In the two probe method, for a long parallel piped shaped of uniform cross-section or a long thin wire-like sample of uniform cross-section, the resistivity can be measured by measuring the voltage drop across the sample due to the transfer of known (constant) current through the sample, as shown in Figure 12. The section a-b is the specimen whose resistivity is to be measured. The battery supplies current ("in" through probe 1 and "out" through probe 2). The current in the specimen is I (Ampere) measured by the amperometer (A). The potential difference between the two contacts (probe 1 and probe 2) at the ends of the specimen is V (Volt). It is measured by a voltmeter (V). The length of the specimen between the two probes is l, and A its area of cross-section, then, the resistivity of the specimen is:

$$\rho = (V/I) \cdot (A/l) = R \cdot (A/l)$$

The four probe method is usually used to overcome the drawbacks of the two probe method: (a) the error due to contact resistance of measuring leads, and (b) its unsuitability for materials having random shapes. [35] However, in the case of the materials tested in this work, the two probe method is very suitable. In addition, the 2-points measurement is the most used method in industry.

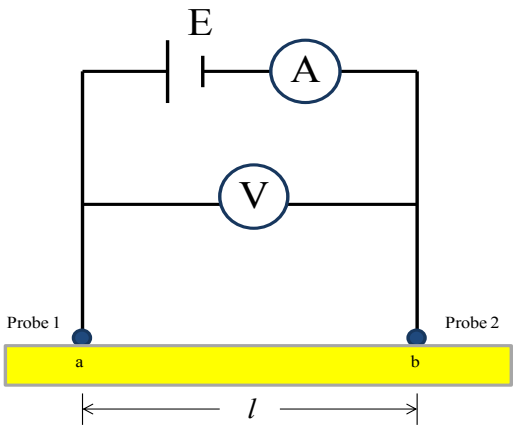

Fig 12. Two probe method of measuring resistivity of a specimen

During the experiments, the standard size specimen was placed between two silver-plated electrodes (Figure 13). The resistance was measured after waiting 60 seconds, and the electrical resistivity was calculated.

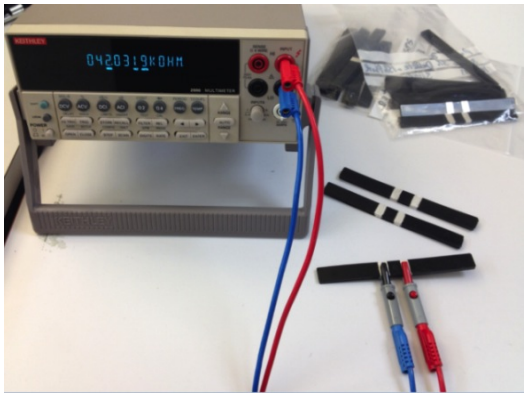

Fig 13. The electrical resistivity measurement

3.6.2 Flammability tests of flame retarded polymers

3.6.2.1 Underwriter Laboratory 94 (UL94) standard

The UL 94 standard provides procedures for bench-scale testing to determine the acceptability of plastic materials for use in appliances or other devices with respect to flammability under controlled laboratory conditions. [36-39]

In the UL94 Vertical Burning test, a plastic bar 125mm x 13mm x 3.2 mm is suspended vertically and clamped at its top. A thin layer of cotton is positioned 300 mm below the test specimen to catch any molten material that may drop from the specimen. Figure 14 shows the test setup according to the UL-94 standard for the Vertical Burning Test.

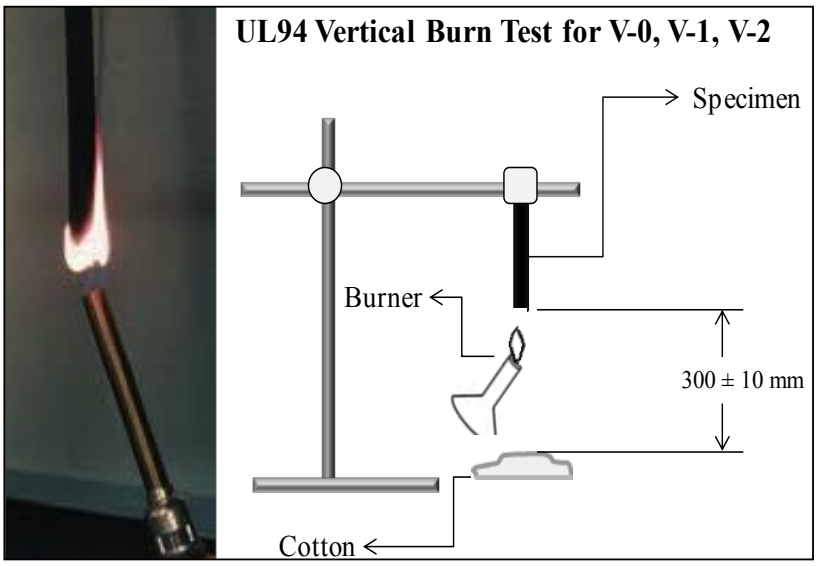

Fig 14. UL 94 Vertical tests

A 20-mm-long flame from a methane burner is applied to the centre point on the bottom end of the specimen. The burner is positioned in order to keep the burner barrel located 10 mm below the bottom end of the material specimen. The flame is maintained for 10 seconds, and then removed to a distance of at least 150 mm. Upon flame removal, the specimen is observed for after-flaming and its duration time recorded (t1). As soon as the after-flame ceases, the burner flame is reapplied for additional 10 seconds, then removed again. The duration of after-flaming (t2) or after-glowing (t3) are noted.

The classification (Table 12) is based on the duration of after-flaming or after-glowing following the removal of the burner flame, as well as the ignition of cotton by dripping particles from the test specimen.

RATING	AFTER-FLAME TIME	BURNING DRIPS
V-0	< 10 s	No
V-1	< 30 s	No
V-2	< 30 s	Yes
n.c. (= not classified)	> 30 s	

Table 12. Classification of materials for the UL 94 V flammability test

The UL 94 standard also includes an horizontal set up, where the polymeric bar is maintained horizontally: this orientation is generally considered less severe than the vertical one. In the vertical UL94 standard, the flame pre-heats the polymer above the

burning area, while in the horizontal set up this effect does not occur.

Apart from the standard tests, the UL94 procedure was also used as test bed of an online acquisition method for monitoring the surface growth of flame retardant protective layers during flammability and combustion tests, which was developed during of this Ph.D work. The system minimizes the disturbances of the flames on the image sensors, thus gathering a video of the material surface. The device continuously records and quantitatively measures the carbonization front growth rate. The apparatus consists of a camera with customized lighting and dedicated software acquiring images of the burning specimen. Chapter 7 is dedicated to the description of this device and its test results.

3.6.2.2 Thermal analysis

Thermal analysis refers to a variety of techniques, in which a property of a sample is continuously measured as the sample is programmed through a predetermined temperature profile. The most common techniques are thermogravimetric analysis (TGA) and differential scanning calorimetry (DSC). [40-42]

A thermal analysis curve is interpreted by relating the measured property versus temperature to chemical and physical events occurring in the sample. It is frequently a qualitative or comparative technique.

- *Thermogravimetric analysis (TGA)*: in a TGA experiment, the mass loss vs. increasing temperature of the sample is recorded. The basic instrumental requirements are a precision balance and programmable furnace, which is generally controlled by software for data reduction. [40-42] TGA makes a continuous weighting of a small sample (c.a., 10 mg) in a controlled atmosphere (e.g., air or nitrogen) as the temperature is increased at a programmed linear rate. Also isothermal analyses can be carried out: for this purpose, the sample is rapidly heated to the programmed temperature before any significant thermal decomposition occurs. TGA allows for quantitatively analysing, for example, the filler content of a polymer compound (e.g., carbon black decomposed in air but not in nitrogen), the amount of residue left at 600°C or 800°C, etc. [40-42]
- *Differential scanning calorimetry (DSC)*: in a DSC experiment, the difference in energy input to a sample and a reference material is measured while the sample and reference are subjected to a controlled temperature program.

DSC requires two cells equipped with thermocouples in addition to a programmable furnace, recorder, and gas controller. [40-42] In DSC, the measured energy differential corresponds to the heat content (enthalpy) or the specific heat of the sample. The sample size is usually limited to less than 10 mg. The DSC measures the power (heat energy per unit time) differential between a small weighed sample of polymer (ca. 10 mg) in a sealed aluminium pan referenced to an *empty pan* in order to maintain a zero temperature differential between them during programmed heating and cooling temperature scans. The technique is most often used for characterizing the glass transition temperature (Tg), melting temperature (Tm), the crystallization temperature (Tc), and heat of fusion of polymers. The technique can be also used for studying the kinetics of chemical reactions, like oxidation and decomposition. [40-42]

3.6.3 Microstructure analysis

3.6.3.1 Scanning Electron Microscopy (SEM)

The resolution of the SEM can approach a few nanometers and it can operate at magnifications that are easily adjusted from about 10x-300,000x. [43]

Together with topographical information, SEM analysis can give information concerning the composition near surface regions of the material.

In the SEM apparatus, a source of electrons is focused (in vacuum) into a fine probe that is rastered over the surface of the specimen. As the electrons penetrate the surface, a number of interactions occur that can result in the emission of electrons or photons from (or through) the surface. A reasonable fraction of the emitted electrons can be collected by appropriate detectors, and the output can be used to modulate the brightness of a cathode ray tube (CRT). An image is produced on the CRT; every point that the beam strikes on the sample is mapped directly onto a corresponding point on the screen. [43]

The main images produced in the SEM are of three types: secondary electron images, backscattered electron images, and elemental X-ray maps. Secondary and backscattered electrons are conventionally separated according to their energies. [43]

The X-ray emission signal can be sorted by energy in an energy dispersive X-ray detector or by wavelength with a wavelength spectrometer. These distributions are characteristic of the elements that produced them and SEM can use these signals to produce elemental images that show the spatial distribution of particular elements in

the field of view as well as semi-quantitative analysis of some elements. Energy-Dispersive X-Ray analysis (EDS) is used in polymer science for element mapping. [43]

3.7 References

[1] I.S. Fahim, W. Mamdouh, H.A.G. Salem, "Nanoscale investigation of mechanical, thermal stability and electrical conductivity properties of reinforced thermoplastic polyurethane/graphene nanocomposite". American Journal of Nanoscience and Nanotechnology 1 (2013), 31-40.

[2] H. Kim, Y. Miura, and C.W. Macosko, "Graphene/polyurethane nanocomposites for improved gas barrier and electrical conductivity". Chem. Mater. 22 (2010), 3441–3450.

[3] R. Smith, "Biodegradable polymers for industrial applications". Woodhead publishing. Cambridge: 2005

[4] F. Laoutid, L. Bonnaud, M. Alexandre, J.M. Lopez-Cuesta, and Ph. Dubois. "New prospects in flame retardant polymer materials: from fundamentals to nanocomposites". Materials Science and Engineering: R: Reports. 63 (2009), Issue 3, 100–125

[5] H. Lia, N. Ninga, L. Zhanga, Y. Wang, W. Liang, M. Tian, "Different flame retardancy effects and mechanisms of aluminium phosphinate in PPO, TPU and PP". Polymer Degradation and Stability 105 (2014), 86–95.

[6] EP 2681279 A1- Flame retardant thermoplastic polyurethane compositions. Feina Cao, Greg S. Nestlerode, Qiwei Lu. Lubrizol Advanced Materials, Inc.

[7] D.R. Hall, M.M. Hirschler, C.M. Yavornitzky, Fire safety Science: Proceedings of the international symposium. In: "Halogen-free flame retardant thermoplastic polyurethanes", 1986.

[8] A.B. Morgan, C.A. Wilkie, editors. "The non-halogenated flame retardant handbook". Wiley (2014), p.194-195

[9] National Research Council (U.S.). Committee on fire- and smoke-resistant materials for commercial aircraft interiors. Fire- and smoke-resistant interior materials for commercial transport aircraft.

[10] G. Marosi, A. Marton, P. Anna, G. Bertalan, B. Marosföi, A. Szép, "Ceramic precursor in flame retardant systems". Polymer Degradation and Stability 77 (2002)

259–265

[11] M. Kilinç (2009). “Production and characterization of boron based additives and the effect of flame retardant additives on pet based composites”. Ph.D Thesis. Middle East Technical University: Turkey.

[12] P. Knauth, J. Schoonman, editors. “Nanocomposite: ionic conducting materials and structural spectroscopies”, Vol. 10, Springer: 2008.

[13] Z. Zhang, K. Friedrich, “Tribological characteristics of micro and nanoparticle filled polymer composites”, Polymer Composites, Springer: 2005.

[14] D.M. Marquis, E. Guillaume and C. Chivas-Joly, “Properties of nanofillers in polymer. nanocomposites and polymers with analytical methods”. Edited by Dr. John Cuppoletti.. Laboratoire national de métrologie et d’essais (LNE) France: 2011, 261-284.

[15] D. Wesolek and W. Gieparda, “Single- and multiwalled carbon nanotubes with phosphorus based flame retardants for textiles”. Journal of Nanomaterials 2014 (2014), Article ID 727494, 6 pages.

[16] K.C. Etika and J.C. Grunlan, “Utilization of clay-carbon nanoparticle synergy for enhancing electrical and mechanical properties of epoxy composites”. Materials Science and Engineering Program, Department of Mechanical Engineering, Texas A&M University, College Station, TX.

[17] Shodhganga. “Flame Retardant Properties“. Chapter 7: Flame Retardant Properties.

[18] A.M.F. Lima, V.G. de Castro, R.S. Borges, G.G. Silva, “Electrical conductivity and thermal properties of functionalized carbon nanotubes/polyurethane composites”. Polímeros 22 (2012), n. 2, 117-124.

[19] J.-C. Huang, “Carbon black filled conducting polymers and polymer blends”. Advances in Polymer Technology 21 (2002), Issue 4, 299–313.

[20] E.K. Sichel, “Carbon black-polymer composites”. Plastics engineering. Marcel Dekker. New York: 1982.

[21] A. Flores, M.E. Cagiao, T.A. Ezquerra, F.J. Balta Calleja, “Influence of filler structure on microhardness of carbon black–polymer composites”. Journal of Applied Polymer Science 79 (2001), 90–95.

[22] I. Krupa, I. Novák, I. Chodák, “Electrically and thermally conductive polyethylene/graphite composites and their mechanical properties”. Synthetic Metals 145 (2004) 245–252.

[23] R. Senguptaa, M. Bhattacharyaa, S. Bandyopadhyayb, A.K. Bhowmicka, "A review on the mechanical and electrical properties of graphite and modified graphite reinforced polymer composites", Progress in Polymer Science 36 (2011), 638-670.

[24] J. Yanga, M. Tiana, Q.-X. Jiab, J.-H. Shia, L.-Q. Zhanga, S.-H. Limc, Z.-Z. Yuc, Y.-W. Maic, "Improved mechanical and functional properties of elastomer/graphite nanocomposites prepared by latex compounding", Acta Materialia 55 (2007), 6372–6382.

[25] L. M. Babcock, M. Altekar, "Use of statistical design to develop flame retardant èpolymer formulations". Chemometrics and Intelligent Laboratory Systems 29 (1995), 141-146.

[26] A. Atikler, H. Demir, F. Tokath, F. Tihminlioglu, D. Balköse, S. Ülkü, "Optimisation of the effect of colemanite as a new synergistric agent in an intumescent system". Polymer Degradation and Stability 91 (2006), 1563-1570.

[27] E.D. Weil, W. Zhu, N. Patel, M. Mukhopadhyay, "A system approach to flame retardancy and comments on modes of action". Polymer Degradation and Stability 54 (1996), 125-136.

[28] H. Dvir, M. Gottlieb, S. Daren, T. Tartakovsky, "Optimization of a flame retarded polypropylene composite". Composites Science and Technology 63 (2003), 1865-1875.

[29] J. Cornell, "Experiments with mixtures. Design, models, and the analysis of mixture data", Wiley, New York: 2002.

[30] C. Rauwendaal. "Polymer extrusion". 5th Edition. Hanser Publications. Munich: 2014, p 1-21.

[31] P. Pötschke, L. Häußler, S. Pegel, Dresden, R. Steinberger, G. Scholz, Lemförde, "Thermoplastic polyurethane filled with carbon nanotubes for electrical dissipative and conductive applications". Presented at the 7th Fall-Rubber-Colloqium, Hannover, Germany: 2006.

[32] Pearlthane: Processing Guidelines. Extrusion/Injection Moulding, Merquinsa. http://www.merquinsa.com/int/p_info/pearlthane/PEARLTHANE_PGL.pdf

[33] W. Wohlleben, M.W. Meier, S. Vogel, R. Landsiedel, G. Cox, S. Hirtha and Z. Tomovi´, "Elastic CNT–polyurethane nanocomposite: synthesis, performance and assessment of fragments released during use". Nanoscale 5 (2013), 369-380.

[34] L.G. Cena and T. M. Peters, "Characterization and control of airborne particles emitted during production of epoxy/carbon nanotube nanocomposites". Journal of Occupational and Environmental Hygiene 8 (2011), 86–92.

[35] S. Singh. “Physics: Study the temperature dependence of resistance of a semiconductor (Four probe method)”. 2012 http://www.sardarsinghsir.com/

[36] R. E. Lyon and M. Janssens, “Polymer flammability”, U.S. Government Final Report number DOT/FAA/AR-05/14, 2005

[37] J.H. Troitzsch in “Plastics flammability handbook”, eds. J. Troitzsch, Hanser Publishers, Munich: 2004.

[38] V. Babrauskas in “Fire retardancy of polymeric materials”, eds. A.F. Grant, C.A. Wilkie, Marcel Dekker, New York, 2000, 81-113

[39] ISO 1210” UL94 Vertical Burning Test”

[40] M.A. Hirschler in “Fire retardancy of polymeric materials”, eds. A.F. Grant, C.A. Wilkie, Marcel Dekker, New York: 2000, 94-280

[41] N.P. Cheremisinoff in “Polymer characterization - Laboratory techniques and analysis”, ed. by N.P. Cheremisinoff, William Andrew Publishing, Noyes, 1996

[42] A. Turi, editor, “Thermal characterisation of polymeric materials”, Academic Press, USA: 1981.

[43] J.H. Moore, editor. “Encyclopedia of chemical physics and physical chemistry”. N.D. Spencer, Institute of Physics, Knovel: 2002.

4 Development of a novel electrically-conductive flame retardant TPU composite

4.1 Introduction

As mentioned in Chapter 1, this work focused on the development of halogen-free UL94-V0 bio-based TPUs with an electrical resistivity ≤ 1000 Ω.cm, and a load ≤ 25 wt%. In order to reach these objectives, this work was supported by the structured experimental approach of Design Of Experiments (DOE) applied to the development of mixtures. Therefore, after identifying and pre-selecting the additives capable of conferring to the polymer of interest the most desirable values of flame retardancy (as high as possible) and electrical resistivity (as low as possible), a strategy based on sequential stages of experiments was adopted to study the mixture.

There were four main phases: (i) screening; (ii) rational reduction of the mixture complexity; (iii) mixture optimization and verification; and (iv) process strengthening and verification. Each of these phases will be explained in detail in the following sections.

4.2 Screening

4.2.1 Experimental design

In this phase, a DOE (DOE 1) was carried out in order to identify what mixture of components may obtain both the low electrical resistivity and the good results in the UL-94 test.

The components, proportions and constraints used to the development of this DOE are shown in Figures 15 and 16.

Component	Type	Minimum	Maximum
A	Mixture	0.000	0.250
B	Mixture	0.000	0.250
C	Mixture	0.000	0.050
D	Mixture	0.000	0.100
E	Mixture	0.000	0.100
F	Mixture	0.000	0.050
G	Mixture	0.000	0.100
H	Mixture	0.000	0.100
		Total =	0.25

Fig 15.Components and their proportions in the mixture system

Low	≤ Constraint	≤ High
0.10	≤ A + B	≤
	≤ C + D + E	≤ 0.10
	≤ G + H	≤ 0.10
0.00	≤ A	≤ 0.25
0.00	≤ B	≤ 0.25
0.00	≤ C	≤ 0.05
0.00	≤ D	≤ 0.10
0.00	≤ E	≤ 0.10
0.00	≤ F	≤ 0.05
0.00	≤ G	≤ 0.10
0.00	≤ H	≤ 0.10
	A+B+C+D+E+F+G+H	= 0.25

Fig 16. Constraints used for the development of DOE 1

It should be noted that the mixtures used for this study are made of 8 components (from A to H) in a total proportion of 0.25 (Figure 15). The remaining proportion of 0.75 is kept constant and made up of TPU (0.72) and CNTs (0.03). It may be useful to note that in this study the total additives load (charge to the polymer) is 0.28 (that is, 0.25 of components A to H + 0.03 of CNTs).

In this design, the responses of the samples are (a) the electrical resistivity (in Ω.cm units) of the extruded samples (not annealed), and (b) the fraction of the specimen producing the worst results of flame retardancy.

According to the stated objective of the study (i.e., screening), the adopted experimental design is an I-optimal design, with 20 runs generated to support a linear model. The mixture system with the formulations is shown in Table 13.

RUN	MIXTURE COMPONENTS								
	A	**B**	**C**	**D**	**E**	**F**	**G**	**H**	**Polymer + CNTs**
1	0.25	0	0	0	0	0	0	0	0.75
2	0.03	0.08	0.011	0.061	0.011	0.008	0.012	0.037	0.75
3	0.25	0	0	0	0	0	0	0	0.75
4	0.03	0.13	0.011	0.011	0.011	0.033	0.012	0.012	0.75
5	0	0.1	0.05	0	0	0	0	0.1	0.75
6	0	0.1	0	0	0	0.05	0.1	0	0.75

7	0.1	0	0.05	0	0.05	0.05	0	0	0.75
8	0	0.1	0	0	0.1	0	0.05	0	0.75
9	0.1	0	0.05	0	0.05	0.05	0	0	0.75
10	0.15	0	0	0.1	0	0	0	0	0.75
11	0.155	0.03	0.011	0.011	0.011	0.008	0.012	0.012	0.75
12	0.1	0	0.05	0	0	0	0.1	0	0.75
13	0	0.25	0	0	0	0	0	0	0.75
14	0	0.1	0	0.1	0	0.05	0	0	0.75
15	0	0.25	0	0	0	0	0	0	0.75
16	0.15	0	0	0	0	0	0	0.1	0.75
17	0	0.2	0.05	0	0	0	0	0	0.75
18	0.0	0.03	0.011	0.061	0.011	0.008	0.037	0.012	0.75
19	0.15	0	0	0	0	0	0	0.1	0.75
20	0.10	0	0	0	0.1	0	0.05	0	0.75

Table 13. Formulations used in the screening DOE 1

4.2.2 Experimental results

Twenty specimens of each formulation were used for the electrical resistivity tests, and ten specimens for the UL-94 tests. The flame retardancy performance and the mean values of the electrical resistivity of these TPU composites are shown in Table 14.

RUN	Extruded Specimens Not Annealed measured at SIPSA [Ω.cm]	UL-94
1	NM*	V0
2	1.82E+06	n.c
3	2.0E+07	V0
4	1.86E+05	n.c
5	NM*	n.c
6	6.46E+02	n.c
7	8.35E+06	V1
8	3.98E+05	n.c
9	4.27E+05	V1
10	1.10E+06	V0
11	7.08E+05	V0
12	3.63E+03	V0
13	3.09E+07	n.c
14	3.39E+04	n.c
15	2.82E+06	n.c
16	7.41E+05	V0
17	1.41E+07	n.c
18	4.27E+04	n.c
19	1.51E+06	V0
20	2.14E+05	V1

Table 14. Electrical resistivity and UL-94 test results for the formulations of DOE 1

**NM =not measurable because the electrical resistivity was higher than E+07 (Ω.cm)*

The Design-Expert® Software was used to analyse the effects of each component in the mixture on the electrical resistivity and burning behaviour. Table 15 compiles the component fractions in each formulation and the responses for each run. It should be

noted that the electrical resistivity of Runs 1 and 6 could not be measured because the electrical resistivity was higher than E+07 (Ω.cm). Therefore, the two runs were excluded from the study. In addition, in order to analyse the flame retardancy performance (Response 2 in Table 15), it was necessary to give a numerical value to each response. The best flame retardancy performance (UL-94 V0) was rated as 0 (no burn) and the worst performance (UL-94 n.c) was rated as 1 (burn). Samples classified as V1 or V2 were rated between 0-1 proportionally to the burning time.

Run	Component 1	Component 2	Component 3	Component 4	Component 5	Component 6	Component 7	Component 8	Response 1	Response 2
	A	B	C	D	E	F	G	H	Resistivity	Burning
1	0.25	0	0	0	0	0	0	0		0
2	0.03	0.08	0.011	0.061	0.011	0.008	0.012	0.037	1.82E+06	1
3	0.25	0	0	0	0	0	0	0	2.0E+07	0
4	0.03	0.13	0.011	0.011	0.011	0.033	0.012	0.012	1.86E+05	1
5	0	0.1	0.05	0	0	0	0	0.1		1
6	0	0.1	0	0	0	0.05	0.1	0	6.46E+02	1
7	0.1	0	0.05	0	0.05	0.05	0	0	8.35E+06	0.4
8	0	0.1	0	0	0.1	0	0.05	0	3.98E+05	1
9	0.1	0	0.05	0	0.05	0.05	0	0	4.27E+05	0.2
10	0.15	0	0	0.1	0	0	0	0	1.10E+06	0
11	0.155	0.03	0.011	0.011	0.011	0.008	0.012	0.012	7.08E+05	0
12	0.1	0	0.05	0	0	0	0.1	0	3.63E+03	0
13	0	0.25	0	0	0	0	0	0	3.09E+07	1
14	0	0.1	0	0.1	0	0.05	0	0	3.39E+04	1
15	0	0.25	0	0	0	0	0	0	2.82E+06	1
16	0.15	0	0	0	0	0	0	0.1	7.41E+05	0
17	0	0.2	0.05	0	0	0	0	0	1.41E+07	1
18	0.0	0.03	0.011	0.061	0.011	0.008	0.037	0.012	4.27E+04	1
19	0.15	0	0	0	0	0	0	0.1	1.51E+06	0
20	0.10	0	0	0	0.1	0	0.05	0	2.14E+05	0.6

Table 15. Component fractions in each formulation and the responses for each run

4.2.2.1 Electrical resistivity

The DOE analysis could find significant effects of the components in the mixture. They are shown by the so-called Cox trace plot (Figure 17), which indicates how the variations of the individual component proportions affect the response.

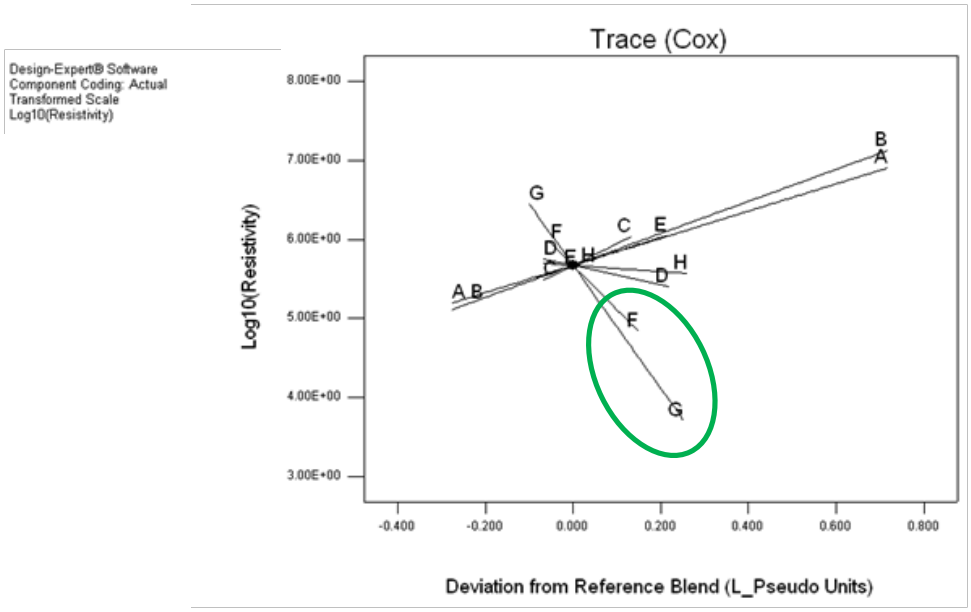

Fig 17. Component effects shown by the Cox trace plot: Response R (Electrical resistivity mean value)

The lines stemming from the reference point (the centre of the experimental domain) towards the right show that components F and G are the most active to decrease the electrical resistivity, while A and B are the components that produce the largest increase in the electrical resistivity. These results are confirmed by the analytical data of the components' effects (that is, the variation in response induced by a component when its proportion changes from minimum to maximum) for each component shown in Table 16. The significant negative effects (probability $p<0.05$) are those of interest, because low values of electrical resistivity are desirable. If a component effect has a large negative effect, it means that it effectively contributes to lower the electrical resistivity.

Component	Component Effect	Prob > | t |	
A	1.71	0.0331	significant
B	2.01	0.0068	significant
C	0.55	0.2086	
D	-0.36	0.2847	
E	0.53	0.2148	
F	-1.12	0.0307	significant
G	-2.74	0.0003	significant
H	-0.13	0.0837	

Table 16. Component effect for the response R (electrical resistivity)

Based on Table 16, it can be concluded that G and, at a lower extent, F are the most important components to decrease the electrical resistivity.

4.2.2.2 Flame retardancy

Operating in the same way than the preceding section, the Cox trace plot (not presented here for brevity), leads to the conclusion that the most important effects are given by A, negative, and B, positive. The analytical data (Table 17) confirm these results.

Component	Component Effect	Prob > | t |	
A	-1.27	< 0.0001	significant
B	0.76	0.0005	significant
C	-0.09	0.3494	
D	0.16	0.0811	
E	0.18	0.1166	
F	0.17	0.1616	
G	0.13	0.2706	
H	-0.11	0.2640	

Table 17. Component effect for the burning response of DOE 1

Since the response of the samples analysed here is the fraction of the specimen producing the worst results of flame retardancy, large negative effects are desirable. Therefore, it can be stated that the component A is the only component capable of improving the flame retardancy test (decrease the materials flammability). It may be noteworthy to mention that, surprisingly, the component B has a strong positive effect, i.e. worsens the flame retardancy properties.

4.2.3 Conclusions

In order to improve both the electrical and the flame retardancy properties of the mixture, it was reasonable to bring forward the following components:

- A, which lowers the burning
- F, which lowers the electrical resistivity
- G, which lowers the electrical resistivity

It should be noted that, unfortunately, the component A also presented the undesirable effect of increasing the electrical resistivity. However, the component A was kept due to the possibility of finding a satisfactory trade-off between the effects of the two responses during the optimization study.

4.3 Rational reduction of the mixture complexity

The rational reduction of the mixture complexity aimed at investigating the mixture

components identified by the screening that could be reduced and thus simplifying the mixture.

The mixture screening study recommended to keep the components A, F, and G in the next phase of experimentation. However, it was decided to maintain only one component that improved the electrical resistivity of the formulations. Therefore, the component G was excluded from further experimentation. Thus, from the screening study, only A and F were selected to bring forward for the rational reduction and the subsequent optimization studies.

In addition, two pre-selected flame retardants (I and J) were included among the materials to be used in the next experimentation because it was necessary for the search of synergistic effects among flame retardants.

A last strategic decision was made in the subsequent experimentation step. According to a requirement of the partner company, the total additives load was reduced from 0.28 to 0.21.

In summary, the following components were selected to carry out the next phase (optimization):

- TPU (Polymeric matrix)
- CNTs
- F
- A
- I
- J

4.4 Optimization and verification

4.4.1 Mixture optimization

In this stage, an experimental plan (DOE 3) was designed to explore the 3 flame retardants mentioned in Section 4.3. Thus, an augmented simplex-lattice design, supporting a quadratic mixture model was implemented, with a total of 12 runs, including 2 replicates (runs 1 and 3).

The fraction of F was kept constant (0.03) together with TPU (0.79) and CNTs (0.03). These components sum to a total of 0.85, and the three flame retardants count a total fraction of 0.15. As required, the total additives load amounts to 0.21 (that is, 0.03 of F + 0.03 of CNTs + 0.15 of FRs). The mixture system with all formulations is shown in Table 18.

RUN	MIXTURE COMPONENTS			
	A	I	J	CNTs + F + Polymer
1	0	0.1125	0.0375	0.85
2	0.075	0.075	0	0.85
3	0.05	0.0875	0.0125	0.85
4	0	0.075	0.075	0.85
5	0	0.15	0	0.85
6	0.0375	0.1125	0	0.85
7	0.0375	0.075	0.0375	0.85
8	0.025	0.10	0.025	0.85
9	0.0125	0.125	0.0125	0.85
10	0.0125	0.0875	0.05	0.85
11*	0	0.1125	0.0375	0.85
12*	0.05	0.0875	0.0125	0.85

Table 18. Formulations used in the optimization DOE 3

**Runs 11 and 12, are replications of runs 1 and run 3, respectively.*

4.4.1.1 Electrical resistivity

Twenty specimens of each run were tested and the electrical resistivity average results are shown in Table 19.

	Electrical Resistivity [Ω.cm]	
Run	Extruded Specimens Not Annealed	Injection Moulded Specimens Annealed
1	2.43E+03	9.59E+04
2	5.20E+02	3.60E+04
3	7.12E+02	9.71E+04
4	2.72E+03	1.32E+05
5	4.77E+02	4.40E+04
6	6.77E+02	2.58E+04
7	1.29E+03	5.77E+04
8	1.02E+03	5.97E+04
9	4.59E+02	4.77E+04
10	1.21+E03	5.95E+04
11	1.13+E03	1.43+E05
12	5.75+E02	8.54+E04

Table 19. Electrical resistivity test results for the mixture of DOE 3

The response of non-annealed specimens was subjected to statistical analysis and resulted in a linear model with a satisfactory fit: $p<0.0001$ (significant), p(Lack-Of-Fit)= 0.2728, Adj-Rsquared= 0.9054. This model was exploited for finding the mixture composition giving the optimum response, corresponding to the minimum electrical resistivity: A = 0.00, I =0.15 and J= 0.00. At this optimum point, the electrical resistivity response is 449.75 Ω.cm.

4.4.1.2 Flame retardancy

The flame retardancy tests were carried according to the UL94 Standard. As explained in Section 3.6.2, the UL94 Vertical Burning test is designed to classify the material by taking into consideration both (i) the performance of each individual specimen, and (ii) the performance of 5 specimens considered collectively. As it is difficult to use this procedure to assign a suitable response in a statistical study, in this work each flame retardancy test result was classified individually according to the following rules:

- V0 = if either at the first or at the second ignition the specimen does not burn or burns within 10 seconds
- V1 = if either at the first or at the second ignition the specimen does not burn or burns within 30 seconds
- V2 = like V1, but the material drips and burns the cotton.
- VA = if at the first ignition the specimen does not burn, and at the second ignition it burns up to 50 seconds without reaching the clamp.
- VB = if at the first ignition the specimen does not burn, and at the second ignition it burns completely and/or reaches the clamp.
- n.c (not classified) = if at the first ignition the specimen burns completely and/or reaches clamp.

Forty specimens of each run were submitted to the UL94 Vertical Burning test. The obtained results, which rated as V0, V1, V2, VA, VB, and n.c., are listed in Table 20.

	UL 94- Injection Moulded Specimens (Not Annealed)					
Run	**V0**	**V1**	**V2**	**VA**	**VB**	**n.c**
1	32	3	-	-	5	-
2	38	2	-	-	3	-
3	38	2	-	-	-	-
4	26	4	-	-	-	-
5	-	4	-	3	-	3
6	-	16	-	-	6	-
7	-	1	-	-	5	-
8	31	6	-	-	3	-
9	26	6	-	1	7	-
10	29	6	-	-	5	-
11	32	3	-	-	2	-
12	38	2	-	-	-	-

Table 20. UL94 Vertical Burning test results classified as V0, V1, V2, VA, VB, and n.c for the mixture of DOE 3

All of these flame retardancy responses are categorical, therefore they cannot be directly used in a statistical analysis. For this reason, a rule to transform these categorical data to numeric data, was created. The new response, FSCORE, describes the burning performance by assigning combustion pseudo-times to the specimens. For combustion classes V0 and V1, FSCORE is the sum of the real observed combustion times of the two ignitions (in seconds). The other classes are conventionally assigned higher and higher times in such a way to produce higher and higher penalizations going through classes V2 = 90, VA = 100, VB = 110 and n.c.= 120, respectively. Note that for our purposes, low values of FSCORE are desirable.

A quadratic mixture model fit the data well: $p<0.0001$ (significant), p(Lack-Of-Fit)= 0.1537 (not significant); Adjusted Rsquared = 0.9583. The numerical optimization led to the mixture composition best suited to improve the flame retardancy properties, corresponding to the minimum FSCORE value. This was found to be located at point A-A= 0.065, I =0.085 and J= 0.00. At this point FSCORE = 5.3 sec.

4.4.1.3 Simultaneous flame retardancy and electrical resistivity

In this analysis, the flame retardancy and the electrical resistivity were considered simultaneously. The combined numerical optimization found the global optimum at the composition point: A = 0.065, I =0.085 and J= 0.00. At this optimum point, the responses are the following: Resistivity = 530; FSCORE = 5.3.

4.4.1.4 Conclusions

This optimization study recommended to repeat the best experimental run (A= 0.065, I =0.085 and J= 0.00), which demonstrated the best flame retardancy and an acceptable electrical resistivity. Therefore, another experiment to verify the optimality of the predicted model was carried out.

4.4.2 Verification

The predicted global optimum was verified by carrying out some experimental trials at the identified mixture composition. The experimental design (DOE 4) was

implemented and the experiments were carried out (Table 21). In this design, the fractions of TPU, CNTs and F were also kept constant.

BLOCK	RUN	MIXTURE COMPONENTS			
		A	I	J	CNTs + F + Polymer
1	1	0.0500	0.0875	0.0125	0.85
1	2	0.0650	0.0850	0.000	0.85

Table 21. Formulations used in the verification DOE 4

Forty specimens of each run were used for the electrical resistivity tests (average values) and the UL94 Standard tests. The results are summarized in Table 22. It is worth to mention that both materials were classified as V0.

Run	Electrical Resistivity of the extruded sample- not annealed [ohm.cm]	UL 94- Standard test
1	1.36E+03	V0
2	8.43E+02	V0

Table 22. Electrical resistivity and UL94 Standard test results of the mixtures of DOE 4

Run 1 and Run 2 were replicated to ensure the selection of the final formulation. Fifty specimens of each run were used for the electrical resistivity and the UL94 Standard tests. The average results are shown in Table 23.

Run	Electrical Resistivity of the extruded sample- not annealed [ohm.cm]	UL 94- Standard test
1	7.50E+02	V0
2	5.17E+02	V0

Table 23. Electrical resistivity and UL94 Standard test results of the mixtures of DOE 4 (replication)

4.4.3 Conclusions

The final composition (Run 2, Table 21) was TPU=0.79; CNTs=0.03; F=0.03; A=0.065; I=0.085 and J = 0.00 (in other words, J was eliminated), for which the predicted values of the maximum flame retardancy and the minimum electrical resistivity were considered satisfactory.

4.5 Process strengthening and verification

In the process strengthening and verification, the compounding of the final selected formulation (Run 2 of DOE 4) shown again in Table 24, was replicated at laboratory and carried out at industrial scale several times in order to confirm the simultaneous

accomplishment of the desired target values of the flame retardancy (V0 compliant) and the electrical resistivity (≤1000 ohm.cm).

Components	Final Formulation
A	0.065
J	0.085
CNTs + F + Polymer	0.85

Table 24. Optimized formulation

48 specimens of this formulation were used for the electrical resistivity tests and ten specimens for the UL94 Standard tests. The average results for the samples compounded at laboratory scale and industrial scale are shown in Table 25 for comparison.

Compound	Electrical Resistivity of the extruded sample-not annealed [ohm.cm]	Electrical Resistivity of the injection moulded sample – not annealed [ohm.cm]	Electrical Resistivity of the injection moulded sample - annealed [ohm.cm]	UL 94 Standard test
Lab scale	3.12E+03	1.50E+07	1.30E+04	V0
Industrial scale	6.82E+02	5.40E+06	3.51+03	V0

Table 25. Electrical resistivity and UL94 Standard test results of the optimized formulation

4.6 Conclusions

An effective formulation of the bio-based polymeric composite with the desirable values of the flame retardancy (V0 compliant) and the electrical resistivity (≤1000 ohm.cm) was developed, exploiting a DOE approach.

A significant difference in the electrical resistivity between extruded samples and injection moulded samples (annealed and not annealed) can be noted from the test results of the final formulation (Table 25).

Therefore, the process type and conditions used during the experiments affected the material electrical conductivity. This finding can be explained by the dynamic percolation behaviour of the CNT network during the melt. The dynamic percolation behaviour refers to the comportment of the composite during processing, when it is in the molten state, in which it is submitted to flow or shear (necessary condition for the dispersion of CNTs). Either if the flow or shear, in the molten state, destroy the formation of conductive networks, or if the conductive fillers re-aggregate forming an efficient conductive network, the final composite will have either a bad or a good

conductivity, respectively [1].

From the experimental results, it can be also noted that the extruded material, which has a lower electrical conductivity (i.e. an increased electrical resistivity) after the injection moulding process, has partially recovered the electrical conductivity (by 3 orders of magnitude) by annealing the material at relatively high temperature (100 °C) for a period of 20 hours.

Cipriano et al. showed that melt annealing at temperatures above the polymer glass transition temperature (but below its thermal degradation temperature) is an efficient way for improving the conductivity of nanocomposites by several orders of magnitude.[2] The explanation given by Cipriano et al. is that, during processing, the exerted shear aligns the CNTs, and thus decreases their degree of inter-connectivity and consequently the conductivity. However, when the material is submitted to annealing, the particle distribution becomes more isotropic and their connectivity increases, thus increasing the electrical conductivity.

4.7 References

[1] F. Jiang, L. Zhang, Y. Jiang, Y. Lu, W. Wang, “Effect of annealing treatment on the structure and properties of polyurethane/multiwalled carbon nanotube nanocomposites”. Journal of Applied Polymer Science 126 (2012), 845–852.

[2] B.H. Cipriano, A.K. Kota, A.L. Gershon, C.J. Laskowski, T. Kashiwagi, H.A. Bruck, S.R. Raghavan, “Conductivity enhancement of carbon nanotube and nanofiber-based polymer nanocomposites by melt annealing”. Polymer 49 (2008), 4846–4851.

5 Characterisation of the electrically-conductive flame retardant TPU composite

5.1 Introduction

This chapter reports on the effects that improve the flame retardancy properties of the TPU blended with phosphinate-based compounds (A and I) and nanofillers (CNTs and F). The fire behaviour of the TPU compounds mixed with CNTs, A, F and I is investigated with UL-94 test. The thermal stability is studied by using TGA and DSC techniques, whereas the dispersion of the additives is assessed by SEM measurements. In addition, EDS measurements help to identify how the elements were distributed on the material surface.

5.2 Experimental setup

5.2.1 Specimens

The samples were obtained using the same extruder and injection moulding machine already employed for the previous experiments. The compositions of the formulations used in this work are described in Table 26.

Components	**Material A: Final Formulation [wt%]**	**Material B: Electrically Conductive composite [wt%]**
A	6.5	-
I	8.5	-
F	3	3
CNTs	3	3
TPU	79	94

Table 26. Formulation composition of materials A and B

5.2.2 Thermal analysis

5.2.2.1 TGA

Thermogravimetric analyses (TGA) were carried out at a heating rate of 10 °C/min under Nitrogen using a Q500 apparatus from TA instruments. In each case, the samples (10 mg) were positioned in opened alumina pans. The precision of the temperature measurements was ±1 °C in the range 50-600 °C.

5.2.2.2 DSC

Heat flow was determined by using a differential scanning calorimeter (DSC Q2000

from TA instruments). The samples were heated from 20 °C to 400 °C at a heating rate of 10° C/min under Nitrogen.

5.2.3 Fire testing- UL-94 test

The test was carried out on barrels of 125mm x 13mm x 3.2 mm according to the American Society for Testing and Materials (ASTM D3801-10). Therefore, five samples were pre-conditioned for 48 hours at 23°C in the presence of 50% RH (relative humidity). Another five samples were pre-conditioned for 168 hours at 70°C.

5.2.4 SEM/EDS

Morphological characteristics were analysed on fractured char surface of samples by means of SEM imaging with integrated EDS (JSM-6010/LA from JEOL)

5.3 Results and discussion

5.3.1 UL94-test results

The UL-94 test results of the final formulation in different pre-conditioning are given in Tables 27 and 28. From both tables it can be seen that all samples were rated as V-0. These results indicate the efficiency of the two flame retardants in this composite.

Sample	**Thickness (mm)**	**t_1 (s)**	**t_2 (s)**	**$t_2 + t_3$ (s)**	**t_f (s)**	**After flame up to the holding clamp**	**Cotton indicator ignited by flaming particles or drops**
1	3,23	0,0	2,1	2,1	10,6	NO	NO
2	3,22	0,0	2,4	2,4		NO	NO
3	3,22	0,0	2,8	2,8		NO	NO
4	3,22	0,0	3,3	3,3		NO	NO
5	3,22	0,0	0,0	0,0		NO	NO
					Classification of the Material		
Average	3,22	0,0	2,1	0,0	V0		
SD	0,0	0,0	1,3	0,0			

Table 27. 48 hours at 23°C; RH 50%

Sample	**Thickness (mm)**	**t_1 (s)**	**t_2 (s)**	**$t_2 + t_3$ (s)**	**t_f (s)**	**After flame up to the holding clamp**	**Cotton indicator ignited by flaming particles or drops**
1	3,22	0,0	2,8	2,8	13,9	NO	NO
2	3,22	0,0	1,5	1,5		NO	NO
3	3,23	0,0	1,7	1,7		NO	NO
4	3,22	0,0	3,2	3,2		NO	NO
5	3,23	0,0	4,7	4,7		NO	NO
					Classification of the Material		
Average	3,23	0,0	2,8	0,0	V0		
SD	0,01	0,0	1,3	0,0			

Table 28. 168 hours at 70°C

5.3.2 Thermal analysis

A preliminary investigation on the potential mechanisms of interactions among the formulation components was carried out by means of thermal analyses (TGA and DSC). The tests were carried out on both the flame retardants chemicals and the final formulation.

5.3.2.1 DSC results

DSC analysis can be used to indicate chemical modifications among the flame retardants through the changes of the heat released. Therefore, DSC tests for the individual flame retardants (Figure 18 and Figure 19) and their combination (Figure 20) were carried out from 20°C to 400°C in the presence of Nitrogen. Due to the appearance of signal disturbances in the plots after 230°C, the curves were analysed up to 230°C only. From Figure 32, it can be seen that the experimental and calculated DSC curves of the combined flame retardants did not show any changes, thus indicating the absence of chemical interaction until 230°C. The reason is that the material decomposition starts after 230 °C (as it will be seen in the TGA studies).

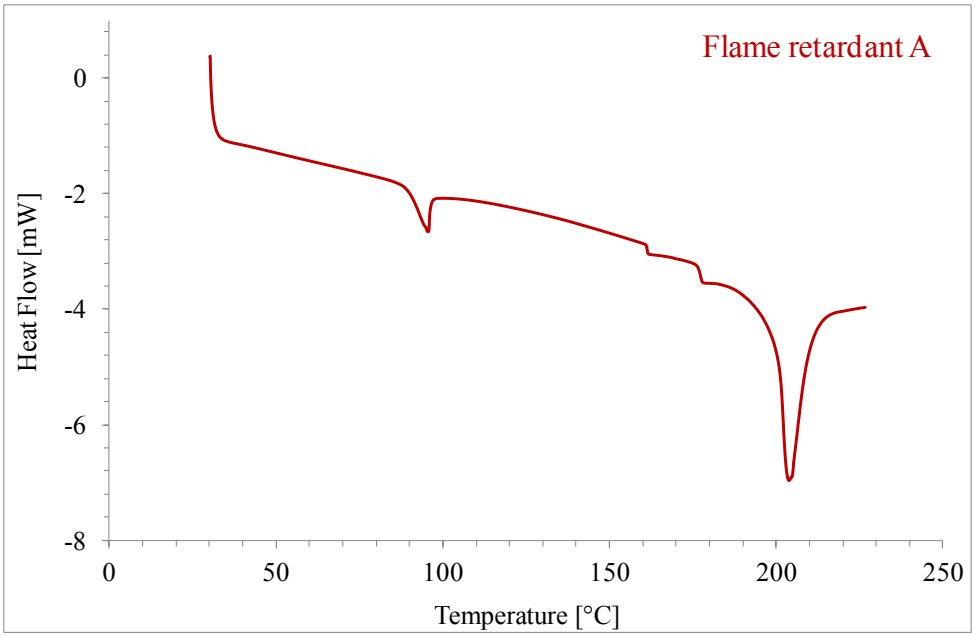

Fig 18. DSC curve of Flame retardant A

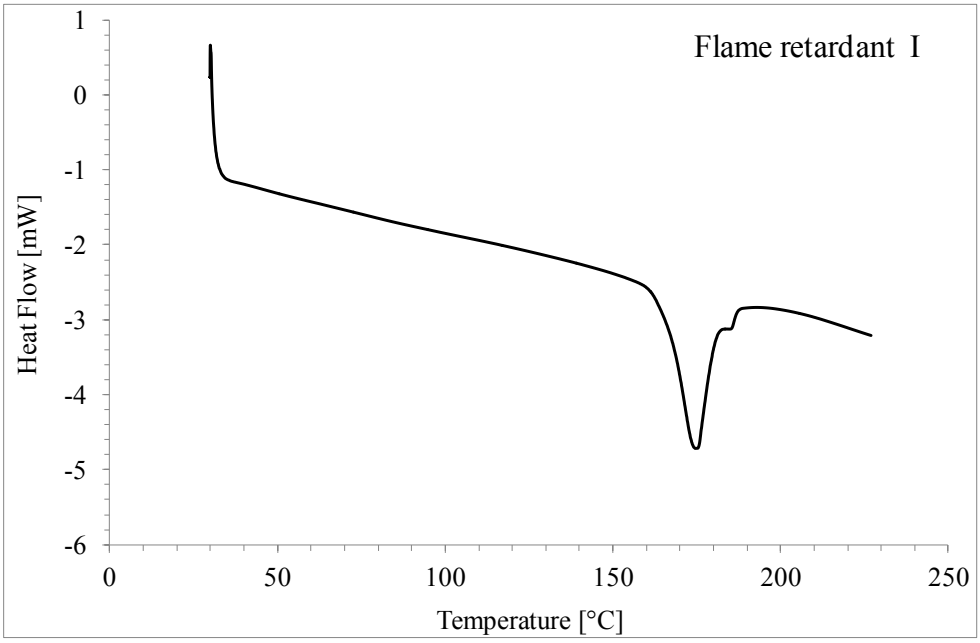

Fig 19. DSC curves of Flame retardant I

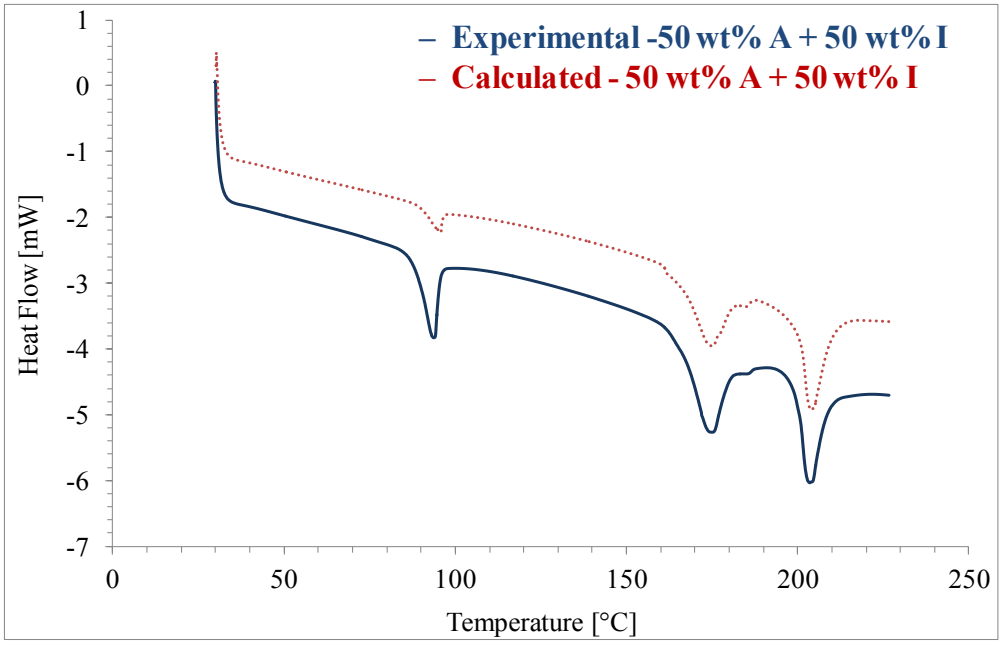

Fig 20. Experimental and Calculated DSC curves of 50 wt% A+ 50 wt% I

5.3.2.2 TGA results

Figure 21 shows the experimental TG curves of A and I. The thermal decomposition of flame retardant A and flame retardant I are characterized by a single step from about 430°C to 480 °C, and from 260 °C to 310 °C respectively.

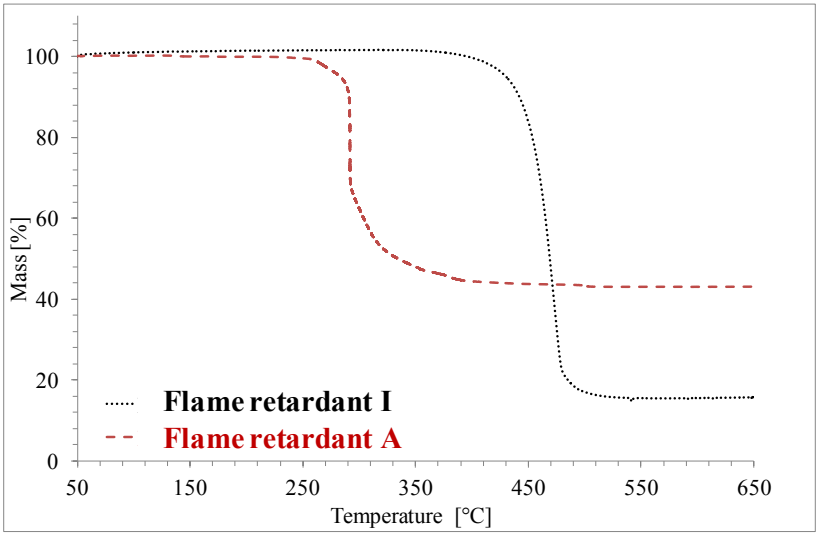

Fig 21. Experimental TG curves of Flame retardant I and Flame retardant A

Figure 22 exhibits the experimental and calculated TGA curves of 50wt% A + 50wt% I. For the calculated curve, the decomposition should take place in two steps, the first from 260 °C to 310 °C, and the second from 370 °C to 490 °C. Also the experimental curve shows two main steps of thermal degradation, but the first step starts 30°C higher than expected, i.e. at 290°C instead of 260°C, and ends at 370°C instead of 310°C. The chemical interaction between the two FR leads to the formation of a higher residue than expected (47%).

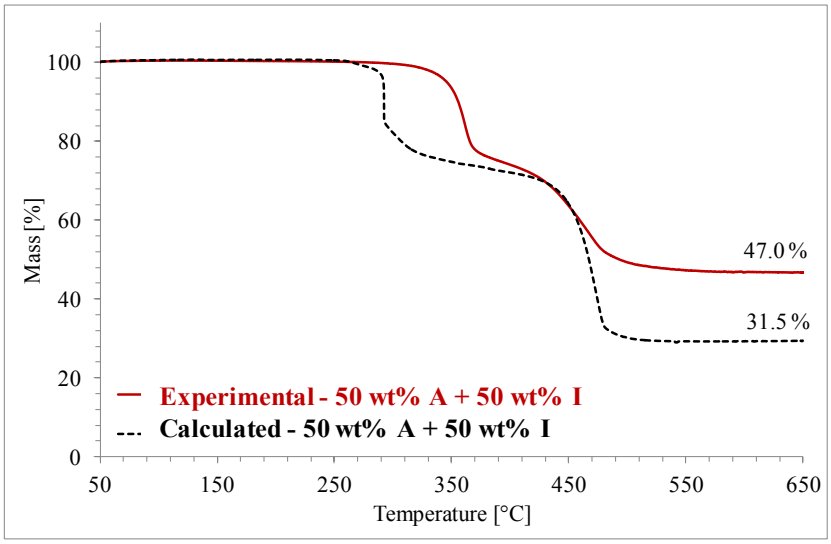

Fig 22. Experimental and Calculated TGA curves of 50 wt% A+ 50 wt% I

Figure 23 shows the TGA curve of the conductive compound (CNTs/F/TPU). It can be seen that there are three decomposition steps: the first step occurs between 230 °C and 300 °C, the second step from 300°C to 365 °C, and the third step between 365°C and 430°C. The residue at 650 °C is 8.0%.

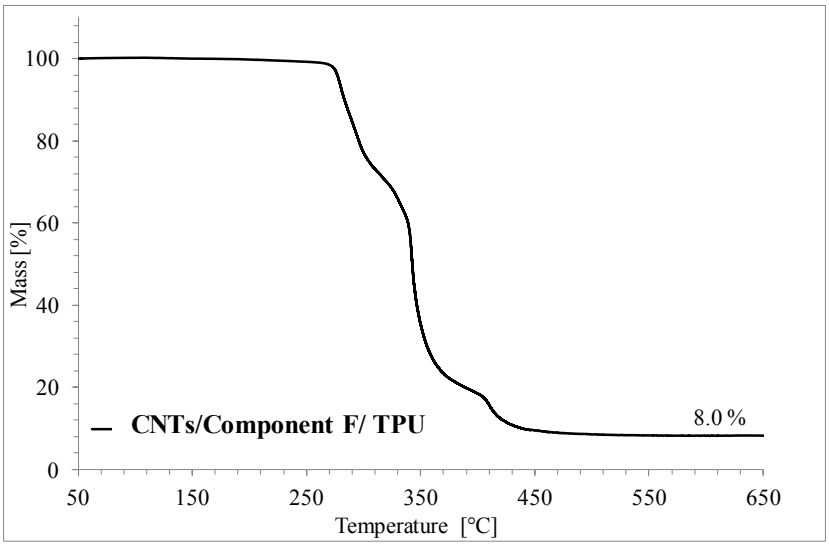

Fig 23. TGA curves of CNTs/Component F/TPU

Figure 24 shows significant differences between the experimental and calculated TGA curves of the final formulation. The differences between the calculated and experimental TGA curves show that the interaction among the flame retardants, the polymer and the conductive fillers leads to a higher on-set of the weight loss and a higher residue than expected, thus confirming the efficiency of the flame retardant system.

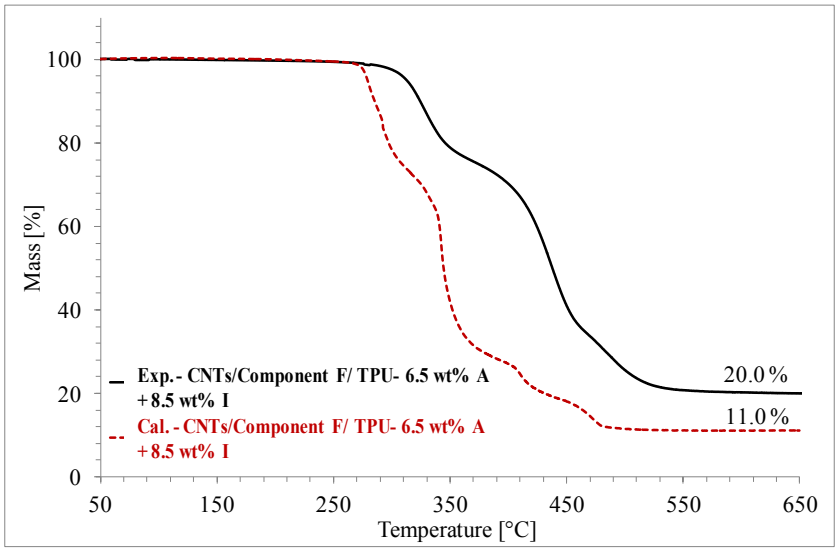

Fig 24. Experimental and Calculated TGA curves of final formulation

5.3.3 SEM/EDS results

The microstructure of the carbonaceous residue of the UL94 V0 specimens was analysed by SEM/EDS.

SEM micrographs at different magnifications (Figure 25a-c) show that the external

surface of the char is smooth with some evidence of bubbles formation (Figure 25a). Small voids are present underneath (Figure 25b). Figure 37c shows that the char surface is mainly closed with only few small cracks. The intumescent shield avoids the formation of cracks and thus the heat and mass transfer are limited, leading to the interruption of the material combustion. [1-3]

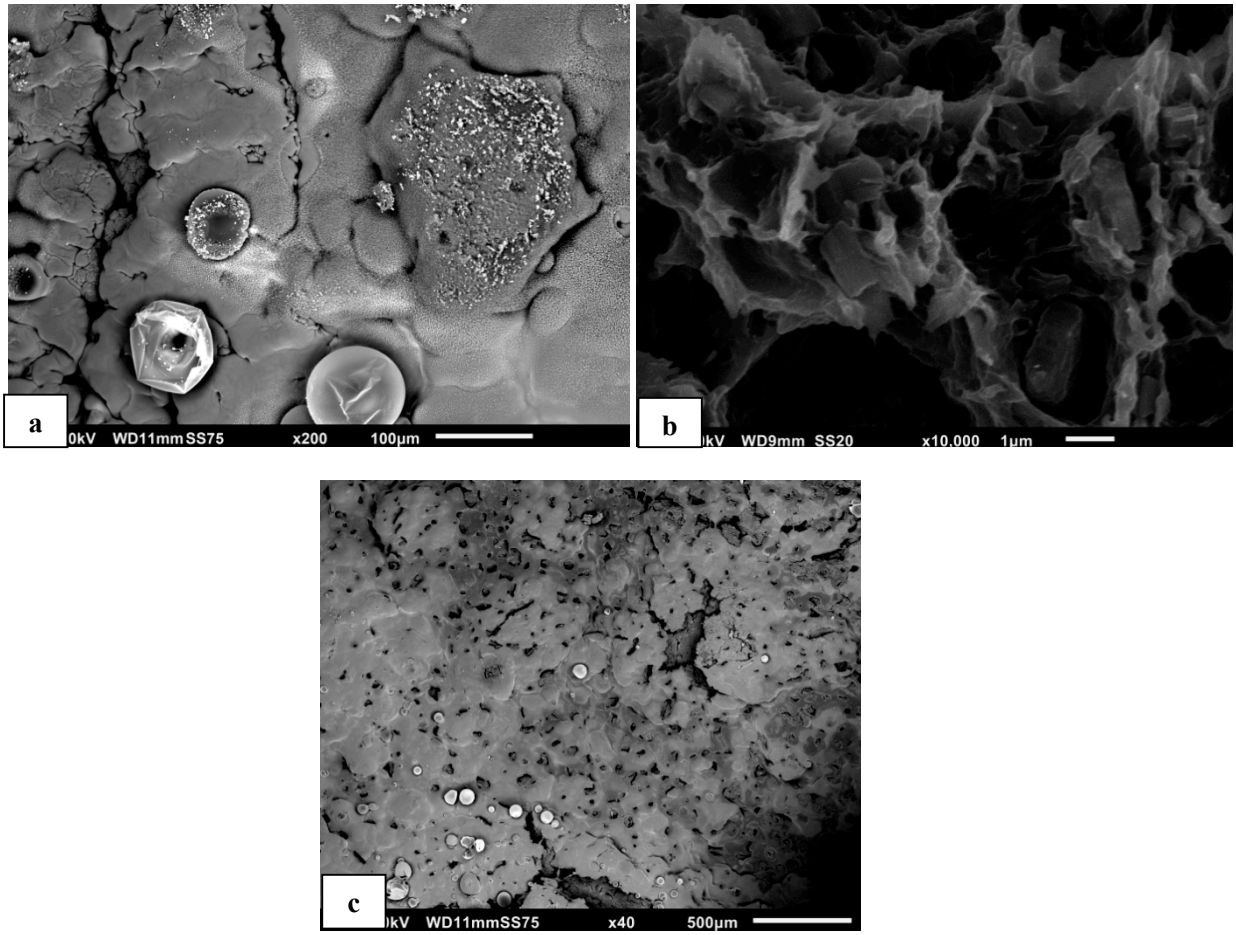

Fig 25. SEM micrographs of combustion chars from: CNTs/ Component F/TPUs fire retarded with Flame retardant I and Flame retardant A. (a) outer surface x200 ; (b) internal structure x70 ; (c) outer surface x40

Figure 26a shows the transition of the burnt to non-burnt area of the material, where the intumescent char is formed protecting the underlying material from degradation. The images (Figure 26 b-g) allowed the chemical analysis of the external surface of the char, showing the presence of Aluminium, Phosphorous, Calcium and Silica, which are residues of flame retardants used in the formulation. There is an homogeneous distribution of these elements on the material char, therefore the formation of the protective layer is built up without segregating any of the organic and inorganic elements of the mixture.

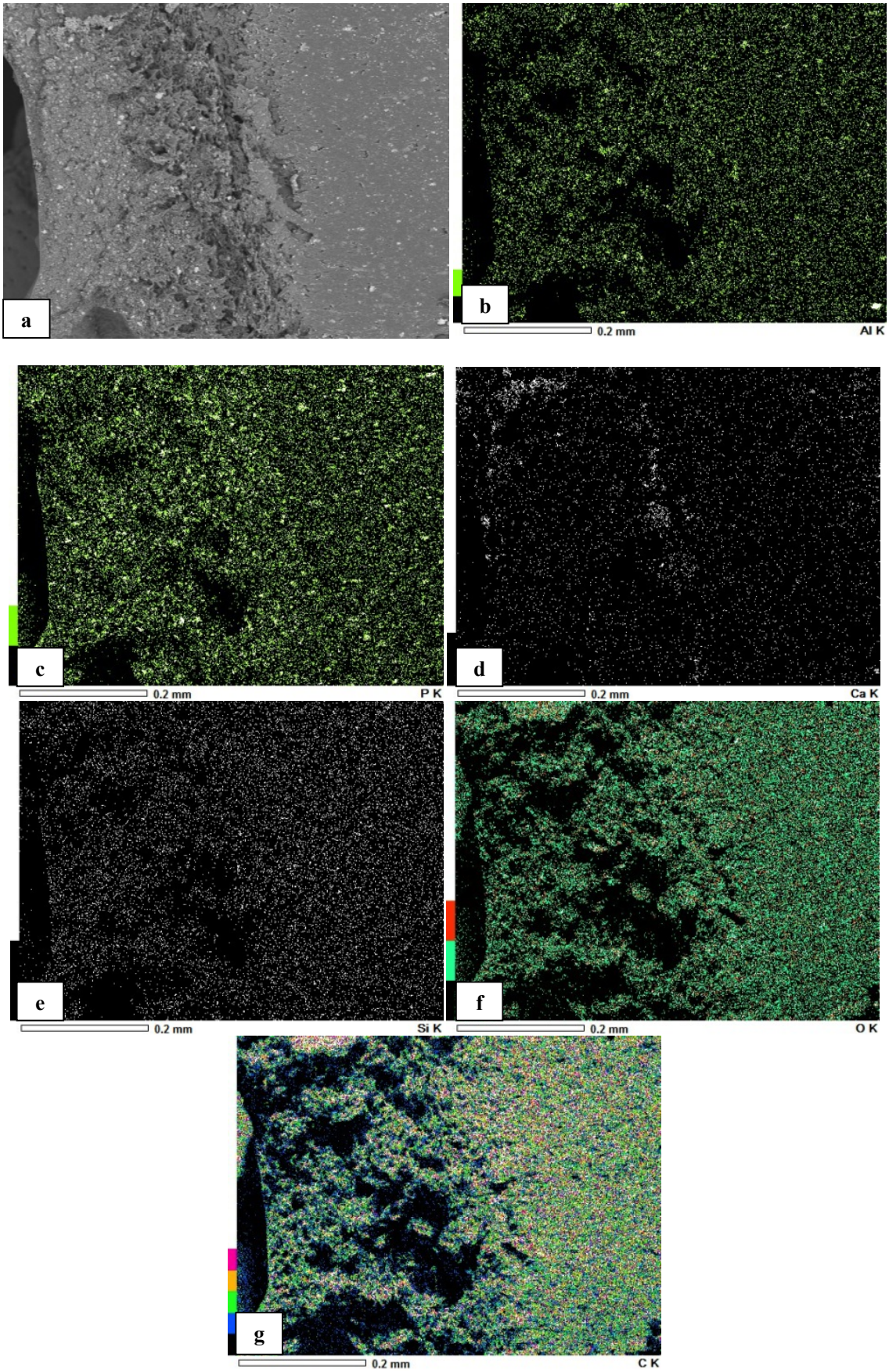

Fig 26 a-g. SEM/EDS micrographs

A typical output of the EDS microanalysis of the combustion char is shown in Figure 27.

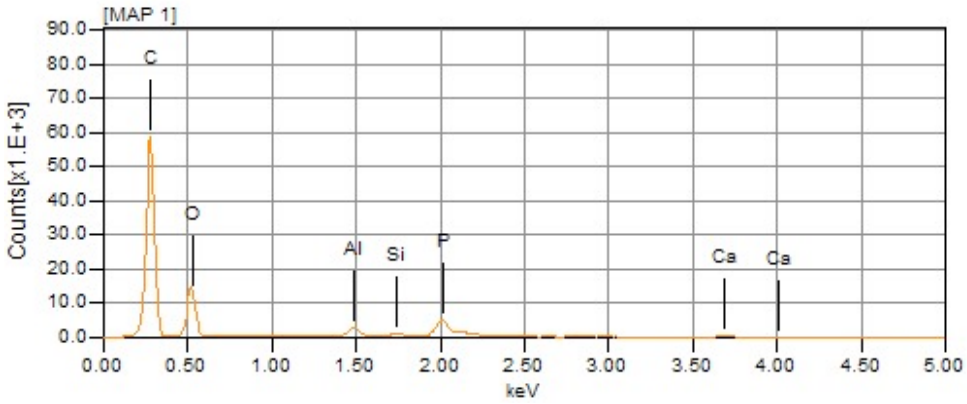

Fig 27. EDS microanalysis of outer surface of combustion char of Figures 38.

5.4 Conclusions

It is difficult to define a chemical action mechanism of the flame retardant system without (i) expanding this study to analyse the possible interactions taking place among all the components; and (ii) using further analytical techniques. Therefore, within this study we can only suggest that the reaction between Flame retardants A and I results in the formation of polyphosphonate salts, which are very stable and avoid the significant weight loss. Further studies are under way to better understand the chemical reactions occurring on heating flame-retarded polymers with these intumescent systems. Preliminary results already showed that the effectiveness of the intumescent flame retardants is due to the foamed char formed on the surface of the burning material, which acts as a physical barrier against heat transfer to the surface of the combustible material.[1]

In addition, in the next chapter a study to correlate the dynamic response of the material to its UL-94 fire test performance will be presented. For that, a novel apparatus was developed to monitor the shield growth even in the presence of flames.

5.5 References

[1] G. Camino, L. Costa, and G. Martinasso, “Intumescent fire retardant systems”. Polymer degradation and Stability 23 (1989), 358-376.

[2] B. Schartel, “Review: Phosphorus-based flame retardancy mechanisms—old hat or a starting point for future development?”. Materials 3 (2010), 4710-4745.

[3] S. Bourbigot, S. Duquesne, “Fire retardant polymers: recent developments and opportunities”. Journal of Materials Chemistry 17 (2007) 2283–2300.

6 An online acquisition method for monitoring the surface growth of flame retardant protective layers

6.1 Introduction

As a consequence of heat activation, flame retardants acting in condensed phase, e.g. intumescent and glass forming systems, build up a protective layer on the underlying material [1-3]. The chemical and physical properties of this protective layer have been extensively studied and the obtained results reported in the open scientific literature. As an example, the structure, chemical composition, expansion temperature interval, mechanical resistance and thermal conductivity of intumescent flame-retardants have been investigated either through experiments or simulations in order to correlate the physico-chemical characteristics of the carbonaceous protective layer with its barrier properties [1-4]. The intumescent volume expansion as a function of temperature has been studied using tailor-made apparatuses [5, 6], heating microscopy [7, 8] and rheometry (plate-plate configuration), which allows correlating the char swelling with its rheological characteristics [9-11].

These experimental set-ups somehow define different scenarios with respect to a real fire and most of flammability and combustion tests, such as UL94, Cone Calorimeter, Limiting Oxygen Index (LOI), etc. The heating source is a furnace [5, 6, 8, 12], and the char expansion measurements are done under controlled temperature [5-10, 12]. In some cases, the facilities introduce some constrains to the evolution of the char: i.e. the expansion takes place in a confined space, and the specimens are subject to a normal force so that the char is not completely free to expand [5,6].

Nevertheless, the systems used so far, usually combined with investigation on mechanisms of thermal degradation of materials [5, 6], have certainly promoted a deeper understanding of intumescent and glass forming systems. Indeed, this knowledge has been extensively used to interpret, ex-post [13, 14] the fire performances achieved by materials subjected to several different fire tests such as UL94, LOI, Glow Wire Ignition (GWI), Cone Calorimeter, etc.

On the other hand, the ex-post fire performances evaluation of flame retardants acting in condensed phase may show some disadvantages, as it can be performed only after the fire test and thus it could miss some noteworthy and useful perspectives directly related to the dynamic evolution of the material during the fire test.

Therefore, the need to investigate some of the dynamics involved in fire tests has pushed this thesis work towards the building up of a specific apparatus aimed at providing information on the growth dynamics of any kind of protective layer upon exposure to a flame source. The system proposed in this work delivers an on-line direct view of the protective layer development, correlating the dynamic response of the material to its fire test performance. The device in situ monitors the shield growth even in the presence of flames that usually hinder the direct observation of the burning surface.

As test bed for the system, flammability measurements according to UL94 standard were performed on phosphorous-containing flame retarded polyurethanes; the obtained data have been correlated with the fire behavior of the selected materials.

6.2 Materials and methods

6.2.1 Materials

UL94 V0 (no burning) and UL94 n.c. (burning) thermoplastic polyurethane formulations comprising different concentrations of flame retardants were prepared and tested. The polyurethane was a Pearlthane® Eco D12T80 from Merquinsa, whereas the flame retardants were commercial phosphonates and phosphinates. The precise composition of the formulations cannot be disclosed, since subject to exploitation by the industrial partner co-baker of this work. Composites were blended by a twin-screw extruder type ZSE 18 HP – 40 D from Leistritz; the testing specimens (125mm x 13mm x 3.2mm) were moulded using an injection moulding machine Allrounder 270/320C from Arburg.

6.2.2 Methods - Flammability test

UL94 (vertical) measurements were performed according to the UL 94 standard test. The specimens (125mm x 13mm x 3.2mm) were ignited at the lower-end with a Bunsen burner flame (20mm in length) for a period of 10s, afterwards the burner was removed for 30 seconds, then reapplied to the same location for 10 additional seconds.

6.3 Video acquisition system and data analysis

The system continuously monitors the material surface recording a video in a non-

invasive way. The acquired images are then processed by a dedicated software, providing quantitative data of the protective layer growth dynamics.

The experimental set-up consists of a CMOS industrial camera from IDS and a personal computer used to acquire and digitize the char image signals from the camera unit (Figure 28). The specifications of the imaging sensor are shown in Table 29. The graphical unit interface (GUI) was written in C# using MS Visual Studio®. The acquired videos were then post-processed with the MVTec Halcon software to extract the key characteristics.

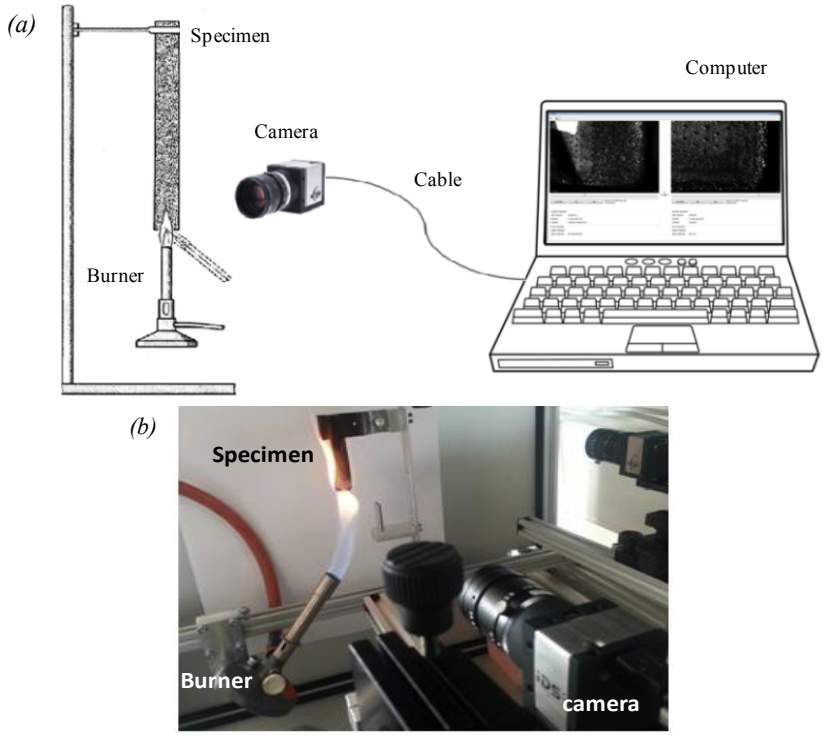

Fig 28. The experimental apparatus. (a) System representation; (b) Experimental set-up.

2D SENSOR SPECIFICATIONS	
Manufacturer and model	IDS uEye UI-1220SE-M-GL
Sensor Technology CMOS	Mono
Resolution (h x v)	752 x 480
Color depth (sensor)	10 bit
Color depth (camera)	8 bit
Pixel Class	WVGA
Sensor Size	1/3"
Shutter Global	Shutter
max. fps in Freerun	Mode 87.2

Table 29. Imaging sensor specifications

Figure 29 shows three snapshots extracted from a video acquired while the flame was surrounding the specimen. These snapshots refer to the first (Figure 29a and b) and

the second flame application (Fig. 29c). The system minimizes the flames disturbances on the sensors providing good quality images of the surface, thus making the formation and growth dynamics of the protective layer clearly visible. Furthermore, layer features such as cracks and holes can be monitored and analyzed. As an example, the timing of holes and cracks in the protective shield can be studied and eventually correlated with the barrier effectiveness.

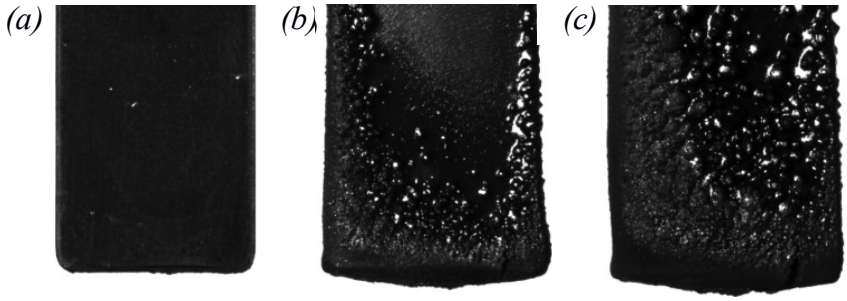

Fig 29. Sequence of images obtained during the UL94 test. (a) and (b) are snapshots taken at the beginning and at the end of the first flame application, respectively. (c) snapshot was taken at the end of the second flame application.

Videos post-processing allows to automatically extract quantitative data on the protective layer growth rate (PLGR), expressed as square millimetres per second [mm^2/s]. The snapshots in Figure 30 show the steps, through which the PLGR is obtained. The first step (Figure 30a) involves the measurement of the 5mm circular moulding mark to calibrate the mm/pixel ratio of the image. The second step (Figure 30b) comprises the identification of flat surface areas and the filtration of the disturbance/interference exerted by smoke and flames. Finally, the third step (Figure 30c) calculates the areas with the features of interest.

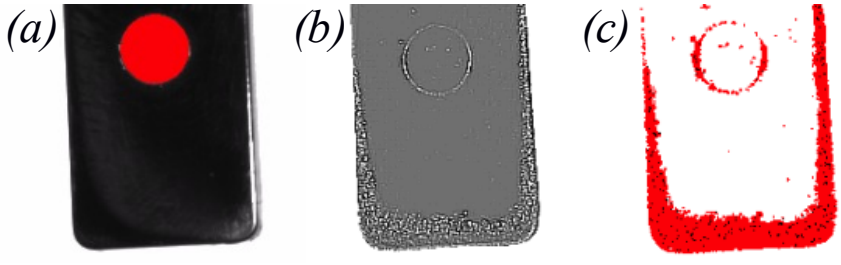

Fig 30. Steps to obtain the char formation rate: (a) Measurement of the 5mm circular moulding mark; (b) Identification of flat surface areas and filtration of smoke/flames influence; (c) Calculation of the areas with the features of interest.

Figure 31a shows an image acquired during the UL94 test, whereas Figure 31b shows the images overlay and the results of the signal processing.

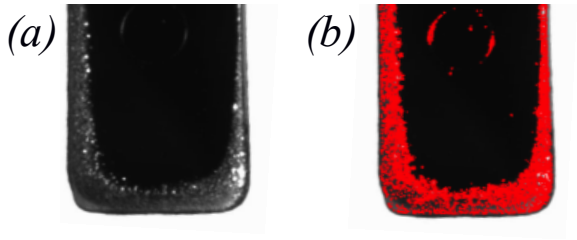

Fig 31. Image from the acquired video: (a) During UL94 test; (b) Images overlay and processing result.

The algorithm developed for the image processing is described in Figure 32. It relies on the fact that the protective layer generates small structures that are easily distinguishable from the white background, the black non-burned surface and flames interference, which are fairly large as compared to the features of interest. High pass filtering of the image separates high frequencies from low frequencies (background, flames, smoke) and returns a flat grey background everywhere except where small structures are observed. It is then possible to count the pixels, which are brighter or darker than average and thus estimate the shielding area.

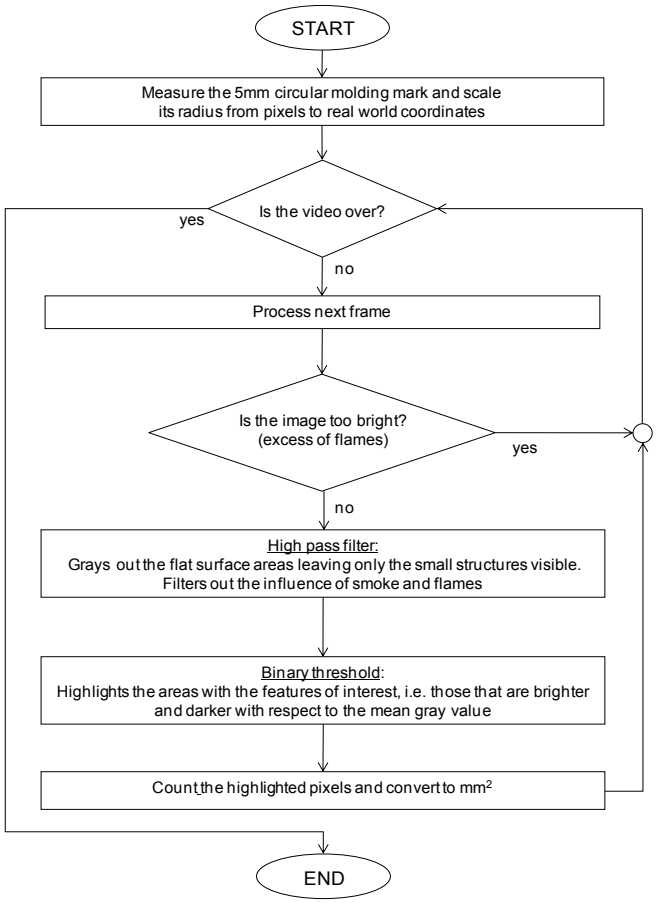

Fig 32. Algorithm used for the image processing.

6.4 Results and discussion

For the first assessment of the vision system, two flame retarded TPUs with opposite performances were selected, i.e. a UL94-V0 (no burning) and a not classified (burning material). Each plot was generated by the average of at least three measurements.

The approaching/leaving of the ignition flame disturbs all the measurements, abruptly changing the camera exposure: as a consequence, in this condition, the Bunsen flame misleads the acquisition system. In order to bypass this measurement lack, a detailed analysis of the curves can be exploited for excluding these time intervals (fitted data in Figures 35, 36, 37, 38, 41 and 42)

6.4.1 UL94-V0 PLGR analysis

A sequence of 6 snapshots is presented in Figure 33. The snapshots show the progressive growth of the protective layer while performing the UL94 test. The images from (a) to (c) refer to the first flame application, whereas images from (d) to (f) correspond to the second flame application.

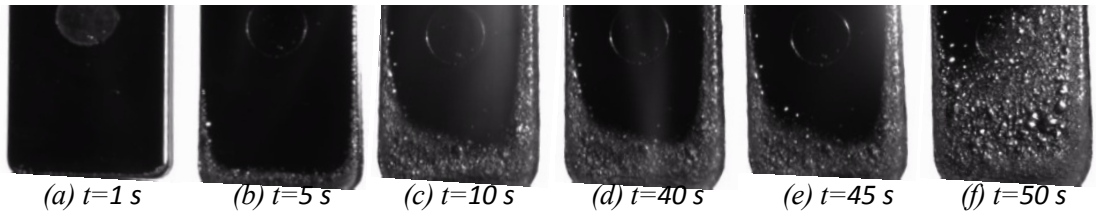

Fig 33. Images extracted from the video of the V0 flame retarded material recorded during the UL 94 flame test. (a) to (c) refer to the first flame application. Images from (d) to(f) correspond to the second flame application.

Figure 34 shows a PLGR plot for the whole UL94 test. The curve plots the extent of surface modification, expressed in mm^2, as a function of UL94 timing (seconds). The plot comprises the first (from 0 to 10 seconds: segments a and b) and the second (from 40 to 50 seconds: segments e and f) ignition flame application and the comprised time interval (30 seconds: segments c and d) (ref. UL94 test procedure).

The curve contains a measurement artefact (segment d) and missing data (end of segment f). The d artefact refers to an apparent reduction of the protective surface area, due to the ignition flame approaching, whereas a too intense flame, leading the image to be overexposed, causes the data missing at the end of segment f. The enhanced flame

intensity is due to local specimen combustion, which increases the overall brightness of the scene. Nevertheless, the material is self-extinguishing as for the UL94 standard. Segment c corresponds to the PLGR plateau at which, after the flame removal, the protective layer growth stops immediately. The most significant steps of the surface modification, corresponding to segments a, b, e and f, are reported in Figures 35, 36, 37 and 38, respectively. The data were fitted to point out the equations that correlate the surface evolution (Y) as a function of time (X).

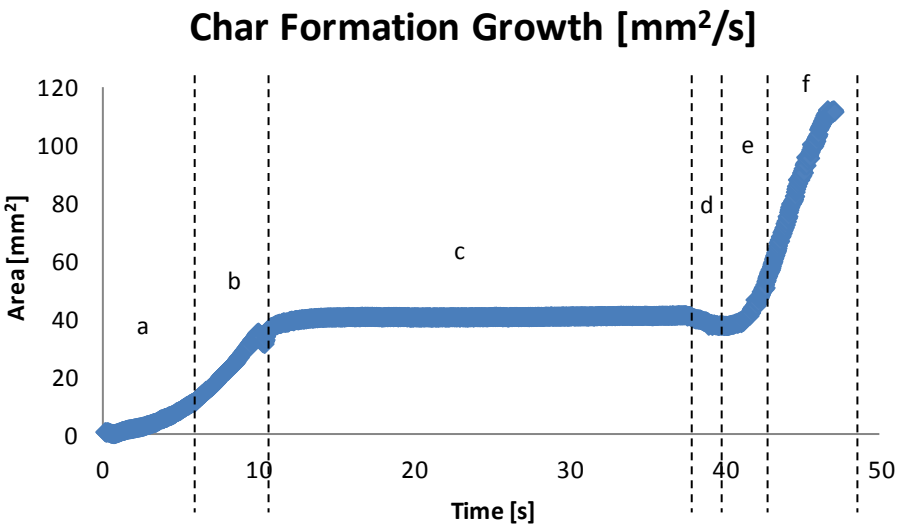

Fig 34. The surface protective layer growth as a function of time for UL94-V0.

First flame application

During the first 5 seconds of forced ignition (segment a, Figure 35), the system shows an unsteady burning behavior [15] and PLGR increases. Then (segment b, Figure 36), the steady burning condition is reached and PLGR shows a constant growth rate of about 5.9 mm^2/s, which does not change up to t = 10 seconds.

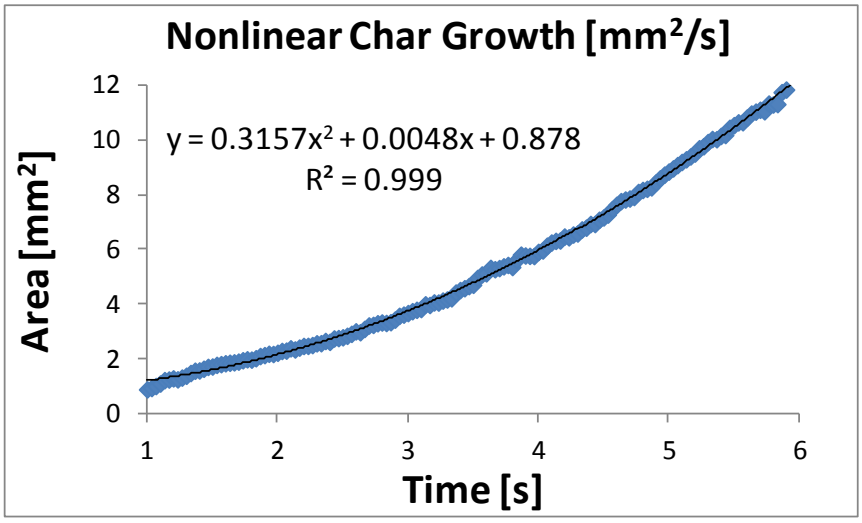

Fig 35. Fitted data in segment a.

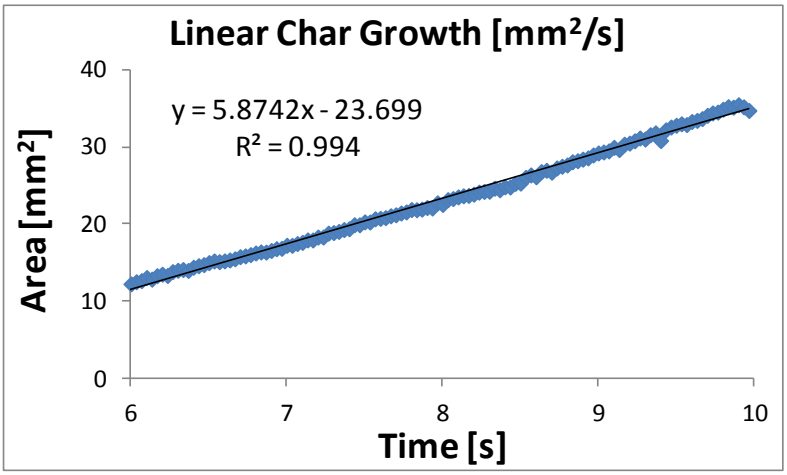

Fig 36. Fitted data in segment b.

Second flame application

Upon a second forced ignition, the transition unsteady/steady burning is also visible. PLGR also shows an early accelerated phase (Figure 37), followed by a constant growth rate of 14 mm^2/s (Figure 38).

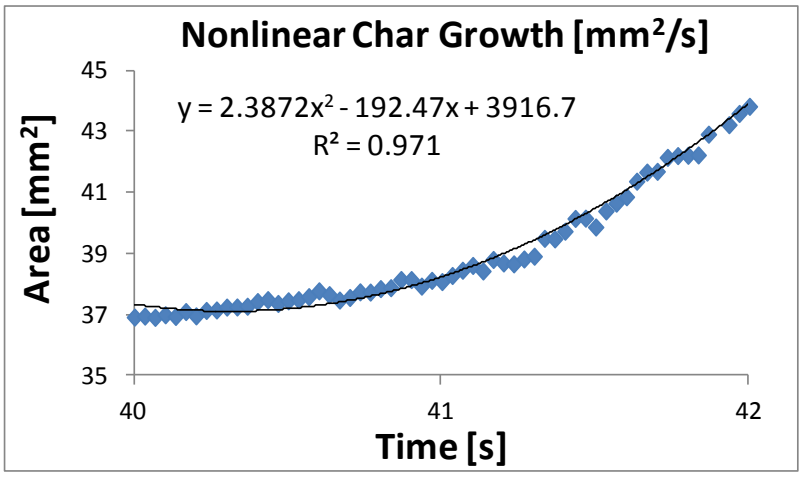

Fig 37. Fitted data in segment e.

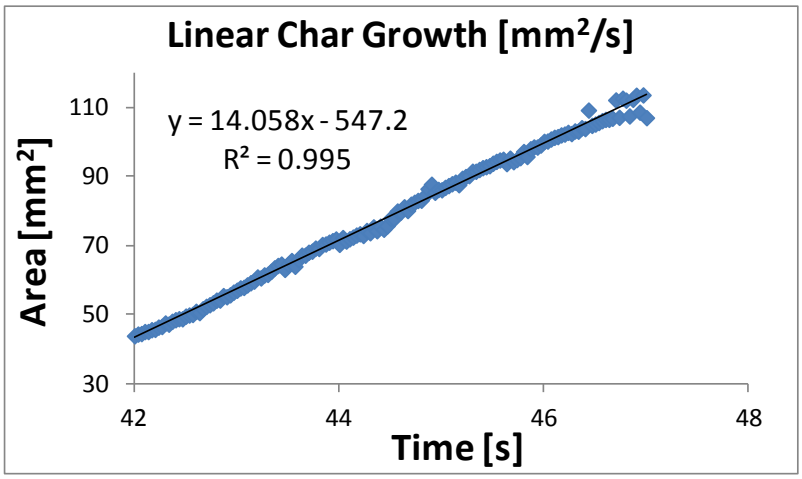

Fig 38. Fitted data in segment f.

The steady PLGR is higher during the second flame application as compared with the first. This behaviour is probably due to different specimen temperatures: indeed, upon the second flame application, the specimen temperature is higher, thus promoting a quicker reaction within the flame retarded formulation.

6.4.2 UL94-n.c.PLGR analysis

Figure 39 collects 6 snapshots from the n.c. UL94 test. Snapshots from (a) to (c) refer to the first flame application. Thereafter, the Bunsen burner was removed and the material continued to burn while generating an ineffective slowly growing protective layer (snapshots from (d) to (f)). The video recording was interrupted at t = 40 seconds.

(a) t=1 s *(b) t=5 s* *(c) t=10 s* *(d) t=15 s* *(e) t=25 s* *(f) t=40 s*

Fig 39. Images extracted from the video of the n.c flame retarded material recorded during the UL 94 flame test. (a) to (c) refer to the first flame application. (d) to (f) show the char growth at different times while the material is still burning.

The formation of an ineffective protective layer leads the material classified as UL94-n.c to burn continuously after the first flame application (Figure 40). The very first segment of PLGR curve is a measurement artefact (Figure 40, segment a) due to the temporary overexposure of the camera. The ineffective protective layer develops with a similar trend as for the V0 material: an unsteady interval (Figure 41), followed by a steady PLGR (Figure 42). The PLRG shows a linear behavior over the time interval from 4 seconds to 10 seconds, where the PLRG is about 1.15 mm^2/s. When the burner is removed, the material continues to burn and the surface shield grows with a linear trend (Figure 40, segment d).

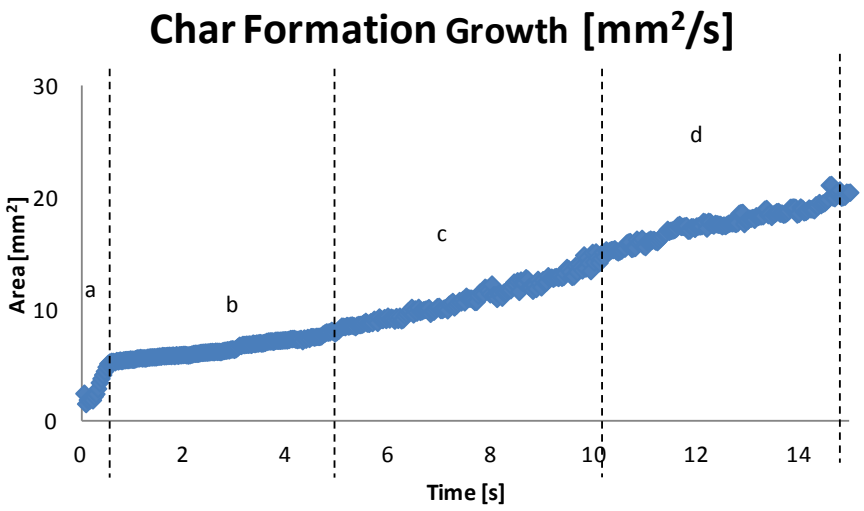

Fig 40. The surface protective layer growth as a function of time for UL94-n.c.

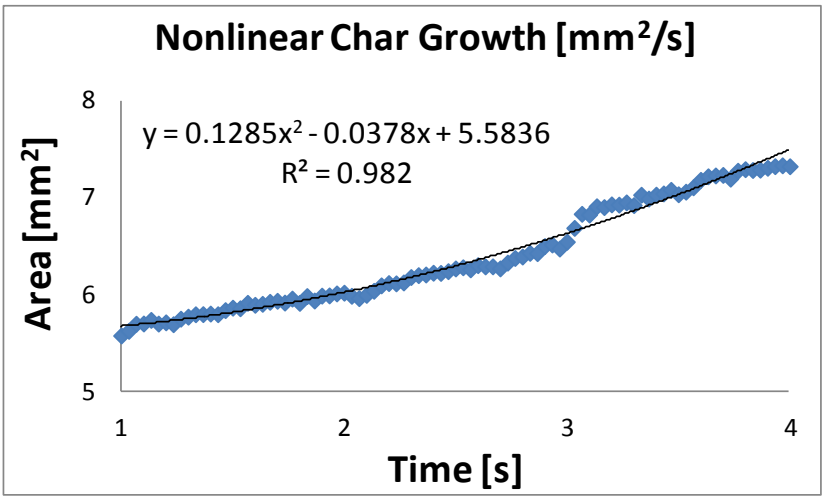

Fig 41. Fitted data in segment b.

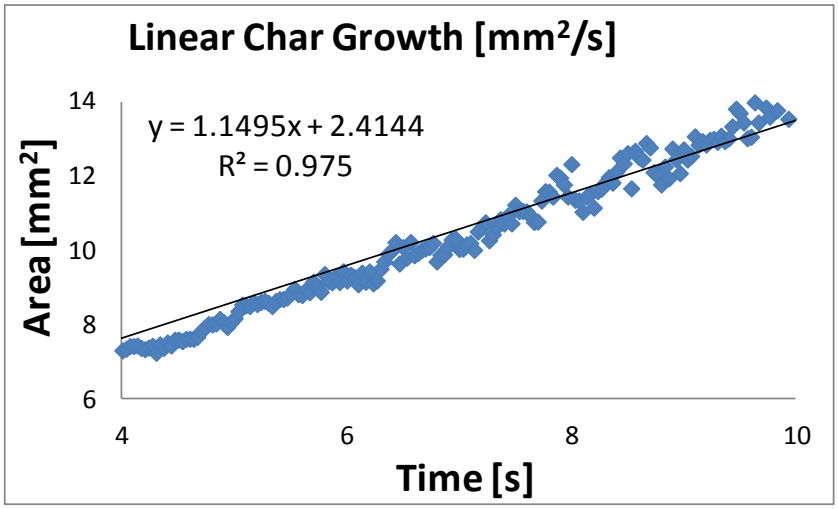

Fig 42. Fitted data in segment c.

Supplementary information consisting of two videos showing the complete sequence of images reported in Figure 33 (V0- UL94 material) and Figure 39 (n.c- UL94

material) can be found in the DVD of this thesis.

6.4.3 PLGR vs UL94 performances

Figure 43 shows the PLGR curves of the V0 and n.c. materials during the first ignition.

After the first second, where the vision system is overexposed, the two materials already behave in a different way. Indeed, V0 material shows a quadratic dependence of area from time, that is, an accelerated growth rate with respect to the n.c. material, where the dependence is linear (Figure 43).

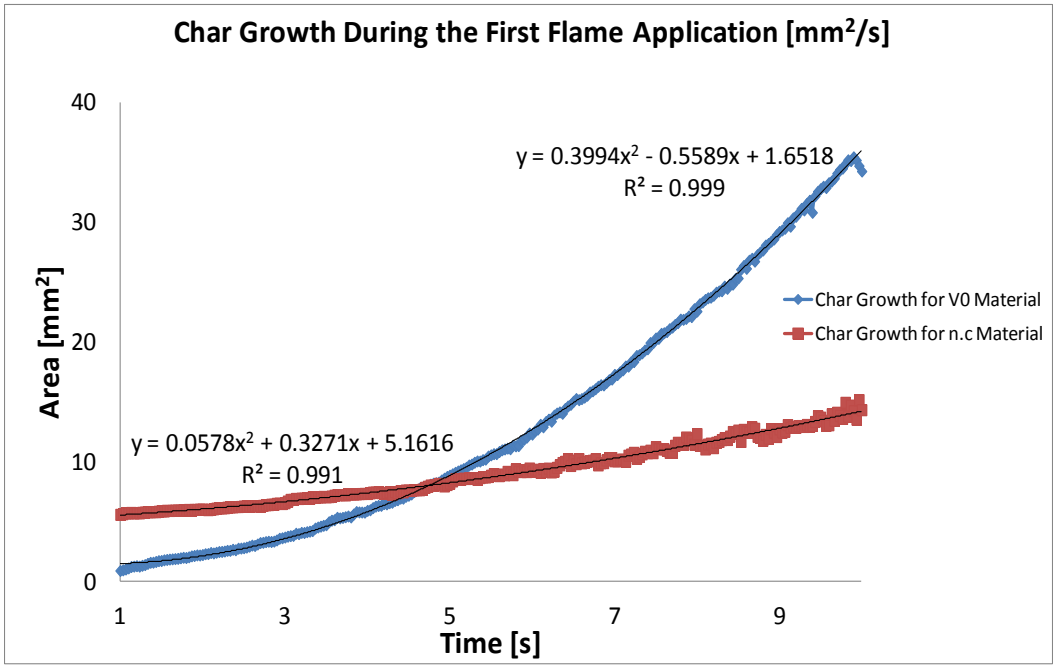

Fig 43. PLGR curves of the V0 and n.c. materials for the first ignition.

However, the n.c. ineffective protective layer area is higher between 1 and about 5 seconds with respect to the V0 counterpart.

As shown in Figure 44, the n.c. material reaches the steady burning condition (linear part of the PLGR curve) before V0 counterpart (i.e. at 4 and 6 seconds, respectively). The V0 effective shield takes more time to build up, while the n.c. materials rapidly generates a poor protective layer, unable to hinder the flux of heat and chemicals between the flame and the material surface.

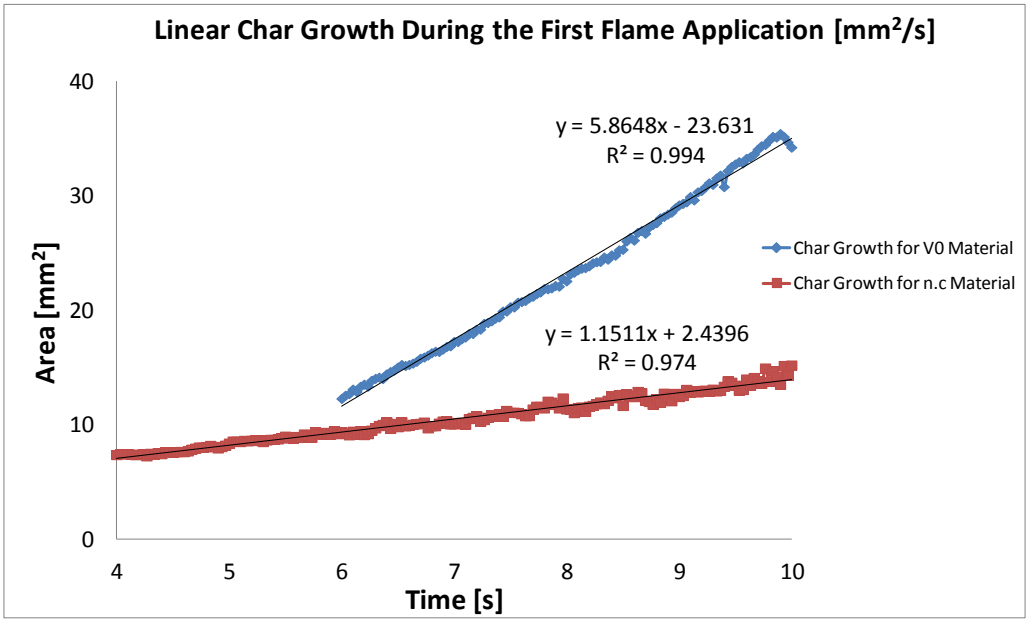

Fig 44. Linear sections of the PLGR curves of V0 and n.c. materials during first ignition.

6.5 Conclusions

In this chapter, a novel apparatus has been proposed for obtaining new insights on the dynamic formation of flame-retardants protective layers, through the acquisition of such important parameters like the growth rate, the timing of holes and cracks formation, and the evolution of the surface texture upon exposure to a flame source [16]. More specifically, the dynamic reaction of the selected materials has been well correlated with the fire performances achieved in UL94 flammability tests. It has been found that the software-aided evaluation of the surface growth rate may represent an interesting tool for the development of flame retardant formulations and the assessment of some of their flame retardant features. Because of the versatility of the proposed small-size apparatus, its possible integration with other standard fire tests is currently under further investigation.

6.6 References

[1] M. Lewin. In: M. Le Bras, G. Camino, S. Bourbigot, R. Delobel, editors. “Fire Retardancy of polymers: The use of intumescence”. Cambridge: The Royal Society of Chemistry: 1998, p. 3-32.

[2] M. Le Bras, S. Bourbigot. In: M. Le Bras, G. Camino, S. Bourbigot, R. Delobel, editors. “Fire Retardancy of polymers: The use of intumescence”. Cambridge: The

Royal Society of Chemistry: 1998, p. 64-753.

[3] G. Camino. In: G. Pritchard, editor. “Flame retardants: Intumescent systems”. Vol. 1: Plastics Additives. Springer:1998, p. 297-306.

[4] R.J. Asaro, B. Lattimer, C. Mealy, G. Steele.” Thermo-physical performance of a fire protective coating for naval ship structures”. Composites: Part A 40 (2009), 11–18.

[5] A. Riva, G. Camino, L. Fomperie, P. Amigouet. “Fire retardant mechanism in intumescent ethylene vinyl acetate compositions”. Polymer Degradation and Stability 82 (2003), 341-346.

[6] A. Castrovinci, G. Camino, G. Drevelle, S. Duquesne, C. Magniez, M. Vouters, “Ammonium polyphosphate–aluminum trihydroxide antagonism in fire retarded butadiene-styrene block copolymer”. European Polymer Journal 41 (2005), 2023- 2033.

[7] L.R.M. Estevão, R.S.V. Nascimento. “The use of heating microscopy in the study of intumescence in waste catalyst containing polymer systems”. Polymer Degradation and Stability 75 (2002), 517-533.

[8] S.P.S. Ribeiro, L.R.M. Estevão, C. Pereira, J. Rodrigues, R.S.V. Nascimento. “Influence of clays on the flame retardancy and high temperature viscoelastic properties of polymeric intumescent formulations”. Polymer Degradation and Stability 94 (2009), 421–431.

[9] S. Duquesne, S. Magnet, C. Jama, R. Delobel, “Thermoplastic resins for thin film intumescent coatings-towards a better understanding of their effect on intumescence efficiency”. Polymer Degradation and Stability 88 (2005), 63-69.

[10] S. Bourbigot, S. Duquesne. In: A.B. Morgan, C.A. Wilkie, editors, “Intumescence and nanocomposites: A novel route for flame-retarding polymeric materials”. Flame Retardant Polymer Nanocomposites. Hoboken: Wiley: 2007, p. 131-162.

[11] M. Jimenez, S. Duquesne, S. Bourbigot, “Characterization of the performance of an intumescent fire protective coating”. Surface and Coatings Technology 201 (2006), 979–987.

[12] L.M.R. Mesquita, P.A.G. Piloto, M.A.P. Vaz, T.M.G. Pinto, “Decomposition of intumescent coatings: Comparison between a numerical method and experimental results”. Acta Polytechnica 49 (2009), 60-65.

[13] S. Bourbigot, S. Duquesne, “Fire retardant polymers: Recent developments and opportunities”. Journal of Materials Chemistry 17 (2007), 2283–2300.

[14] S. Bourbigot, M. Le Bras, S. Duquesne, M. Rochery, “Recent advances for

intumescent polymers". Macromolecular Materials and Engineering 289 (2004), 499–511.

[15] R.E. Lyon, M.L. Janssen, "Polymer flammability". Final Report. U.S. Department of Transportation Federal Aviation Administration, 2005. Report No.: DOT/FAA/AR-05/14.

[16] R. Dos Santos, M. Floris, M. Banfi, E. Oberrauch, M. Marchizza, G. Malucelli, G. Tognola, A. Castrovinci. An online acquisition method for monitoring the surface growth of flame retardant protective layers. (submitted to Fire and Materials)

7 Final conclusions and perspectives

This work was devoted to the design and development of a novel electrically conductive flame retardant material, which can take benefits from the potential synergisms between flame retardants and conductive fillers.

The combination of the scientific knowledge with the DOE approach was essential to achieve the main technological objective of this work, which consisted of developing a bi-functional bio-based TPU composite with the following specifications: halogen-free UL94-V0, electrical resistivity ≤ 1000 Ω.cm and fillers content not exceeding 25 wt.%.

During this work, the main tasks were identifying the ingredients (in a first stage) and defining the optimal proportions of additives (in a second stage) capable of simultaneously conferring to the polymer of interest the most desirable values of flame retardancy (as high as possible) and electrical resistivity (as low as possible).

The materials (flame retardants and electrically conductive additives) used in the development of this novel formulation were pre-selected mainly based on bibliographical studies. Then, the experimental activities and the analysis of the test results allowed to identify positive and negative effects among the components of the formulation (synergisms among flame retardants).

The obtained *final formulation: TPU=0.79; CNTs=0.03; Component F=0.03; Component A=0.065; Component I=0.085* showed the maximum flame retardancy and the minimum electrical resistivity, which are considered simultaneously satisfactory. After the final formulation was obtained, some experiments were replicated both at laboratory and at industrial scale in order to confirm the simultaneous accomplishment of the desired target values of flame retardancy (V0 compliant) and electrical resistivity (≤1000 Ω.cm).

Table 30 compares the technical specifications of the *final formulation* developed in this thesis under the ELYSA project with the technical specifications of similar products from the companies RTP, BASF and LUBRIZOL. The final formulation has a lower electrical resistivity than the commercially available products supplied by these companies, it is bio-based and it still has an excellent flame retardancy (that is, V0 in the UL-94 test).

Manufacturer	Product name	TPU Polymer base	Bio-based	Halogen-free	UL94	Surface resistivity [ohm/sq]	Hardness shore A	Tensile strength [MPa]	Elongation at break [%]	Filler load [wt%]
RTP	ESD C 1200T-85A	ether	no	no	N/A	<1E+6	90	15 *	>300*	N/A
BASF	Elastollan® 1190 A FHF	ether	no	yes	V0	N/A	90	25	550	N/A
LUBRIZOL	Estane® ZHF 95AT3 TPU	ether	no	yes	V0	5.6E+14	95	13.8	360	N/A
This thesis	**ELYSA**	**esther**	**yes**	**yes**	**V0**	**< 1E+03**	**93**	**9****	**134****	**21**

Table 30: Comparison among the technical specifications of the final formulation and the technical specifications of similar products from RTP, BASF and LUBRIZOL. *500mm/min, **100mm/min

The analysis to understand the interactions between flame retardants and CNTs, and between flame retardants and the polymer, is under way.

In this work, an innovative online acquisition apparatus for monitoring the surface growth of flame retardant protective layers was also designed and developed, which provided a deep insight of the dynamic behavior of a phosphorous-based flame retarded material. The measurement of the surface protective layer growth rate provided a better understanding of the behavior of the flame retardant systems, correlating the speed of the chemical reaction with the performances of the material.

Dynamic monitoring of cracks formation could help to adjust the flame retardant formulations in order to minimize/avoid this behaviour. Therefore, the identification of the cracks formation in the char is clearly possible with this apparatus and some measurements are currently under way (Figures 45 and 46). In addition, a 3D scan, which could measure the volume expansion and inspect features that are not visible with the 2D camera, is also possible with this apparatus. Preliminary results are shown in Figure 47.

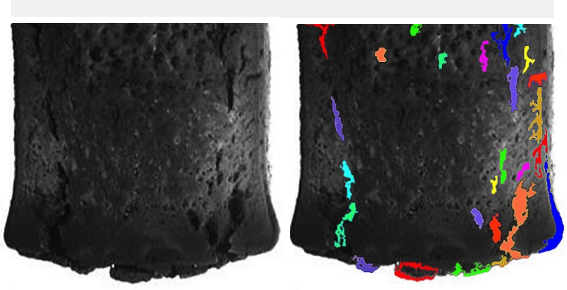

Fig. 45: Images of cracks in the material surface before and after processing.

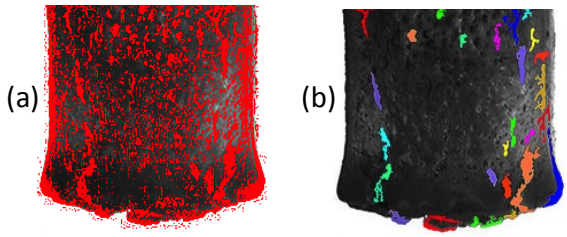

Fig. 46: Steps of cracks identification

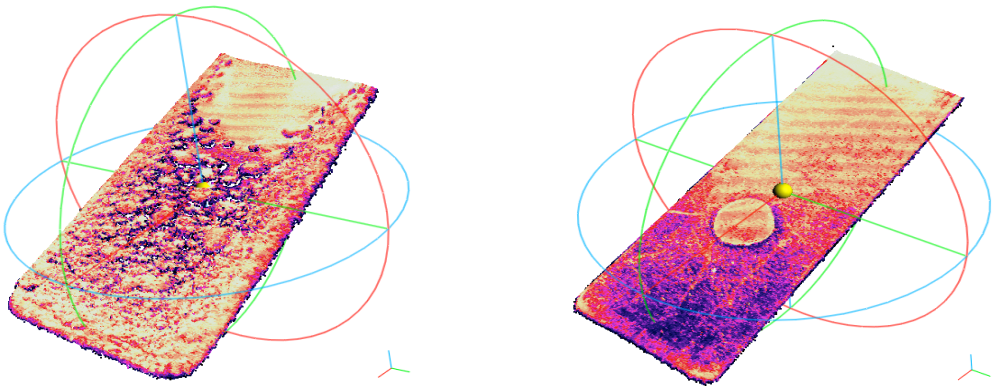

Fig. 47: 3D scan of the material surface.

Annexes

Annex 1

Material Manufacturer/ Supplier	Commercial Reference	Aggregation State	Composition	Brief Description
FR PHOSPHOROUS-BASED				
ADEKA-PALMAROLE	ADK STAB FP-2100J	Powder	Nitrogen/phosphorus-based	Halogen free flame retardant for polyolefins (excellent flame retardancy with retention of polymer mechanical properties).
BUDENHEIM	BUDIT 3202	Powder	Ammonium polyphosphate	This formulation was optimized for TPU enables to meet stringent flammability requirements conforming to regulations such as UL 94 V-0 and V-2 at lower cost. The additive shows almost no impact on processability.
KREMS CHEMIE CHEMICAL SERVICES	KCCS DOB11	Powder	6H-Dibenz [c,e] [1,2] oxaphosphorin-6-propanoic acid, butyl ester, 6-oxide	Gas phase active; additive character; for polyurethanes.
	KCCS EP11	Powder	Ethylenediamine-o-phosphate	For intumescent flame retardant systems for polyurethanes.
RHODIA	AMGARD TOF	Powder	Trioctyl phosphate	Halogen free phosphate plasticizer with a very good resistance to low temperatures and weathering.
THOR	AFLAMMIT® PPN 967/ AFLAMMIT® PPN 978	Powder	Multi-component blend based on ammonium polyphosphate	Designed for use in polyolefins and thermoplastic elastomers. Stable up to 250-260^{o}C (to pass UL 94 V-0)

LANXESS	DISFLAMOLL DPK	Liquid	Cresyl diphenyl phosphate (phosphoric acid esters)	Acts as a flame retardant and as a plasticizer. Compatible with Polyether-TPU as well as with Polyester-TPU.
ITALMACH CHEMICALS	FLAME RETARDANT A B85AX	Powder	Calcium inorganic phosphinate	Flame retardant A B85AX is a very effective solution for flameproofing PBT, PA 6 and glass fibres reinforced, showing outstanding mechanical properties. Synergistic effect are known with some other flame retardants like Melamine Cyanurate.or Zinc Borates.
CHEMTURA	REOFOS RDP	Liquid	Bisphosphate (RDP)	High molecular weight phosphate ester flame retardant, which can impart superior flammability performance and lower volatility when compared with triaryl phosphate.
SUPRESTA	FYROLFLEX® RDP/ FYROLFLEX® BDP	Liquid	Resorcinol bis (diphenyl phosphate)	Oligomeric phosphate ester flame retardant, is designed for use in engineered resin applications. Due to its low volatility and high heat stability, this non-halogen flame retardant can tolerate high temperature processing required of many engineered resins.
FRX POLYMERS	NOFIA™ OL1100/ NOFIA™ OL5000	Pellets	(polyphosphonate homopolymers)	Low molecular weight flame retardant additives. The oligomers are phosphorus-based additives suitable for flame retarding thermoplastic polyurethanes, polyester elastomers, unsaturated polyesters.
BUDENHEIM	FR CROS C40	Powder	Ammonium polyphosphate	Flame retardant for PUR, polyurethane, thermoplastics, other and as a catalyst for intumescent systems in polymers (Polyolefins)
ALBEMARLE	NCEND™ P-30	Liquid	Triphenyl phosphate	NcendX P-30 flame retardant provides a halogen-free solution for flame retarding PC/ABS, PPO/HIPS and other polymers.
CLARIANT	EXOLIT® OP 930/OP 935	Powder	Aluminium phosphinates (Et PO Et O3Al)	A new class of halogen free and environmentally friendly flame retardants for electronic applications.
CERAMIC AND LOW MELTING GLASS PRECURSOS				
WILLIAM BLYTHE	FLAMTARD H S1050	Powder	Zinc Hydroxystannate and ZHS)	Flame retardant synergist that simultaneously suppresses the generation of smoke and prevents the surface spread of flame.

RIO TINTO MINERALS	FIREBRAKE® ZB	Powder	Zinc borate (2zno·3b2o3·3.5h2o)	Smoke and afterglow suppressant, and anti-arcing agent in polymer systems such as polyvinyl chloride, nylon, epoxy, polyethylene, polypropylene, polyesters, thermoplastic elastomers and rubbers.
THOR	AFLAMMIT® PCI 511	Powder	Zinc borate (2zno·3b2o3·3.5h2o)	Standard grade of zinc borate, available as a fine, white powder. Multipurpose FR and smoke suppressant additive. Stable up to 290°C.
CARBON SOURCE				
PERSTORP	CHARMOR™ DP40	Powder	Dipentaerythritol derivative	Carbon source for halogen free systems demanding lower smoke release and non-toxic fumes.
LUBRIZOL	ESTANE® 54610 NAT 021		aromatic TPU	Aromatic polyester-based thermoplastic polyurethane.
SILICON-BASED SYSTEM				

WACKER CHEMIE	GENIOPLAST® PELLET S	Pellets	Silicone gum Formulation with high loading of Ultrahigh molecular weight (uhmw) siloxane polymer.	Improve burning characteristics of thermoplastic resins, especially when applied in combination with halogen free flame retardant fillers. It is expected to give improved benefits compared to conventional lower molecular weight siloxane additives, e.g. less screw slippage, improved release, a lower coefficient of friction, fewer paint and printing problems, and a broader range of performance capabilities.
DOW CORNING	DOW CORNING 4-7081 RESIN MODIFIER	Powder	Si powder resin modifiers (methacrylate)	Halogen-free powdered siloxanes recommended as additives in highly filled flame-retardant (FR) plastic formulations. Benefits observed include reduced die drool, torque, heat release rate, smoke, rate of toxic gas evolution, and water absorption, as well as increased impact strength.
LEHMANN & VOSS	AMINOSILAN DL-PTEO	Liquid	Aminosilane	Compared with pure silane this dry liquid improves handling and dosage, gives a better dispersion and optimum distribution of the active ingredient inside the compound. Suitable for substrates like glass fibers, mineral wool, silica, clay mica, aluminium hydroxide, magnesium hydroxide and other OH- group containing fillers.
POLYMER				
LUBRIZOL	Pearlthane® ECO D12T80		Bio-based Thermoplastic Polyurethane	High performance bio-based TPU with ca. 42% bio-based content as determined according to ASTM D6866 for Injection Moulding applications. This natural TPU resin features properties similar to standard TPU of same hardness, i.e. excellent mechanical properties and abrasion resistance.
CONDUCTIVE FILLERS				

ROCKWOOD ADDITIVES	CLOISITE® 30B	Powder	Natural montmorillonite modified with a quaternary ammonium salt (MT2EtOH: methyl, tallow, bis-2-hydroxyethyl, quaternary ammonium)	Additive for plastics and rubbers to improve various physical properties, such as reinforcement, CLTE, synergistic flame retardant and barrier.
LAVIOSA CHIMICA	DELLITE® 72T	Powder	Natural montmorillonite derived, modified with a quaternary ammonium salt (DTDMAC)	Used to improve some physical, thermal and mechanical properties of the polymer matrix.
CYTEC	THORNEL®MAT VMC CARBON FIBER		Carbon fibre	Shorter fibers for injection molding. Fiber lengths average 200 µm - inadequate for good mechanical property improvement but can result in improved shrinkage, thermal and electrical conductivity, and frictional characteristics.
NANOAMOR	NANOAMOR 95%		Carbon nanofibers	80-200 nm Carbon Nanofibers 200-500 nm Carbon Nanofibers
NANOAMOR	NANOAMOR 95%		Graphitized carbon nanofibers	80-200 nm Graphitized Carbon Nanofibers 200-500 nm Graphitized Carbon Nanofibers
AMERICAN ELEMENTS	CARBON NANOTUBES	Powder	Carbon(c) nanotubes	Single walled, double walled and multi-walled forms, bundled and unbundled, with tube lengths from 5 to 30 nanometers (nm) and specific surface area (SSA) in the 50 to 500 m 2 /g range.
NANOCYLTM	NC7000	Powder	Carbon nanotubes	Thin multi-wall carbon nanotubes, produced via the catalytic carbon vapor deposition (CCVD) process. Small size and high aspect ratio (>150) let them form a network of conductivity at a very low concentration.
TIMCAL	TIMREX	Powder	Synthetic Graphite	Produced using a highly-controlled graphitization process which a consistent purity, perfect crystalline structure and well defined texture.
EVONIK-CARBON BLACKS	PRINTEX® XE 2	Powder	Carbon black	Carbon black. Used as reinforcing filler in rubber compounds. Offers very good electrical conductivity.
CABOT	VULCAN® P	Powder	Carbon black	Highly reinforcing furnace black. Used to impart electrical conductivity to rubber and plastic compounds.

				Offers high surface area, very good chemical purity and surface porosity. Can be used in conjunction with other furnace blacks. Possesses very low solvent extract, sulphur content and sieve residue.
TIMCAL	ENSACO®	Powder	Carbon black	Slightly more graphitic than furnace blacks. They combine to a certain extent the properties of a furnace black and an acetylene black.
ZOLTEK	PANEX® 35 TYPE -65		Chopped fiber	Chopped fiber for engineering thermoplastic applications. It provides excellent mechanical and electrical properties for reinforcement in thermoplastic molding compounds requiring high strength and modulus, low density, electrical conductivity, dimensional stability, low thermal expansion and excellent friction/wear properties.

Annex 2

A.2.1 Design of Experiments (DOE) for mixtures

DOE suggests a relatively small set of very informative runs (experimental design) which allow the experimenter to efficiently reach the desired objective, being it screening (identification of the key factors among all) or optimization (identification of the combination of factors capable of providing the most desirable response or set of responses)

The polymer products, which are the object of the present study, are mixtures obtained by mixing various components together. Experimentation involving mixtures is different from that involving physical factors like temperature, pressure or time. Indeed, in mixtures the proportions of the components are not free to vary independently of one another.

In general, letting x_i, $i = 1, 2, \ldots, q$, be the variables representing the proportions of the q mixture components, the constraints are the followings:

$$\sum_{i=1}^{q} x_i = 1 \qquad x_i \geq 0 \qquad i = 1, 2, \ldots . q.$$

The DOE methodologies especially applied to mixtures are described in several books [1-3], and book chapters [4-6].

A.2.2 Statistical models for mixtures

Models for mixtures are different from models for independent factors, because they must take into account the constraint existing among the components proportions $(\sum_{i=1}^{q} x_i = 1)$

The mixture models for three components (Scheffè models) are the following:

- Linear model: $Y = b_1 x_1 + b_2 x_2 + b_3 x_3$

- Quadratic model: $Y = b_1 x_1 + b_2 x_2 + b_3 x_3 + b_{12} x_1 x_2 + b_{13} x_1 x_3 + b_{23} x_2 x_3$

Looking at these equations and comparing them to the correspondent models for independent factors, it is immediately apparent that they lack the constant term, b_0 , and the quadratic terms, x_i^2. To show how these equations come from, let's consider the simple case of linear model for two independent factors (x_1 , x_2):

$$Y = b_0 + b_1 x_1 + b_2 x_2$$

Taking into account the constraint $x_1 + x_2 = 1$, this equation can be written as follows:

$$Y = b_0 (x_1 + x_2) + b_1 x_1 + b_2 x_2 = b_0 x_1 + b_0 x_2 + b_1 x_1 + b_2 x_2$$

$$Y = b_1' x_1 + b_2' x_2$$

with:

$$b_1' = b_0 + b_1$$

$$b_2' = b_0 + b_2$$

Acting in a similar way, the equations representing the mixture models for any number of components (2, 3, 4, etc.) and for any order (linear, quadratic, cubic, etc.) can be obtained. The simplest models are reported in the next table, which also shows the number of model parameters.

Two components

Model	Equation	Number of parameters
Linear	$Y = b_1 x_1 + b_2 x_2$	2
Quadratic	$Y = b_1 x_1 + b_2 x_2 + b_{12} x_1 x_2$	3

Three components

Model	Equation	Number of parameters
Linear	$Y = b_1 x_1 + b_2 x_2 + b_3 x_3$	3
Quadratic	$Y = b_1 x_1 + b_2 x_2 + b_3 x_3 + b_{12} x_1 x_2 + b_{13} x_1 x_3 + b_{23} x_2 x_3$	6
Cubic	$Y = b_1 x_1 + b_2 x_2 + b_3 x_3 + b_{12} x_1 x_2 + b_{13} x_1 x_3 + b_{23} x_2 x_3 + c_{12} x_1 x_2 (x_1 - x_2) + c_{13} x_1 x_3 (x_1 - x_3) + c_{23} x_2 x_3 (x_2 - x_3) + b_{123} x_1 x_2 x_3$	10

In general, it can be shown that a mixture model of order k for f components has the following number of parameters:

$$\frac{(f + k - 1)!}{(f - 1)k!}$$

In order to explain the meaning of the coefficients, let's consider first the term $b_1 x_1$ in the three components models. If $x_1 = 1$, due to the constraint $x_1 + x_2 + x_3 = 1$, x_2 and x_3 must be zero and this means that $Y = b_1$. Therefore, the coefficient b_1 represents the response of pure component 1. The interpretation of all the other linear components is the same.

In general, the interpretation of the coefficients of a mixture model is the following:

- Coefficients b_i represent the responses correspondent to pure components i. In a graphical representation, b_i represents the height of the mixture response surface

above vertex *i*.

- In a model of order higher than linear, there are additional terms that induce an "excess" on the response, which can be either positive (synergistic) or negative (antagonistic). These terms express the amount of deviation of the response from linearity. For example, the term b_{ij} expresses the joint non-linear effect of components *i* and *j*.
- Constant term b_0 and quadratic terms of each same component $b_{ii}x_i^2$ are lacking because they are included in the existing coefficients.

A.2.3 Experimental designs for mixtures

Many types of experimental designs for mixtures exist according to the shape of the experimental region: their generation and analysis are described in detail in the above cited books [1-3].

Simplex-lattice and augmented simplex-lattice designs

One important case is when the experimental region is a geometrical figure called *simplex*. For two components, a simplex is a line, for three components, a triangle, for four components a tetrahedron, and so on. A simplex design has the component ranges all having the same spread, and extra multi-linear constraints are not allowed. When mixture space is a simplex, simplex lattice designs are the most popular design.

A simplex-lattice design, denoted with the symbol {f,k}, where f is the number of mixture components and k is the order of the design (with k≤f). In the {f,k} simplex lattice design each of the f components is studied at k+1 equispaced values:

$$x_i = 0, \frac{1}{k}, \frac{2}{k}, ..., 1$$

The choice of k determines the dimension of the design: the higher the k value is, more closely spaced is the lattice and the higher is the number of trials, which make up the design.

It can be calculated that the number of design points in a simplex lattice design is given by the same formula, which gives the number of mixture model parameters:

$$\frac{(\mathrm{f}+\mathrm{k}-1)!}{(\mathrm{f}-1)!\,\mathrm{k}!}$$

When k=2 the possible fractions of each components are 0, ½, 1. For k=3 they are 0, ⅓, ⅔, 1. The above description is about the *base simplex lattice designs*. The next figure shows the graphical representation of the {3,2} simplex lattice design in its base form, which has 6 design points.

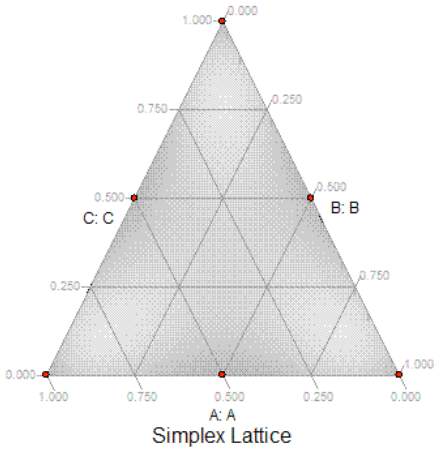

Simplex Lattice

The {f,k} simplex lattice design supports a mixture design of order k in its base form. However, as the number of points exactly equals the number of model parameters that have to be estimated, there are no degrees of freedom left for the estimation of the experimental error and the lack-of-fit (the need to add higher order terms to the model).

For this reason, the designs used in practice require some extra points: the corresponding designs are called *augmented simplex lattice designs*. Augmentation of a simplex design adds f+1 interior check points to allow the detection of the lack-of-fit: one center point and f points halfway between the center point and each vertex are added. Furthermore, in order to estimate the pure error, some replicated points (generally 5 points) are also added.

Therefore, the number of design points in a {f,k} simplex lattice augmented design is approximately:

$$\frac{(f+k-1)!}{(f-1)!\,k!}+f+6$$

The next figure shows a {3,2} simplex lattice augmented design: there are 6 points pertaining to the base simplex lattice plus 4 check points plus 5 replicated points (not specified in the figure) for a total of 15 design points.

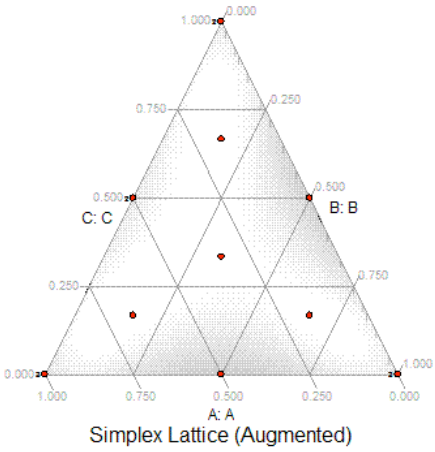

Simplex Lattice (Augmented)

Optimal designs

When the mixture space is not a simplex and/or there are multi-linear constraints, one must use mixture optimal designs. Unlike the simplex designs, where there is a specific pattern to the design points, the points in this design are computer-generated by a special algorithm in order to achieve a given property.

Just to mention two of the most popular optimal designs, D-optimal design provides the most accurate estimates of the model coefficients and I-optimal design provides the lower prediction variance across the entire design space.

The common practice is to set the number of design points equal to the number of the model parameters plus 5 replicate points plus 5 extra points for the lack-of-fit. Therefore, the number of design points in an optimal mixture design of order k for f components is approximately:

$$\frac{(f+k-1)!}{(f-1)!\,k!}+10$$

A.2.4 References

[1] J. Cornell: Experiments with mixtures (3rd edition). Wiley-Interscience (2002)

[2] W.F. Smith: Experimental design for formulation. Siam (2005)

[3] J.A. Cornell: A primer on experiments with mixtures. Wiley (2011)

[4] G.E.P. Box, N. R. Draper: Response surfaces, mixtures and ridge analysis. Wiley-Interscience (2007). Chapters 16-18.

[5] R. Myers, D.C. Montgomery, C.M. Anderson-Cook: Response surface methodology (3rd edition). Wiley (2009). Chapters 11-12.

[6] D. Voinovich, B. Campisi, R. Phan-Tan-Luu, “Experimental Design for Mixture Studies”. In: Comprehensive Chemometrics Edited by Steven D. Brown, Romà Tauler and Beata Walczak. Elsevier (2009). Chapter 1.13.

List of Publications

Papers in peer-reviewed journals

R. Dos Santos, M. Floris, M. Banfi, E. Oberrauch, M. Marchizza, G. Malucelli, G. Tognola, A. Castrovinci. An online acquisition method for monitoring the surface growth of flame retardant protective layers. *(submitted)*

Papers in international conferences

- *Poster:* R. Dos Santos, M. Banfi, M. Floris, M. Marchizza, G. Tognola, G. Malucelli, A. Castrovinci. "A 2d/3d Vision System to Quantitatively Assess the Evolution of a Protective Layer on Flame Retarded Polymers." FRT14: Fire Retardant Technologies 2014. Preston, United Kingdom, April 14-17 2014

- *Poster:* R. Dos Santos, G. Nardi, M. Marchizza, G. Tognola, M. Banfi, M. Floris, E. Oberrauch, G. Malucelli, A. Castrovinci. "Electrically Conductive Fire Safe Polymers." FRPM:14th Fire Retardancy and Protection of Materials Conference. Lille, France. 30th June- 4th July 2013.

Acknowledgements

First of all, I would like to give praise and worship to God, for Him nothing is unfeasible.

Then, I would like to thank Dr. Andrea Castrovinci from the University of Applied Sciences of Southern Switzerland (SUPSI) for giving me the opportunity to pursue a Ph.D. degree in his research group and to work in an industrial research project. I also express my sincere gratitude for the opportunity to attend international courses and conferences that allowed me to learn what other research groups are doing in this research field and stimulated me as a researcher. Furthermore, I would not have learned and accomplished as much as I did in the last three years without his support and for that I am truly grateful.

A special thanks goes to my Ph.D. advisor Prof. Dr. Giulio Malucelli from the Politecnico di Torino for his academic support and guidance, for proofreading this thesis, and for being always available for me.

I would like to thank the partner company SIP Industrial Promotion, in special the Ing. Matteo Marchizza, Giorgio Nardi and Guido Tognola for their support and cooperation during the industrial research project.

I would also like to thank the companies Chemtura, Italmach Chemicals, Clariant, FRX Polymers, Wacker Chemie, TIMCAL, and Lanxess for providing free material samples.

I owe special thanks to Ermanno Oberrauch for the help with the DOE and for his support in the revision of this thesis. In addition, I would like to thank Dr. Giulio Scocchi, Ing. Daniele Crivelli and Ing. Samuele Scarlioni from SUPSI-ICIMSI for the SEM images, mechanical tests and DSC measurements, respectively. I would also like to thank Dr. Jenny Alongi, Giuseppina Iacono and Samuele Colonna from the Politecnico di Torino for helping me to carry out some of the experiments.

I also want to thank Michele Banfi and Moreno Floris for their help in the development of the imaging acquisition system used to monitor the surface of flame-retarded polymers subjected to burning tests.

I am really grateful to my husband Diego for his love and for proofreading this thesis. He supported me all the time and helped me when there were times that I thought I would never make it in time (thank you for your patience during all the late nights and long weekends). A very special thanks also goes to my mother Maria Rosa,

my father Joaquim, my sisters and brothers (thanks for giving me amazing nephews), who stimulated me to continue my studies and always offered me their support and best wishes. In addition, I would like to thank Mrs. Erminia Camillotti for her unconditional support and help outside the university.

I am deeply indebted to the SUPSI-ICIMSI staff, Cinzia Dolci and Franco Barilone for the administrative and technical support and for their friendship.

Moreover, I would also like to extend my gratitude to my co-workers who contributed in making the working place a lively and friendly place for me, in special my colleagues Ehsan, Marco, Luca and Giovanni, who helped me to accomplish this thesis in many different ways.

Finally, I would like to express my gratitude to all those who (in)directly gave me the support to complete this work. They may have not been mentioned here, but they are not forgotten.